# Characterization of recombinant Modified Vaccinia virus Ankara delivering Zika virus nonstructural proteins NS2B and NS3$^{pro}$

von Jan Hendrik Schwarz

Inaugural-Dissertation zur Erlangung der Doktorwürde
der Tierärztlichen Fakultät der Ludwig-Maximilians-Universität München

# Characterization of recombinant Modified Vaccinia virus Ankara delivering Zika virus nonstructural proteins NS2B and NS3$^{pro}$

von Jan Hendrik Schwarz

aus Pforzheim i. BaWü

München 2021

Aus dem Veterinärwissenschaftlichen Department der
Tierärztlichen Fakultät der Ludwig-Maximilians-Universität München

**Lehrstuhl für Virologie**

Arbeit angefertigt unter der Leitung von:

Univ.-Prof. Dr. Gerd Sutter

Mitbetreuung durch:

Univ.-Prof. Dr. Asisa Volz

**Gedruckt mit Genehmigung der Tierärztlichen Fakultät**

**der Ludwig-Maximilians-Universität München**

| | |
|---|---|
| **Dekan:** | Univ.-Prof. Dr. Reinhard K. Straubinger, Ph.D. |
| **Berichterstatter:** | Univ.-Prof. Dr. Gerd Sutter |
| **Korreferent:** | Univ.-Prof. Dr. Heidrun Potschka |

**Tag der Promotion:** 17. Juli 2021

*Meinen lieben Eltern*

*Meinem großen Bruder*

*Meinen wunderbaren Freunden*

*Meiner kleinen Muse*

*Für 13*

***„Je kaputter die Welt draußen,***

***desto heiler muss sie zu Hause sein.“***

Reinhard Mey

# TABLE OF CONTENTS

# I. ABBREVIATIONS

| | |
|---|---|
| **aa** | amino acids |
| **ADE** | antibody-dependent enhancement |
| **APC** | antigen-presenting cell |
| **ATCC** | American Type Culture Collection |
| **BHQ** | Black Hole Quencher™ |
| **BSA** | bovine serum albumin |
| **BSL** | biosafety level |
| **°C** | Degree Celsius |
| **C-protein** | Capsid protein |
| **CAM** | chorioallantois membranes |
| **CD** | cluster of differentiation |
| **CDC** | Centers for Disease Control and Prevention |
| **CEF** | chicken embryo fibroblasts |
| **CMC** | carboxymethyl cellulose |
| **CNS** | central nervours system |
| **CTL** | cytotoxic T lymphocyte |
| **$CO_2$** | carbon dioxide |
| **CVA** | chorioallantois vaccinia virus Ankara |
| **CZS** | congenital Zika syndrome |
| **DAPI** | 4′,6-Diamidin-2-phenylindol |
| **DC-SIGN** | Dendritic Cell-Specific Intercellular adhesion molecule-3-Grabbing Non-integrin |
| **dd$H_2O$** | double-distilled water |
| **DENV** | Dengue virus |
| **DMEM** | Dulbecco`s modified Eagle`s medium |
| **DMSO** | dimethyl sulfoxide |
| **DNA** | deoxyribonucleic acid |
| **dNTP** | deoxynucleosidtriphosphate |
| **DPBS** | Dulbecco`s phosphate buffered saline |
| **dpc** | days post infection |
| **dsRNA** | double-stranded RNA |

| | |
|---|---|
| **ECDC** | European Centre for Disease Control |
| **E-protein** | Envelope protein |
| **EDTA** | ethylene-diamine tetraacetatic acid |
| **ELISA** | enzyme-linked immunosorbent assay |
| **ELISpot** | enzyme-linked immunosorbent spot assay |
| **ER** | endoplasmic reticulum |
| **FACS** | fluorescence-activated cell sorting |
| **FAM** | 6-FAM-phosphoramidit |
| **FBS** | fetal bovine serum |
| **FcR** | Fc receptor |
| **FFU** | foci forming units |
| **FDA** | Food and Drug Agency |
| **FP** | fusion protein |
| **f.p.** | footpad |
| **GAG** | glycosaminoglycane |
| **GPT** | glutamate pyruvate transaminase |
| **hpi** | hours post infection |
| **HA** | human influenza hemagglutinin |
| **HEPES** | 4-(2-hydroxyethyl)-1-piperazineethanesulfonic acid |
| **HE** | hematoxylin / eosin |
| **HIV** | Human Immunodeficiency Virus |
| **HR** | heptad repeat |
| **HRP** | horseradish peroxidase |
| **ICS** | intracellular cytokine staining |
| **ICU** | intensive care unit |
| **IEDB** | Immune Epitope Database |
| **i.m.** | intra muscular |
| **IF** | immunofluorescence |
| **IFN** | interferon |
| **IFNAR** | type I interferon receptor knockout mice |
| **i.p.** | intraperitoneal |
| **Ig** | immunoglobulin |
| **IL** | interleukin |
| **IRF** | interferon regulatory factor |
| **I.T.** | intracellular tail |

| | |
|---|---|
| **kDa** | kilodalton |
| **kb** | kilo base pairs |
| **LB** | lysogeny broth |
| **l** | liter |
| **M** | Mol |
| **M-protein** | Membrane protein |
| **MEM** | minimal essential medium |
| **MHC** | major histocompatibility complex |
| **mg** | milligram |
| **min** | minute |
| **ml** | milliliter |
| **mM** | millimol |
| **MOI** | multiplicity of infection |
| **MVA** | Modified Vaccinia virus Ankara |
| **MVA-ZIKV-NS3$^{pro}$/** | Modified Vaccinia virus Ankara expressing Zika virus |
| **MVA-NS3$^{pro}$** | nonstructural protein NS3$^{pro}$ |
| **MVA-ZIKV-NS2B/** | Modified Vaccinia virus Ankara expressing Zika virus |
| **MVA-NS2B** | nonstructural protein NS2B |
| **nM** | nanomol |
| **NS** | non-structural protein |
| **NS2B** | nonstructural protein NS2B |
| **NS3$^{pro}$** | nonstructural protein NS3 protease |
| **NTD** | *N*-terminal domain |
| **OD** | optical density |
| **o/n** | over night |
| **ORF** | open reading frame |
| **PBS(T)** | phosphate buffered saline (tween20) |
| **PCR** | polymerase chain reaction |
| **PFU** | plaque-forming units |
| **PMA** | phorbol 12-myristate 13-acetate |
| **PNGase F** | peptide-N-glycosidase F |
| **PRNT** | plaque reduction neutralization test |
| **rMVA** | recombinant Modified Vaccinia virus Ankara |
| **RNA** | ribonucleic acid |
| **RPMI** | Roswell Park Memorial Institute |

| | |
|---|---|
| **rpm** | rounds per minute |
| **RT** | room temperature |
| **RT-PCR** | reverse transcription polymerase chain reaction |
| **SARS-CoV-2** | severe acute respiratory syndrome coronavirus 2 |
| **SDS-PAGE** | sodium dodecyl sulfate polyacrylamide gel electrophoresis |
| **sec** | second |
| **SFC** | spot-forming cells |
| **SPF** | specific-pathogen-free |
| **STING** | stimulator of interferon genes |
| **T.A.** | transmembrane anchor |
| **TAE** | tris-acetate-EDTA |
| **TBS** | tris-buffered saline |
| **$TCID_{50}$** | 50 % tissue culture infective dose |
| **TCR** | T cell receptor |
| **Th** | T helper |
| **TMB** | 3,3′,5,5′-Tetramethylbenzidine |
| **TNF** | tumor necrosis factor |
| **UV** | ultraviolet |
| **V** | volt, volume |
| **VACV** | Vaccinia virus |
| **VARV** | Variola virus |
| **VNT** | virus neutralization test |
| **VP-SFM** | virus production serum-free medium |
| **VSV** | vesicular stomatitis virus |
| **WB** | Western blot |
| **WHO** | World Health Organization |
| **WNV** | West Nile virus |
| **YFV** | Yellow fever virus |
| **ZIKV** | Zika virus |

# II. INTRODUCTION

Zika virus (ZIKV) was largely ignored for many years after it was first isolated in 1947. Unexpectedly, in 2007 ZIKV caused outbreaks in the Federate States of Micronesia, and from there spread throughout the South Pacific and to Latin America. These outbreaks were associated with neurological diseases and congenital birth disorders, which resulted in the World Health Organization (WHO) declaring the ZIKV outbreak as a “Public Health Emergency of International Concern” in 2016. To date, there are no vaccines or therapeutic agents against ZIKV licensed.

As ZIKV shares similarities in immunodominant epitopes of its structural proteins with other related flaviviruses, infections with these pathogens can result in a cross-reactive antibody response. These non-neutralizing immunoglobulins can lead to increased viral replication and disease severity through the phenomenon of antibody-dependent enhancement (ADE). Moreover, flavivirus-vaccines based on structural proteins can also exacerbate the course of infection through this pathomechanism. Consequently, a new strategy to design a vaccine that avoids eliciting ADE could potentially be achieved by targeting the nonstructural proteins of ZIKV. This approach is suggested to mitigate the risk of ADE by inducing a balanced humoral and cellular immune response. However, the role of nonstructural proteins in the immune response against flaviviruses is still poorly understood.

Modified vaccinia virus Ankara (MVA), a highly attenuated and replication deficient vaccinia virus with an exceptional safety profile, represents one of the most advanced recombinant viral vector platforms for the development of new vaccines against infectious diseases. This study aims to providing new approaches for a better understanding of the involvement of the cellular immune response in protection against ZIKV and thus to improve future flavivirus vaccine design. To accomplish this goal, we evaluated the safety, immunogenicity, and protective capacity of recombinant MVA-vaccine candidates expressing the ZIKV nonstructural proteins ZIKV-NS2B and ZIKV-NS3$^{pro}$ (MVA-NS2B and MVA-NS3$^{pro}$).

# III. LITERATURE REVIEW

## 1. Zika virus: a re-emerging pathogen

In 1947, scientists at the East African Virus Research Center in Entebbe, Uganda, released sentinel rhesus monkeys into Zika Forest for epidemiological investigations of Yellow Fever Virus (YFV) (Dick et al. 1952). One of these animals developed mild disease symptoms characterized by low-grade fever and rash and was examined further for possible causes of the disease. In the context of the intended study, the investigations were carried out in particular with regard to different strains or related viruses of YFV. In fact, the scientists had discovered a previously unknown pathogen: the Zika virus (Musso and Gubler 2016).

### 1.1. Virological characterisics of Zika virus

Zika virus (ZIKV) belongs to the genus *Flavivirus* within the *Flaviviridae* family, which consists a large group of other globally prevalent human pathogenic viruses, including Dengue virus (DENV), Japanese encephalitis virus (JEV), West Nile virus (WNV), and Yellow fever virus (YFV). Flaviviruses are enveloped viruses with a single-stranded RNA genome of positive polarity that are transmitted by arthropods and thus also referred to as "*arboviruses*" – an acronym for "*arthropode-borne viruses"* (Musso and Gubler 2016).

The ZIKV genome encodes a methylated 5´nucelotide cap, and a single ~11kb open reading frame (ORF) flanked up- and downstream by highly structured untranslated regions (UTRs) of ~100 and 400 nucleotides respectively (Wolford and Schaefer 2020). The ORF is translated into a single polyprotein. Similar to other flaviviruses, the polyprotein is co- and post-translationally cleaved by cellular and virus-encoded proteases into ten functional proteins. These consist of three structural capsid (C) proteins, one precursor membrane (prM) protein, one envelope (E) protein and seven nonstructural proteins (NS1, NS2A, NS2B, NS3, NS4A, NS4B and NS5), which enable virus replication (Mukhopadhyay et al. 2005, Baronti et al. 2014, Musso and Gubler 2016).

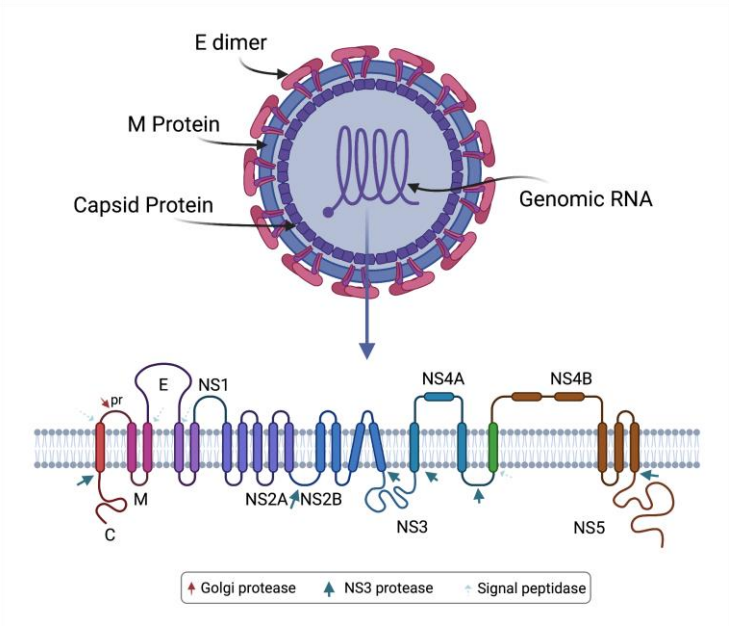


**Figure 1: Structure and genome of ZIKV. The whole genome of ZIK is translated in a polyprotein, which is co- and post-translationally processed by host and viral proteases. It encodes three structural proteins: membrane (M) protein (blue), envelope (E) protein (red) and capsid (C) protein (purple) capsuling the viral RNA. Created with BioRender.com**

ZIKV has the ability to infect a variety of human cells. In doing so, it utilizes various cellular receptors for attachment as well as internalization through cell-mediated endocytosis. In principle, sulfated glycosaminoglycans linked to cellular surface proteins (GAGs), which are present on numerous human cells, have been shown to play a role in cellular attachment and subsequent entry of ZIKV (Kim et al. 2017). However, because ZIKV primarily infects dendritic and endothelial cells, it utilizes C-type lectins expressed on these cells as the main portal for host entry. In particular, the dendritic cell-specific intercellular adhesion molecule-3-grabbing-nonintegrin (DC-SIGN) and the liver-specific ICAM3-grabbing-nonintegrin (L-SIGN) are known to be key receptors interacting with glycans on the E protein of ZIKV (Jameson et al. 2002, Perera-Lecoin et al. 2013). It is known that other members of flaviviruses also utilize these receptors. For example, DENV can infect DC-SIGN or L- SIGN

expressing cells, while WNV primarily infects only L-SIGN expressing cells (Davis et al. 2006, Mondotte et al. 2007).

After the virus has attached to the surface, it enters the target cell by receptor-mediated endocytosis (Gollins and Porterfield 1985). The acidification in the endosome triggers an irreversible conformational change of the E protein that results in fusion of cellular and viral membranes (Allison et al. 1995).

The following viral replication and assembly occurs in close association with intracellular membrane structures. Right after endocytosis, the nucleocapsid is released into the cytoplasm, RNA and capsid protein are separated and particle assembly is initiated (Allison et al. 1995, Brinton 2002, Lindenbach and Rice 2003). In the next step, the 5´cap-structure of the viral RNA starts to interact with cellular ribosome-subunits, where the translation of the viral polyprotein starts (Abrams et al. 2017). This process is briefly interrupted at the capsid protein in the amino-terminal region of the polyprotein, since a specific domain of the carboxy-terminal region of this protein acts as a signal peptide. Consequently, the entire translational complex is transported into the endoplasmic reticulum (ER), where immature particles are formed. These particles - containing the lipid membrane, E and prM protein, and nucleocapsid - are not infectious at this stage because they lack the ability to induce host cell fusion (Guirakhoo et al. 1991, Guirakhoo et al. 1992).

Next, the growing chain of amino acids in the ER is anchored to the lipid layer through the transmembrane domains of the prM and E protein (Abrams et al. 2017). Initially, the ER-associated signal peptidase cleaves the precursor protein to generate the C-, prM-, E- and NS1 proteins. The remaining parts get cleaved by the protease-domain of the heterodimer NS2B/NS3 (NS2B/NS3$^{pro}$) (Abrams et al. 2017). After post-translational polyprotein processing, the viral RNA genome is replicated at the ER membrane (Lindenbach and Rice 2003). In this process, the NS3 helicase supports the activated polymerase domain of the NS5 protein by appropriate deconvolution of the corresponding RNA strands (Luo et al. 2008). Several transcription steps later, the newly synthesized (+)ssRNA strands are finally available for virus assembly (Luo et al. 2008). ER membrane-associated C proteins interact with the newly formed RNA genome

and contribute to its correct folding in order to form viral particles with the E and prM proteins, which are also located in the membrane of the ER (Wu et al. 2015). At this point, the precursor domains of the M protein prevent the premature pH-mediated fusion of the E protein with the cell membrane. Inside the Golgi apparatus, the prM is cleaved into the subsequently smaller and mature M protein by cellular furin (Ma et al. 2004, Mukhopadhyay et al. 2005). Mature virus particles are released outside the cell through the secretory pathway of the trans-Golgi-network (Mukhopadhyay et al. 2005).

## 1.2. Epidemiology of ZIKV

In the years following its discovery, Zika virus was sporadically detected in humans in Africa and Southeast Asia in the 1960s (Dick et al. 1952, Hayes 2009, Haddow et al. 2012). Due to the benign nature of the infection caused by this virus, it firstly remained obscure (Hayes 2009, Brasil et al. 2016).

It was not until local and short-lived outbreaks were documented in 2007 in the Yap Islands, in the Federated States of Micronesia and in the Pacific Ocean, that the world became aware of ZIKV.

In a second outbreak that occurred between 2013 and 2014 in French Polynesia in the South Pacific, more than half of the population was infected (Musso et al. 2018). During this epidemic, the first associations between ZIKV and neurological disorders and even serious fetal abnormalities were described. This connection was increasingly observed when ZIKV spread to other Pacific regions and South America, where it was initially detected in the north of Brazil in 2015 (Musso et al. 2014).

While the incidence of the inflammatory polyneuropathy Guillain–Barré syndrome has been predominantly described in French Polynesia during the ZIKV epidemic (Mier et al. 2018), a broad spectrum of fetal and birth defects, ranging from spontaneous abortion to microcephaly was associated with the Brazilian epidemic (Costa et al. 2016, Miranda-Filho Dde et al. 2016). Finally, the ability of ZIKV to be transmitted via blood and sexual contacts was also confirmed, the WHO declared these outbreaks as a “Public Health Emergency of International Concern in February 2016” (PHEIC) (Saiz et al. 2016). Since then, almost 4000 cases of severe birth defects, also known as “congenital ZIKV syndrome” (Moore et al. 2017), were reported in South America by 2018 (Musso

et al. 2019). As a result of the linkage between ZIKV infection and these severe disease outcomes, the virus was recently added to the medically relevant list of TORCH pathogens (acronym in the field of obstetrics for various infectious diseases that can potentially lead to embryopathy, fetopathy or abortion during pregnancy) (Mehrjardi 2017).


**Figure 2: Emergence and spread of ZIKV. Map of regions where cases of ZIKV infections have been reported between 2007 and 2018. Created with BioRender.com**

Remarkably, phylogenetic studies indicate that a single introduction of the virus must have occurred almost a year before the first reports of ZIKV in Brazil (Faria et al. 2016). These findings can explain the severe course of the pandemic in Latin America: the local population had never been exposed to ZIKV before and was therefore fully susceptible to the virus (Rossi et al. 2018, Rodriguez-Barraquer et al. 2019). In addition, the study illustrates that ZIKV can be efficiently transmitted in mosquito rich areas and can spread across regions through human mobility (Musso and Gubler 2016).

While the spread of the virus can be easily tracked, the link between ZIKV infection and the occurrence of severe neurological complications is very difficult to assess due to the insufficient data situation. Thus, there are only inadequate scientifically validated data on these diseases before and during the pandemic available (Victora et al. 2016). For example, more than half of the cases of microcephaly were incorrectly recorded because the required measurements were not taken more than once during comparable time periods,

resulting in an overall result that falsely overstated the number of reported cases of microcephaly (Krow-Lucal et al. 2018). Beyond that, a large proportion of the measurements were not even carried out according to an international standard, which makes the comparability of the results even more difficult (Victora et al. 2016). The causal relationship between ZiKV and severe neurologic complications is furthermore difficult to determine, due to the fact that the occurrence of the virus and the corresponding symptoms varied territorially and temporally, as shown by the different cases in French-Polynesia and Brazil (Costa et al. 2016, Miranda-Filho Dde et al. 2016, Hay et al. 2018, Mier et al. 2018).

Years after the first outbreaks, there is still an ongoing debate as to whether these diseases were already prevalent before the pandemic and may have been exacerbated, but not caused by the virus. In any case, it is not yet clear whether these cases of disease can really be attributed to ZIKV alone or whether these observations are based on multifactorial reasons, which are still unknown (Petzold et al. 2021).

In 2017, only a few months after the WHO defined ZIKV as a global threat, its incidence began to decrease as dramatically as the cases had initially risen. Since neither a vaccine nor preventive therapeutics were available at that time, this phenomenon can only be explained by herd immunity in the effected population. This theory certainly applies only to countries of high incidence, such as Brazil or French Polynesia. However, it is not yet clear how the pandemic could decrease in the rest of the world (Aubry et al. 2017, Rodriguez-Barraquer et al. 2019).

The different lineages of ZIKV could have a crucial influence on the spread and occurrence of ZIKV-associated symptoms, although their impact on ZIKV spread and pathogenesis is poorly understood. So far, two major lineages have been defined through genetic analyses: the Asian and African lineage (Metsky et al. 2017, Liu et al. 2019). The outbreaks in Micronesia were caused by a subclade of the Asian lineage, which was also responsible for the epidemic in the Americas and consequently is referred to as the American lineage. Although this American lineage is responsible for the largest and most severe outbreaks

of ZIKV, the original Asian strain also poses the risk of an epidemic: in 2018, nearly 150 cases of ZIKV infection were detected in India, attributable to a strain of the "old" Asian lineage (Watts et al. 2018). Studies had demonstrated that strains of both the “old” Asian and American line are responsible for the severe birth defects and neurological disorders described during the epidemic outbreaks between 2013 and 2017 (Wongsurawat et al. 2018). In contrast to this, no correlations between such symptoms and strains of the African lineage have been reported so far, despite the fact that ZIKV has circulated in Africa for decades (Simonin et al. 2017). Notably, several *in vitro* and *in vivo* approaches suggest an impact on enhanced pathogenesis of the African lineage compared to the Asian lineage (Duggal et al. 2017, Sheridan et al. 2018). Even in the 2016 ZIKV outbreak in Angola, the numerous congenital birth defects could be attributed to the Asian lineage (Hill et al. 2019).

By mid-2019, the WHO reported mosquito-borne autochthonous transmission of ZIKV in up to 87 countries in Africa, North-and South America, South-East Asia and Western Pacific. Following the severe outbreaks in South America, isolated cases of microcephaly have also been reported in Africa, although the total number was nowhere near the scale of the previous outbreaks (WorldHealthOrganization 2019).

Prior to 2019, autochthonous transmission of ZIKV has not been observed in Europe, although more than 2000 cases of imported ZIKV infections had already been reported there by 2017 (Wilder-Smith et al. 2018). In 2019, the first autochthonous infection with ZIKV in Europe has been reported by the European Centre for Disease Control (ECDC) in southern France. The mosquito species *Aedes aegypti*, which mainly transmits the virus to humans, is not native to France. However, there are established populations of the related species *Aedes albopticus* in the affected region, which can also transmit ZIKV (Kraemer et al. 2019). This issue illustrates the potential for ZIKV to occur in all countries where *Aedes species* are indigenous. Of course, this assumption also implies that ZIKV can re-emerge in countries where it was already endemic (Parola and Musso 2020).
Consequently, there is still a risk of new outbreaks of ZIKV with unpredictable effects (Badolo et al. 2019). As shown by the cases identified in France, the

next epidemic could possibly even occur in Europe (Giron et al. 2019) . At this point, however, it must be emphasized that mosquito species present in Europe are not yet known to be capable of causing large ZIKV outbreaks (Hugo et al. 2019, Chouin-Carneiro et al. 2020). Nevertheless, the potential of the African ZIKV lineage and an unexpected expansion of the vector spectrum due to climate change could favor this situation.

### 1.3. Transmission

The vast majority of transmissions are caused by mosquitoes (Gutiérrez-Bugallo et al. 2019) which thus are the most significant factor for epidemic spreading. As with DENV or YFV, mosquitoes of the genus *Aedes* are responsible for this horizontal transmission of ZIKV to humans. In turn, the mosquito species *A. aegypti* is responsible for the majority of ZIKV transmissions (Gutiérrez-Bugallo et al. 2019). Despite the fact that the related species *A. albopictus* is more widespread than *A. aegypti* in areas where flaviviruses are endemic and has also been shown to be a competent vector for these pathogens, this species plays only a minor role in ZIKV transmission (Gutiérrez-Bugallo et al. 2019). However, these ratios may continue to evolve in favor of *A. aegypti* due to climatic changes, urbanization, and population growth (Kraemer et al. 2019, Musso et al. 2019).

In addition to vector-based transmission, ZIKV also has a unique characteristic among arboviruses: it can be transmitted both sexually and from mother to fetus (Musso et al. 2019). However, only 1 % of the ZIKV infections in Europe and the United States can be traced back to sexual transmission. Owing to a lack of data, these figures cannot be adequately assessed in countries where the pandemic was rampant (Wilder-Smith et al. 2018). Corresponding reports suggest that ZIKV infections are predominantly male-to-female transmitted and independent of whether the affected individual is symptomatic or not (Polen et al. 2018). Interestingly, infectious particles can be detected in the testes and semen of affected males for up to 30 days after the disease has been contracted (Mead et al. 2018).

In addition, several confirmed cases of ZIKV infection via blood transfusion also represents another uncommon feature of horizontal transmission of arboviruses

(Musso et al. 2016, Bloch et al. 2018). However, in the absence of appropriate monitoring, even these observations are difficult to reliably quantify with concrete numbers, so that the prevalence of ZIKV among blood donors can be estimated at just 1 % (Liu et al. 2019).

In contrast, maternal-fetal transmission can be characterized quite precisely. Transmission can occur in all trimesters of pregnancy and, similar to sexual transmission, is independent of whether the infected mother is symptomatic or not (Brasil et al. 2016, Reynolds et al. 2017, Shapiro-Mendoza et al. 2017, Pomar et al. 2018). Data from outbreaks in South America show that more than a quarter of all infected mothers transmit ZIKV to their fetuses (Pomar et al. 2018).

### 1.4. Clinical manifestations

While 50 to 80% of ZIKV infections are asymptomatic in adults (Musso and Gubler 2016, Petersen et al. 2016, Musso et al. 2018), ZIKV can cause a broad spectrum of fetal and birth defects, ranging from spontaneous abortion to microcephaly (Costa et al. 2016, Miranda-Filho Dde et al. 2016). These different clinical pictures are a consequence of severe malformations caused by ZIKV infections and are collectively referred to as congenital Zika syndrome (CZS). Pathological manifestations of CZS include calcifications in the cortex, lesions of the medulla oblongata, pigmentary abnormalities and atrophy of retinal structures (Moore et al. 2017, Pomar et al. 2018). These are all fairly common clinical pictures in congenital infection, but actually are significantly more common in CZS (Moore et al. 2017, Musso et al. 2019). While almost half of maternal-fetal transmissions of ZIKV lead to no damage or symptoms in newborns, 21 % of them, however, have a risk of 5 to 14 % for congenital Zika syndrome. Mostly studies from Brazil show that 6 % of infected fetuses have a risk of ZIKV-associated microcephaly and 14 % even get aborted (Pomar et al. 2018). However, neurological damage characterized by motor impairment can also be found in children who do not show these abnormalities at birth (López-Medina et al. 2020). This indicates that long-term studies must continue for a better understanding of the extent of ZIKV infections (Mulkey et al. 2020).

In addition to these serious abnormalities, the association between ZIKV infection and the occurrence of Guillain-Barré syndrome (GBS) has also been

confirmed in adults (Mier et al. 2018). Due to the neurotropism of ZIKV, this inflammatory polyneuropathy may arise from rather mild disease courses predominantly characterized by mild fever, arthralgia, conjunctivitis, and myalgia (Duffy et al. 2009, Musso and Gubler 2016, Musso et al. 2018). Other severe nerve diseases such as meningoencephalitis and myelitis can also be a consequence of the infection. The incidence of ZIKV-associated GBS amounts to 2-3 cases per 10,000 ZIKV infections, which is comparable to other infections that can cause GBS. The first GBS-specific symptoms appear approximately 6-10 days after the infection, which include inflammatory demyelinating polyneuropathy, acute motor axonal neuropathy, ophthalmoplegia and ataxia (Cao-Lormeau et al. 2016, do Rosario et al. 2016, Dos Santos et al. 2016, Mulkey et al. 2020). Studies suggest that ZIKV-associated-GBS cases result in a higher mortality rate than those caused by other reasons (Dirlikov et al. 2018, Mulkey et al. 2020).

## 1.5. Prevention and treatment

Intensive global efforts to find a safe and effective vaccine against ZIKV have so far been unsuccessful, and as result there is still no licensed vaccine available (Wilder-Smith et al. 2018). Nevertheless, there are many promising vaccine candidates. A total of ten have entered phase I clinical trials worldwide, including various vaccine platforms such as mRNA vaccines, recombinant subunit vaccines, virus-like particles and also inactivated virus vaccines (Masmejan et al. 2018). One DNA-based candidate has entered a clinical phase II trial (Wilder-Smith et al. 2018). However, several years after the pandemic, phase II/III clinical trials are particularly challenging due to the current low case numbers of ZIKV which make it very difficult to evaluate the efficacy and safety of a vaccine candidate (Wilder-Smith et al. 2018, Vannice et al. 2019, Pattnaik et al. 2020). Therefore, even human infection models are now being discussed as alternative evaluation methods for approval processes (Vannice et al. 2019).

Efforts to obtain regulatory approval for specific therapeutics against ZIKV have been as unsuccessful as the search for a suitable vaccine. Although none of the drugs has yet been tested in a clinical trial, there are numerous promising antiviral agents that show efficacy against ZIKV in vitro and in various animal models (Masmejan et al. 2018). Some of these potential therapeutics consist of agents directed against the virus, such as polymerase, protease inhibitors or nucleoside analogs, which are commonly used against other human pathogenic viruses (Bernatchez et al. 2020). Other potential drugs such as purine or pyrimidine synthesis inhibitors exhibit antiviral activity by targeting the viral life cycle (Baz and Boivin 2019). However, since these are only theoretical approaches, clinical treatment of ZIKV infected patients still only consists of supportive symptomatic therapy (Musso et al. 2019). Thus, patients suffering from GBS receive the same treatment as those whose disease has not been caused by ZIKV infection: intravenous immunoglobulin administration and plasma exchange (Musso et al. 2019).

If CZS is suspected, more frequent and targeted monitoring of pregnant women through regular laboratory and ultrasound examinations is recommended. Children suffering from CZS can only be treated by extensive surveillance and intensive medical interventions, with very low chances of survival (Adebanjo et

al. 2017). Since transmission routes of ZIKV are very well recorded, preventive measures including health recommendations for persons at risk can be applied in a targeted manner. These include protection against mosquito bites and targeted screening of mosquito species, as well as recommendations for protected sexual intercourse after suspected infection for two months for women and three months for men (WorldHealthOrganization 2016, Musso et al. 2019).

# 2. Immune response to Flaviviruses

Viral entry to host cells are initially detected by cellular pattern recognition receptors (PRRs), which mediate the initiation and retrieval of an effective antiviral immune response. PRRs recognize conserved molecular pathogen features, so-called pathogen-associated molecular patterns (PAMPs), which enable the immune system to distinguish between foreign organisms and host cells. In case of flaviviruses, viral PAMPs include single-stranded RNA (Boehme et al. 2004).

## 2.1. Innate immune response

Recognition of these specific patterns initiates both an immediate immune response to prevent viral spread in the host and a pathogen-specific adaptive immune response. Dependent on the corresponding cell type, flaviviral infections result in the production of specific cytokines, such as type I (α, β), type II (γ), and type III (λ) IFN as well as the activation of several IFN-stimulated genes (ISGs) (Hamel et al. 2015, Bayer et al. 2016, Quicke et al. 2016). The IFN response is critical for the control of flaviviral infections. This is reflected by the susceptibility of mice lacking components of the IFN signaling pathway to infections with ZIKV (Shrestha and Diamond 2004, Lazear et al. 2016). In turn, they induce a number of other cytokines, the expression of multiple effector molecules, integrins and also interact with the Jak-STAT pathway (Karaghiosoff et al. 2000, Shimoda et al. 2000). Various studies show numerous mechanisms of how ZIKV attenuates the IFN response. For example, the ZIKV NS5 and NS2A proteins have been shown to reduce interactions of STAT2, a key signaling molecule of type I IFN pathway, leading to increased viral replication (Grant et al. 2016). Moreover, ZIKV seems to mediate IFN inhibition by antagonising STAT1 and STAT2 phosphorylation (Bowen et al. 2017).

## 2.2. Adaptive immune system

Effective control of viral infection, viral clearance and protection against re-infection requires activation of the humoral and cellular immune response.

Especially for virus clearance, the formation of neutralizing antibodies is of utmost importance. In the course of humoral immunity, the WNV neutralizing antibodies are of particular importance. The flaviviral envelope protein is the

main target antigen for eliciting this type of immunoglobulins (Colombage et al. 1998, Throsby et al. 2006) Antibodies against prM (Vázquez et al. 2002) or the non-structural protein NS1 are also detected in high amounts during flavivirus infection, although these do not exhibit any neutralizing capacity (Chung et al. 2007, Heinz and Stiasny 2012). Remarkably, different experimental vaccines expressing ZIKV prM and E protected mice from viral challenge. Passive transfer experiments showed that this protection was mediated by E-specific antibodies (Bayer et al. 2016). However, another immunoglobulin subclass plays a decisive role in the early control of flavivirus infection. As early as four days after infection, a high level of neutralizing WNV-specific IgM can be found in the serum of infected mice (Diamond et al. 2003). IgM-specific neutralization at an early stage of infection could help to prevent or limit further spread of the virus into the central nervous system (CNS). In contrast, the IgG response to infection gets effective at a later stage, when the viral infection may already have caused severe damage (Diamond et al. 2003).

T lymphocytes (hereafter referred to as T cells) represent another important component of the immune system for combating pathogens. CD8+ T cells, also called cytotoxic T lymphocytes (CTL), are essential for protection against WNV and ZIKV infection (Purtha et al. 2007). Their function is based on two different strategies: on the one hand, they secrete cytokines, including IFN-γ and tumor necrosis factor (TNF) (Shrestha et al. 2006, Brien et al. 2007). On the other hand, they can secret cytotoxic proteins such as granzyme B and perforin leading to the elimination of virus-infected cells (Shrestha et al. 2006, Ramos et al. 2012). Whereas the nonstructural proteins NS3 and NS5 of DENV are clearly known to be targeted by CD8+ T-cell response, CTLs are primarily directed against prM, E, NS2B and NS5 during an infection of ZIKV (Elong Ngono et al. 2017, Hassert et al. 2019).

CD4+ T cells are also needed for virus defense due to their diverse functions. Thus, mice lacking CD4+ T cells or MHC-II molecules show higher susceptibility to experimental infection with ZIKV (Lucas et al. 2018). Furthermore, CD4+ T cells help B cells mounting the humoral immune response (Sen et al. 1992), support CD8+ T cell responses, segregate cytokines (Sitati and Diamond 2006) and are also able to kill infected cells directly (Heller et al. 2006). Of note, T cell

depleted wild-type and IFN-deficient mice lose weight after challenge infection with ZIKV, underlining their necessity in immune responses against this pathogen (Winkler et al. 2017). This may suggest that the reduced CD4+ and CD8+ T cell responses against ZIKV during pregnancy may be the crucial cause of the congenital diseases associated with ZIKV infections. Therefore, the role of T cells during ZIKV infections has to be investigated in more detail, especially with regard to the design of possible vaccines against various flaviviruses.

# 3. Antibody-Dependent enhancement

Flaviviruses are endemic to many regions and exhibit immunological cross-reactivity amongst themselves. Similar antigenic structures lead to both humoral and cell-associated immune responses. This fact may lead to a beneficial immune response against these different pathogens. However, especially for DENV, this principle is known to turn into a dangerous disadvantage and cross-reactive antibodies can exacerbate flavivirus disease through the phenomenon of antibody-dependent enhancement (ADE) (Halstead 2014).

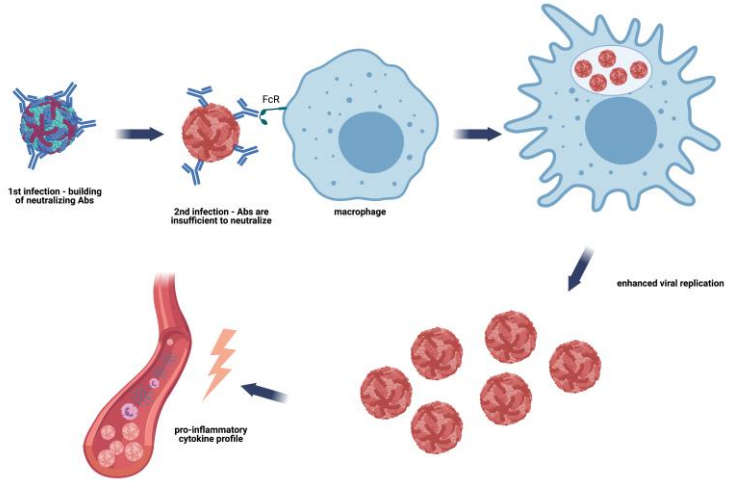


**Figure 3: Antibody-dependent enhancement. Non-neutralizing or partially neutralizing antibodies elicited by prior infection with ZIKV may cause increased viral infection of macrophages via FcR-mediated endocytosis during subsequent DENV infection, resulting in a more severe disease progression. Created with BioRender.com**

To this end, flaviviruses appear to exploit a vulnerability of the host immune system: for efficient pathogen clearance, macrophages recognize antibody-coated viruses - in a class-dependent manner - via their Fc receptors (FcR), which significantly increases the phagocytic activity of these cells. Thus, virus-antibody complexes are recognized, internalized and destroyed via a FcR-mediated pathway in case of a primary DENV infection. This process initially leads to only mild, acute disease with production of efficient neutralizing antibodies. However, this process can also lead to immunopathology when a second DENV infection with a different viral serotype occurs. Antibodies

induced by the first infection can recognize and bind the second infectious strain but have only a reduced neutralizing capacity (Halstead, 2014). Thus, viruses that are only partially coated with these sub-neutralizing antibodies can be taken up by macrophages and replicate within them. This process leads to early and high viremia and also impairs further immune modulation (Halstead 2014).

Several studies not only show an increased risk of developing severe dengue fever in people with pre-existing anti-DENV antibodies (Katzelnick et al. 2017). The presence of antibodies triggered by ZIKV infection can also worsen the course of dengue disease (George et al. 2017, Katzelnick et al. 2017, Katzelnick et al. 2020). Of note, no disease-exacerbating effect has been observed to date with subsequent ZIKV infection in the presence of prior DENV infection. Although it should be noted that the data on pre-existing DENV antibodies during ZIKV infection to date is weak (Katzelnick et al. 2020). Dengue-ADE has been associated with the production of cross-reactive antibodies against the prM protein on the viral surface of DENV, which may increase the infectivity of immature virions carrying high levels of uncleaved prM (Dejnirattisai et al. 2010).

Therefore, vaccines directed against prM may also induce ADE as in natural infection. Sanofi-Pasteur's live-attenuated vaccine Dengvaxia® against several DENV serotypes was given a limited approval because of concerns regarding this issue. It could sensitize some of the dengue-naïve recipients to severe dengue fever (Martinez-Vega et al. 2017, Thomas and Yoon 2019). This fact underlines the difficulty of producing an effective and safe vaccine against flaviviruses. Since the E protein displays the most prominent structure on the flaviviral surface and mediates receptor binding and virus entry, this protein is - beside the prM protein - a major target for vaccine development. Given the potentially catastrophic consequences of vaccine-induced ADE between ZIKV and other flaviviruses, entirely new approaches need to be found to replace the commonly used target antigens (Wilder-Smith et al. 2018).

# 4. Modified Vaccinia virus Ankara (MVA) as viral vector vaccine

Vaccinia viruses (VACV) are enveloped DNA viruses that belong to the genus *Orthopoxviruses* within the family *Poxviridae*. This genus includes variola virus (VARV), the causative agent of human smallpox - one of the world's most dangerous infectious diseases of humans. The WHO vaccination program that led to the eradication of this pathogen was carried out with different strains of VACV (Bhattacharya 2008).

## 4.1. MVA - an attenuated virus with strong properties

One of these smallpox vaccines was the chorioallantois vaccinia virus Ankara (CVA) strain of VACV, produced by the Turkish vaccine institute in Ankara by donkey-calf-donkey passages (Volz and Sutter 2017). CVA was also used in Germany as a smallpox vaccine from 1953 onwards (Staib and Sutter 2003, Volz and Sutter 2017), but was discontinued due to association with several cases of post-injection secondary lesions (Herrlich and Mayr 1957).

Nevertheless, CVA provided the basis for an improved vaccination approach. Due to its well-characterized biological properties, it was the ideal virus to trace the evolution from a poxvirus with a broad host range to a poxvirus with a more limited host range – just like VARV (Herrlich and Mayr 1957). Indeed, after more than 500 passages on chicken embryo fibroblasts, the resulting virus did not replicate in human cells anymore, although infectivity was preserved in most mammalian cells (Mayr and Danner 1978, Carroll and Moss 1997, Drexler et al. 1998). These new properties led to a renaming of the virus: Modified Vaccinia virus Ankara (MVA) (Mayr 1975).

Between 1968 and 1976, MVA was used to immunize more than 120,000 people. During this time, it showed its potential as an effective and safe vaccine because the adverse events associated with the conventional smallpox vaccine, were not observed for MVA. Consequently, MVA also received its first approval as a pre-vaccine for smallpox vaccination in Germany in 1977 (Mayr and Danner 1978). Despite the eradication of smallpox and the associated abolition of compulsory vaccination in 1980, interest in MVA did not wane, especially

because of MVA's versatility as a gene expression vector.

### 4.2. High genetic stability of MVA

CVA and MVA show clear differences in infectivity in cell culture. These observations are explained by the fact that the MVA genome is reduced by about 15 % compared to the CVA genome (Meyer et al. 1991). The 572 long-term passages on CEF resulted in several point mutations and six large genomic deletion sites in the genome (Antoine et al. 1998, Meisinger-Henschel et al. 2007). These changes are crucial for its replication deficiency in human cells and its avirulence in mammals (Mayr and Danner 1978, Volz and Sutter 2017). Consequently, these genomic deletions have a huge impact on some of the structural and immunomodulatory proteins of CVA. However, crucial for virulence properties are the changes in host-range genes, such as the K1L and C12L/SPI-1 genes (Blanchard et al. 1998). Despite the numerous differences from the parental CVA, the stability of the MVA genome is considered assured by several independent genomic sequence analyses (Mayr and Danner 1978, Antoine et al. 1998).

The high genetic stability is only one of many properties that qualify MVA as a recombinant vector. Nevertheless, it should be noted that recombinant gene products can exert negative selection pressure on the growth of recombinant MVA (rMVA). To prevent this, codon optimization must be carried out for the insertion of heterologous sequences between two essential genes to prevent the instability of the flanking regions of the insertion sites and to prevent frame shifts in recombinant genes (Wyatt et al. 2009). Due to its biological activity, the gene product itself can also negatively affect the stability and vitality of the vector and its growth. This can occur in the case of overexpression, which can be safely controlled by using the modified H5 promoter, thus ensuring the stability of the vector (Wyatt et al. 1996).

### 4.3. Versatile gene expression of MVA

The 178 kb large genome of MVA further allows the integration of large amounts of heterologous DNA and thus high variability for the expression of many foreign proteins (Antoine et al. 1998). Moreover, replication of MVA is independent from host cell genome and gene expression is controlled by virus-specific promoters,

which can activate the viral transcription complex during the entire viral life cycle. Therefore, mRNA needs no splicing and genes contain no introns (Tolonen et al. 2001). But most importantly, it shows that even in host cells in which no new infectious virions can be produced due to reduced replication capacity of MVA, all viral gene classes can be expressed (Broyles 2003). In contrast to other replication-deficient poxvirus vectors, there is an almost unrestricted production of viral and recombinant proteins (Sutter and Moss 1992). Taken together, these features facilitate the design, generation and utilization of MVA as a recombinant vector. The methods required for this are very well established and are based on the principle that the insertion of foreign genes occurs by homologous recombination between the viral DNA genome and DNA of a shuttle plasmid, carrying the corresponding gene sequence. As described above, transcription of target genes can be controlled by early-late vaccinia virus (VACV)-specific promoter sequences (Kremer et al. 2012).

### 4.4. Immunizing properties of MVA

However, the most important characteristic that qualifies MVA as an efficient vaccine platform is its ability to stimulate strong immune responses (Greiner et al. 2006). As numerous pre-clinical and clinical studies have shown, MVA not only has the ability to activate antigen-specific antibodies and T cells (Greiner et al. 2006, Pascutti et al. 2011), it also enables early activation of the host innate immune system. These observations are probably explained by the absence of many viral immune evasion factors in the MVA genome, so that MVA-mediated immunizations can effectively activate important innate immune responses. Specifically, MVA induces type I interferons and the production of other cytokines and chemokines that stimulate the migration of immune cells to the regions of MVA inoculation, in turn activating antigen-specific adaptive immune responses (Förster et al. 1994, Büttner et al. 1995, Delaloye et al. 2009, Halle et al. 2009, Lehmann et al. 2009). Thus, MVA not only mediates antigen production, it also elicits adjuvant effects (Price et al. 2013). This may explain the strong humoral and cellular immune responses after boost-immunization studies. Even the characterization of the first recombinant MVA vector vaccine against influenza A virus H1N1 showed a highly efficient stimulation of influenza antigen-specific antibodies and cytotoxic CD8+ T cells after immunization of mice (Sutter et al. 1994). Also, the administration of relatively low doses of the

MVA vaccine showed the induction of protective immunity (Drexler et al. 2003, Kreijtz et al. 2009, Volz et al. 2014).

### 4.5. MVA-based vaccines against emerging infectious diseases

Newly emerging viruses are a serious threat to public health and have become a global concern in recent years. Zoonoses play a decisive role in these outbreaks: since 2003, highly pathogenic influenza A viruses have appeared as the causative agent of severe respiratory diseases, Ebola virus kept the world in suspense between 2014 and 2016 and MERS-CoV has pandemic potential since its first appearance in 2012 (de Jong and Hien 2006, Haagmans et al. 2016, Feldmann et al. 2020). The current SARS-CoV-2 pandemic in particular, with its drastic consequences for global health and economy, proves the need for a safe and efficacious vaccine platform.

Already advanced generation procedures, preclinical characterization and clinical testing of recombinant MVA offer the possibility of rapid development of vaccines against such emerging viral infections. Initial clinical trials have been conducted with recombinant MVA vaccines against HIV and malaria (Cosma et al. 2003, Rochlitz et al. 2003, Webster et al. 2006). No serious adverse events were reported during these clinical trials, nor in subsequent studies with different MVA influenza vaccine candidates. Furthermore, a MVA-based vaccine against the spike-protein of the Middle East respiratory syndrome coronavirus (MERS-CoV-S) showed high immunogenicity and protective efficacy in different preclinical models (Song et al. 2013, Haagmans et al. 2016). Safety and immunogenicity of this MVA-MERS-S candidate vaccine were already verified in a first phase I clinical study (Koch et al. 2020). Several MVA-based vaccine candidates also showed high immunogenicity and productive efficacy against SARS-CoV-2 in l independent preclinical studies. These are promising data in the search of suitable vaccines to combat the current global pandemic.

Of note, the only vaccine against Ebola with marketing authorization in Europe, is a combination of two different viral vectors, in which a recombinant MVA vaccine serves as a booster vaccine in a heterologous prime-boost immunization schedule after prime vaccination with an adenovirus-based vaccine (Ewer et al. 2016). This underlines the potential of MVA as a safe

vaccine platform for human infections with highly pathogenic viruses.

# IV. OBJECTIVES

Since there is no vaccine or antiviral agent against ZIKV licensed yet, the aim of this work is to investigate a possible new strategy to develop a safe and effective vaccine against this pathogen. For this purpose, this thesis describes:

1. **the generation of two recombinant MVA constructs expressing the ZIKV-nonstructural proteins NS2B and NS3$^{pro}$ (MVA-NS2B and MVA-NS3$^{pro}$)**

2. ***in vitro* characterization of recombinant MVA-NS2B and MVA-NS3$^{pro}$**

- genetic analysis
- analysis of protein expression
- replication analysis

3. ***in vivo* characterization of recombinant MVA-NS2B and MVA-NS3$^{pro}$ in IFNAR -/- mice**

- protective capacity upon challenge infection
- analysis of induced humoral immune response
- analysis of induced cellular immune response
- analysis to determine correlate of protection

# V. MATERIAL AND METHODS

## 1. Materials

### 1.1. Antibodies

**Table 1: Primary Antibodies used for Western blot analysis**

| Antibody | Dilution | Company |
|---|---|---|
| rabbit anti-ZIKV-NS2B | 1:1,000 | GeneTex, Irvine, USA |
| mouse anti-HA-Epitope-Tag | 1:1,000 | Invitrogen, Rockford, USA |

**Table 2: Secondary Antibodies used for Western blot analysis**

| Antibody | Dilution | Company |
|---|---|---|
| anti-rabbit IgG | 1:5,000 | Cell Signaling Technology, Leiden, The Netherlands |
| anti-mouse IgG | 1:5,000 | Agilent Dako, Glostrup, Denmark |

**Table 3: Primary Antibodies used for Immunostaining**

| Antibody | Dilution | Company |
|---|---|---|
| rabbit anti-VACV | 1:2,000 | Acris GmbH, Arnbruck, Germany |
| rabbit anti-ZIKV-NS2B | 1:1,000 | GeneTex, Irvine, USA |
| mouse anti-HA-Epitope-Tag | 1:1,000 | Invitrogen, Rockford, USA |

**Table 4: Secondary Antibodies used for Immunostaining**

| Antibody | Dilution | Company |
|---|---|---|
| goat anti-rabbit | 1:5,000 | Jackson Immuno Research, West Grove, USA |
| fluorescent (Alexa) goat anti-mouse | 1:1,000 | Life Technologies, Darmstadt, Germany |
| fluorescent (Alexa) goat anti-rabbit | 1:1,000 | Life Technologies, Darmstadt, Germany |

**Table 5: Antibodies used for ELISA**

| Antibody | Dilution | Company |
|---|---|---|
| rabbit anti-ZIKV-NS2B | 1:1,000 | GeneTex, Irvine, USA |
| anti-rabbit IgG | 1:5,000 | Cell Signaling Technology, Leiden, The Netherlands |
| anti-mouse IgG | 1:5,000 | Agilent Dako, Glostrup, Denmark |

**Table 6: Antibodies used for depletion of CD8+ T cells in mice**

| Antibody | Dilution | Company |
|---|---|---|
| mouse anti-CD8 | 1:7,000 | Harlan Bioproducts, Indianapolis, USA |

**Table 7: Antibodies used for Flow cytometry**

| **Antibody** | **Dilution** | **Company** |
|---|---|---|
| anti-mouse CD3 phycoerythrin (PE)-Cy7 | 1:100 | Biolegend, San Diego, California, USA |
| anti-mouse CD4 Brilliant Violet 421 | 1:6,000 | Biolegend, San Diego, California, USA |
| anti-mouse CD8α Alexa Fluor 488 | 1:1,000 | Biolegend, San Diego, California, USA |
| anti-mouse IFN-γ | 1:200 | Biolegend, San Diego, California, USA |
| anti-mouse IFN-γ plus TNF-α | 1:200 | Biolegend, San Diego, California, USA |

**Table 8: Secondary Antibodies used for Histochemistry**

| **Antibody** | **Dilution** | **Company** |
|---|---|---|
| rabbit anti-Flavi-E | 1:1,000 | Abcam, Oxford, UK, |
| goat anti-rabbit antibody | 1:200 | Burlingame, CA, USA |

## 1.2. Oligonucleotide primers

**Table 9: MVA specific oligonucleotide primers for PCR reactions**

| Primers | Sequence | Size |
|---|---|---|
| Del 1-F | 5'-CTT TCG CAG CAT AAG TAG TAT GTC-3' | 291 |
| Del 1-R | 5'-CAT TAC CGC TTC ATT CTT ATA TTC-3´ | |
| Del 2-F | 5'-GGG TAA AAT TGT AGC ATC ATA TAC C-3' | 354 |
| Del 2-R | 5'-AAA GCT TTC TCT CTA GCA AAG ATG-3' | |
| Del 3-F | 5'-GAT GAG TGT AGA TGC TGT TAT TTT G-3' | 446 |
| Del 3-R | 5'-GCA GCT AAA AGA ATA ATG GAA TTG-3' | |
| Del 4-F | 5'-AGA TAG TGG AAG ATA CAA CTG TTACG-3' | 502 |
| Del 4-R | 5'-TCT CTA TCG GTG AGA TAC AAA TAC C-3' | |
| Del 5-F | 5'-CGT GTA TAA CAT CTT TGA TAG AAT CAG-3' | 603 |
| Del 5-R | 5'-AAC ATA GCG GTG TAC TAA TTG ATT T-3' | |
| Del 6-F | 5'-CGT CAT CGA TAA CTG TAG TCT TG-3' | 702 |
| Del 6-R | 5'-TAC CCT TCG AAT AAA TAA AGA CG-3' | |
| Insert NS2B-F | 5'-CGA TAG TCG AAG ATA CAA CTG TTACG-3' | 432 |
| Insert NS2B-R | 5'-CCT CTG TCG GTG AGG TAC AAA TAC C-3' | |
| Insert NS3$^{pro}$-F | 5'-CAT GGT TAA CAT CTT TGA TGG AAT CAG-3' | 512 |
| Insert NS3$^{pro}$-R | 5'-ATC ATA GTG GTG TAA TAT TTG GTT A-3' | |
| C7L-F | 5'-CAT GGA CTC ATA ATC TCT ATA C-3' | 447 |
| C7L-R | 5'-ATG GGT ATA CAG CAC GAA TTC-3' | |

**Table 10: ZIKV specific oligonucleotide primers for qPCR reactions**

| **Primers** | **Sequence** |
|---|---|
| ZIKV-NS5-F | 5‘-CGGAGACCCTAGAGACCATTAT-3‘ |
| ZIKV-NS5-R | 5’-CATCTTCCCTATGCCCTTGTT-3´ |
| Probe | 5’-FAM/CTGGGAACAGTCTCGCTGGGAATC/BHQ1-3´ |

## 1.3. Peptides

**Table 11: Amino acid sequences of overlapping peptides used for ELISA**

| **Epitope identities** | **Amino acid sequence** |
|---|---|
| NS2B1425 | IERAGDITWEKDAEV |
| NS2B1429 | GDITWEKDAEVTGNS |
| NS2B1433 | WEKDAEVTGNSPRLD |
| NS2B1437 | AEVTGNSPRLDVALD |
| NS2B1441 | GNSPRLDVALDESGD |
| NS2B1445 | RLDVALDESGDFSLV |
| NS2B1449 | ALDESGDFSLVEDDG |
| NS2B1453 | SGDFSLVEDDGPPMR |
| NS2B1457 | SLVEDDGPPMREIIL |

**Table 12: Amino acid sequence of a ZIKV-NS2B specific epitope used for ELISPOT and FACS analysis**

| **Epitope identity** | **Amino acid sequence** |
|---|---|
| NS2B1478 | ICGMNPIAI |

### 1.4. Bacterial strain

*Escherichia coli* NEB 10-beta bacteria (New England Biolabs, Frankfurt, Germany) were used for heat-shock transformation and amplification of plasmid DNA.

### 1.5. Plasmids

**Table 13: Expression and shuttle plasmids used for generation of rMVA**

| Plasmid | Purpose | Supplier |
|---|---|---|
| pUC57-ZIKV-NS2B | cloning | Genewiz, Leipzig, Germany |
| pUC57- ZIKV-NS3$^{pro}$ | cloning | Genewiz, Leipzig, Germany |
| pIIIH5red- ZIKV-NS2B | cloning | Jan Hendrik Schwarz, LMU |
| pIIIH5red- ZIKV-NS3$^{pro}$ | cloning | Jan Hendrik Schwarz, LMU |
| pIIIH5red | cloning | Gerd Sutter, LMU |

# 2. Methods

## 2.1. Cell culture

### 2.1.1. Cultivation of permanent cells

Vero (African green monkey kidney; ATCC CCL-81) cells were maintained in Dulbecco`s Modified Eagle`s Medium (MEM) (SIGMA-ALDRICH, Taufkirchen, Germany) supplemented with 5 % heat-inactivated FBS, 1 % penicillin-streptomycin and 1 % MEM non-essential amino acid solution. Human HaCat (CLS Cell Lines Service GmbH, Eppelheim, Germany) cells were cultured in Dulbecco`s Modified Eagle`s Medium supplemented with 10 % heat-inactivated FBS, 2 % HEPES-solution (SIGMA-ALDRICH, Taufkirchen, Germany) and antibiotics as described above. All cells were maintained at 37 °C and 5 % $CO_2$ atmosphere.

### 2.1.2. Cultivation of primary cells

10-day-old chicken embryos (SPF eggs, VALO, Cuxhaven, Germany) were used for preparation of Primary chicken embryo fibroblasts (CEF) and maintained in MEM (SIGMA-ALDRICH, Taufkirchen, Germany) containing 10 % heat-inactivated fetal bovine serum (FBS) (SIGMA-ALDRICH, Taufkirchen, Germany), 1 % penicillin-streptomycin (SIGMA-ALDRICH, Taufkirchen, Germany), and 1 % MEM non-essential amino acid solution (SIGMA-ALDRICH, Taufkirchen, Germany).

### 2.1.3. Cell count

After trypsinizing, cells were diluted 1:10 with Trypan blue solution containing 0.1 % trypan blue and 0.2 % sodium azide in sodium phosphate buffer for live/death staining. Living cells were counted with a Neubauer Chamber.

## 2.2. Generation of recombinant virus

The generation of the recombinant viruses used in this study was based on the clonal MVA isolate F6, which was also used as the appropriate control in the following experiments. Analysis of viral DNA confirmed clonal genetic homogeneity in comparison to its ancestor MVA stock virus (MEYER et al., 1991).

The following viruses have been generated by homologous recombination for this study:

(a) MVA-ZIKV-NS2B (referred to as MVA-NS2B)

(b) MVA-ZIKV-NS3$^{pro}$ (referred to as MVA-NS3$^{pro}$)

### 2.2.1. Plasmid construction and transfection

Using an *in silico* approach, cDNA encoding the complete amino acid (aa) sequences of ZIKV-NS2B (415 aa) and the sequences coding for the protease portion of ZIKV-NS3 (NS3$^{pro}$) (447 aa) (Zika virus isolate Yap 2007, GenBank accession no. EU545988.1) was modified by inserting silent codon alterations to remove three termination signals (TTTTTNT) for vaccinia virus early transcription and G/C nucleotide runs. cDNA, containing fragments of ZIKV non-structural protein gene sequences, was generated by DNA synthesis (Invitrogen Life Technology, Regensburg, Germany) and cloned into the MVA transfer plasmid pIIIH5red (Kremer et al. 2012) to place the ZIKV gene sequences under the transcriptional control of the vaccinia virus early/late promoter PmH5 (Wyatt et al. 1996) finally leading to the MVA vector plasmids pIIIH5red-ZIKV-NS2B and pIIIH5red-ZIKV-NS3$^{pro}$ (Figure 4). To obtain recombinant MVA, permissive CEF (90-95 % confluent) were firstly infected with non-recombinant MVA at low multiplicity of infection (MOI=0.05) and 45 min later transfected with pIIIH5red-ZIKV-NS plasmid DNA in six-well tissue culture plates (Sarstedt, Nümbrecht, Germany) using X-tremeGENE DNA Transfection Reagent Lipofectamine (Roche Diagnostics, Penzberg, Germany). Transfected cells were harvested after 48 h and MVA-NS2B and NS3$^{pro}$ were clonally isolated by screening for the transient co-expression of the red fluorescent marker protein mCherry in plaque passages on CEF.

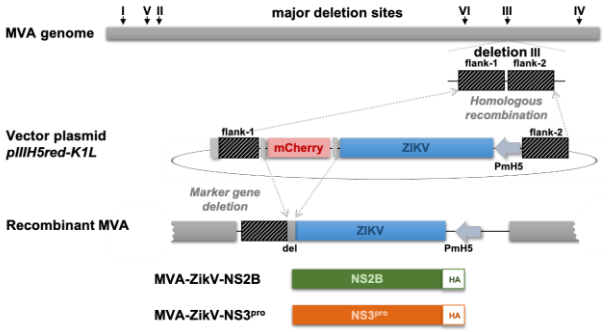


**Figure 4: Schematic depiction of the generation of recombinant MVA-NS2B and ZIKV-NS3$^{pro}$.** I-VI indicate the major deletion sites in MVA. The black boxes symbolize flank-1 and flank-2, which surround the areas of the MVA genome where the insertion site is located. In this case, deletion III was used to insert ZIKV non-structural protein gene sequences, here shown as blue boxes. The vaccinia virus early/late promoter PmH5, indicated by an arrow, guarantees control of the transcription. The mCherry gene was used for plaque picking and was removed by intragenomic homologous recombination using repetitive sequences.

### 2.2.2. Virus amplification, purification and handling

CEF cells grown in T175 cell culture flasks were used for amplification of viruses. The monolayers were infected and incubated at 37 °C for 3-4 days, respectively until cytopathic effects were clearly observed. Flasks were frozen at -20 °C until further processing.

### 2.2.3. Virus purification and handling

To enable further purification of the virus suspension in the media of infected cells, they were three times freeze-thawed prior to centrifugation at 15,000 rpm for three hours at 4 °C (Avanti J-26XP, Beckman Coulter). After discarding the supernatant, the remaining pellets were resuspended in 30 ml Tris-buffer (10 mMTris-HCl, pH 9.0). In the further course, the pellet suspension was sonicated three times for 15 seconds and vortexed between every sonication. Afterwards, the suspension was centrifuged at 1,200 rpm for five minutes at 4 °C and the supernatant was collected. To achieve higher purification, the remaining pellet was again resuspended in 5 ml Tris-buffer and the entire process was repeated 4-5 times.

For the final purification process, the collected supernatant was purified by 36 % sucrose gradient centrifugation: 15 ml sucrose was gently overlaid with 20 ml supernatant in specific plastic tubes. Tubes were centrifuged at 15,000 rpm for 90 min at 4 °C (OptimaTM LE-80K Ultracentrifuge, Beckman Coulter). After discarding the supernatant, the remaining pellets were resuspended in 2-4 ml Tris-buffer. Finally, the stocks were aliquoted in 300 µl portions in cryo-tubes and long-term stored at -80 °C.

### 2.2.4. Virus handling

For experimental use, virus stocks were thawed on ice. To avoid mutual adhesion of virus particles in aliquoted stocks, they were sonicated three times for one minute before usage.

### 2.2.5. Virus titration and immunostaining

To determine an accurate virus titer of wild-type and recombinant MVA, viruses were prepared in 10x serial dilutions steps ranging from $10^4$ to $10^9$. These dilutions were used to infect 90-95 % confluent CEF cells in 6-well tissue plates. Infected cells were incubated for 48 h and afterwards, fixed with ice-cold methanol:acetone (1:1) for 5 min. Plates were blocked with PBS (+ 3 % FBS) for 1 h at RT or 4 °C o/n. Afterwards, plates were washed 3 times with PBS. Primary antibody (anti-Vaccinia virus or anti-HA) was diluted in PBS (+ 3 % FBS) and plates were incubated for 1 h at RT. Thereafter, plates were washed 3 times with PBS. Secondary antibody (goat anti-mouse HRP) was diluted in PBS (+ 3 % FBS) and plates were incubated for 1 h at RT. Subsequently, plates were washed 3 times with PBS and TrueBlueTM Peroxidase Substrate was added to each well until staining could be observed. Titers were expressed by Plaque-forming units per ml (PFU/ml).

## 2.3. Characterization of recombinant viruses

### 2.3.1. Polymerase chain reaction (PCR)

PCR samples were obtained by infection of 90 % confluent CEF monolayers at an MOI of 5. Cells were incubated for 2 days prior harvesting and centrifugation at 13,000 rpm for 15 seconds. Viral DNA was extracted and purified out of 200 µl of resuspended supernatant using the QIAmp DNA Mini Kit (Qiagen) following the manufacturer's protocol.

Polymerase chain reaction (PCR) was performed with 50 ng of DNA (2 µl) per sample and 23 µl of PCR Master Mix.

**PCR Master mix composition:**

- 18.8 µl distilled water
- 2.5 µl buffer (10x)
- 0.5 µl dNTP's
- 0.5 µl forward oligonucleotide primer
- 0.5 µl reverse oligonucleotide primer
- 0.2 µl Dynazyme II (DNA-Polymerase)

As listed in table 9, specific oligonucleotide pairs were used for the respective PCR reaction. The corresponding thermocycling conditions for the specific PCRs were applied using the peqSTAR 2x thermocycler (PEQLAB Biotechnology GmbH).

**Table 14: Cycle conditions for Del I-VI-PCR**

| **Step** | **Temperature** | **Time** |
|---|---|---|
| Initial duration | 95 °C | 3 minutes |
| 30 cycles | 95 °C<br>57 °C<br>72 °C | 30 seconds<br>45 seconds<br>45 seconds |
| Final extension | 72 °C | 5 minutes |
| Storage | 4 °C | forever |

**Table 15: Cycle conditions for C7L-PCR**

| **Step** | **Temperature** | **Time** |
|---|---|---|
| Initial duration | 95 °C | 3 minutes |
| 30 cycles | 95 °C<br>57 °C<br>72 °C | 30 seconds<br>45 seconds<br>45 seconds |
| Final extension | 72 °C | 5 minutes |
| Storage | 4 °C | forever |

**Table 16: Cycle conditions for Insert PCR (MVA-NS2B)**

| **Step** | **Temperature** | **Time** |
|---|---|---|
| Initial duration | 95 °C | 3 minutes |
| 30 cycles | 95 °C<br>55 °C<br>72 °C | 30 seconds<br>45 seconds<br>45 seconds |
| Final extension | 72 °C | 5 minutes |
| Storage | 4 °C | forever |

**Table 17: Cycle conditions for Insert PCR (MVA-NS3$^{pro}$)**

| **Step** | **Temperature** | **Time** |
|---|---|---|
| Initial duration | 95 °C | 3 minutes |
| 30 cycles | 95 °C<br>56 °C<br>72 °C | 30 seconds<br>45 seconds<br>45 seconds |
| Final extension | 72 °C | 5 minutes |
| Storage | 4 °C | forever |

**Table 18: Cycle conditions for qPCR (ZIKV-Detection)**

| | | |
|---|---|---|
| Reverse Transcription | 50 °C | 30 minutes |
| Activation of Polymerase | 95 °C | 15 minutes |
| 42 cycles | 95°C<br>60 °C | 15 seconds<br>45 seconds |

2.3.2. Gel electrophoresis

Gel electrophoresis was used for fractionation of PCR products. For visualization of the separated fragments, Gel RedTM was added to a 1 % agarose gel. The samples were loaded onto the gel together with a molecular weight marker (1 kD) (New England Biolabs, Frankfurt am Main, Germany). TAE buffer was used as running buffer and nucleic acid was visualized with a ChemiDocTMMP Imaging system (Bio-Rad, München, Germany).

2.3.3. Multi-step analysis of virus growth

Replication capacity of MVA-NS2B and MVA-NS3$^{pro}$ was tested in one-step and multiple-step growth experiments in CEF and human HaCat cells (Boukamp et al. 1988). Amplification of recombinant MVA was done in CEF. To guarantee high titers for preclinical studies, virus stocks were purified using sucrose cushions (36 %) for ultracentrifugation. Viruses were resuspended in 10 mM Tris-HCl buffer (pH 9.0) and stored at −80 °C until usage. Viral titers were determined as previously described (Kremer et al. 2012) indicated in plaque forming units (PFU).

2.3.4. Western blot analysis of recombinant proteins

To test the expression of ZIKV-NS2B and ZIKV-NS3$^{pro}$, confluent CEF monolayers were infected at high multiplicity of infection (MOI=5) with recombinant MVA, whereas cells infected with wild-type MVA and uninfected cells (mock) served as controls. At different time points of infection, proteins were extracted from infected cells and stored at −80 °C until further investigation by Western Blot analysis. Briefly, cell proteins were separated by

electrophoresis in a sodium dodecyl sulfate (SDS)-10 % polyacrylamide gel (SDS-PAGE) and afterwards transferred to a nitrocellulose membrane by electroblotting. The membranes were blocked in a phosphate buffered saline (PBS) buffer containing 1 % (w/v) non-fat dried milk and 0.1 % Tween-20 (SIGMA-ALDRICH, Taufkirchen, Germany) detergent for 1 h and then incubated with primary antibodies, using a polyclonal rabbit anti-ZIKV non-structural 2B antibody (1:1000; GeneTex, Irvine, USA) for detection of ZIKV-NS2B and a monoclonal HA epitope tag antibody (1:7000; Invitrogen, Rockford, USA) to detect ZIKV-NS3$^{pro}$. Hereinafter, the membranes were washed with 0.1 % Tween-20 in PBS and incubated with an anti-rabbit IgG antibody (1:5000; Cell Signaling Technology, Leiden, The Netherlands), resp. anti-mouse IgG (1:5000; Agilent Dako, Glostrup, Denmark), both conjugated to horseradish peroxidase. After subsequent washing, blots were developed using SuperSignal® West Dura Extended Duration substrate (Thermo Fisher Scientific, Planegg, Gemany) prior to detecting the signal by the chemiluminescent western blot imaging system (Image Lab, Bio-Rad, Munich, Germany).

### 2.3.5. Immunostaining of MVA-ZIKV infected cells

Confluent Vero cells were infected at a low multiplicity of infection (MOI=0.01), 24 h later fixed at room temperature with 4 % paraformaldehyde for 10 min on ice and washed two times with PBS. Subsequently, cells were permeabilized using 0.1 % Triton X-100 (SIGMA-ALDRICH, Taufkirchen, Germany) solution in PBS. Hereafter, a rabbit polyclonal antibody against ZIKV-NS2B (1:1000 GeneTex, Irvine, USA) was used as well as a monoclonal HA epitope tag antibody (1:7000; Invitrogen, Rockford, US) for detecting ZIKV-NS3$^{pro}$. Fluorescent (Alexa) polyclonal rabbit/goat anti-mouse antibodies (Life Technologies, Darmstadt, Germany) were used to detect first bound antibodies. Finally, a 1 µg/ml solution of 4,6-diamidino-2-phenylindole (DAPI) (SIGMA-ALDRICH, Taufkirchen, Germany) was used for staining nuclear DNA prior of analysis of stained cultures by a fluorescence microscope (Keyence BZ-X700, Keyence, Neu-Isenburg, Germany) with a ×100 objective.

### 2.3.6. Generation of Synthetic Peptides

The protein sequence for ZIKV-NS2B was obtained from the NCBI database (ID: 6441). To detect CD8+ T cell epitopes, we used the previously described NS2B epitope $NS2B_{1478}$ (ICGMNPIAI) (Hassert et al. 2019) for identification by IFN-γ Enzyme-Linked Immunospot assay (ELISPOT). CD4+ T cell epitopes for ELISPOT analysis were identified by using the MHC II Binding tool of the T Cell Epitope Prediction analysis resource in the Immune Epitope Database (IEDB) as described previously (Dhanda et al. 2019). For coating of enzyme-linked immunosorbent assay (ELISA) plates, we generated a pool of overlapping peptides, consisting nine 15-mer sequences with a 11 amino acid overlap, covering the entire ZIKV-NS2B amino acid sequence. Synthesis of all peptides was performed by Thermo Fisher Scientific as crude material with a purity <50 % on a 1–4 mg scale. All peptides were dissolved to a concentration of 2 mg/ml in PBS, aliquoted, and stored at −20 °C until use.

## 2.4. Zika virus

### 2.4.1. Virus used for this study

ZIKV Isolate H/PF/2013 (EVAg, clinical isolate, French Polynesia 2013, GenBank Sequence Accession: KJ776791) was propagated on Vero cells and used for both *in vitro* and *in vivo* assays.

### 2.4.2. Virus handling

Since RNA viruses are vulnerable to mechanical stress and temperature changes, the viruses were only shaken gently or thawed slowly over a very long period of time for experimental use. The viruses were only handled under constant cooling during the experiments.

### 2.4.3. Virus titration

To determine infectivities of ZIKV stock viruses, seven serial dilutions of each sample were prepared (range: $10^3$-$10^8$). Dilutions were used to infect Vero cells and incubated at 37 °C and 5 % $CO_2$ for 1 h.

After the 1 h adsorption period, the virus suspension was discarded and wells were washed 3 times with PBS. Afterwards, a 1:1 solution of carboxymethyl cellulose sodium salt (CMC) and DMEM was added to each well as overlay. Plates were incubated at 37 °C and 5 % $CO_2$ for 4 days. After this incubation period, the overlay was removed and plates were washed with PBS three times. 100 µl of crystal violet solution was given to each well for plaque staining.

### 2.4.4. Plaque Reduction Neutralizing Assay

For quantification of ZIKV neutralizing antibodies, sera of mice were taken on day 18 and 36 (=8 days post challenge (dpc) after immunization and analyzed by plaque reduction neutralization test (PRNT). First, sera were heat-inactivated for 30 min at 56 °C, 2x serially diluted in 96-well plates, and 200 PFU of ZIKV strain H/PF/13 were added to the same volume of serum dilution. After incubating for 2 h at 37 °C, the mixture was used to inoculate Vero cells (80 % confluent) in 24 well plates. After 1 h, 2 % CMC diluted in demineralized water was added to each well as overlay and cells were incubated at 37 °C. After 48 h, the overlay medium was removed and crystal violet was used to stain cells for identification of plaques.

The PRNT90 titer was defined as the reciprocal of the serum dilution that reduced ZIKV plaque formation by ≥90 %.

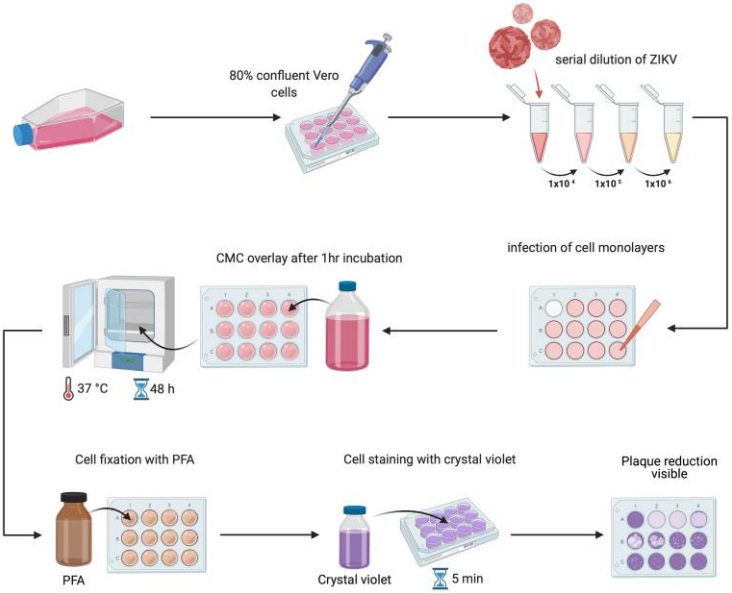


**Figure 5: Experimental scheme for Plaque reduction neutralization test (PRNT).** Titers of ZIKV neutralizing antibodies are quantified by PRNT. Created with BioRender.com

## 2.5. In vivo characterization

### 2.5.1. Mice

IFNAR-/- mice lacking the type I IFN system (Muller et al. 1994) have been backcrossed more than 20 times with C57BL/6 mice and bred under specified-pathogen-free (SPF) conditions. Mice were housed in isolated cage units (IsoCage, Tecniplast, Hohenpeißenberg, Germany) for experiments and had free access to food and water. The Government of Upper Bavaria, Munich, Germany approved all shown experiments which were performed in compliance with the German Animal Welfare Act.

### 2.5.2. IFNAR-/- challenge study

To assess the protective efficacy of recombinant MVA, ZIKV challenge studies were performed in a biosafety level 2 laboratory. In two independent experiments, mice (n = 5) were vaccinated via the intramuscular (i.m.) route into the left hind leg using 100 µl of virus suspension with a dose of $10^8$ PFU of recombinant MVA. Wild-type MVA and PBS were used as controls. 28 days after prime vaccination, mice were infected with a dose of $10^3$ foci-forming-units (FFU) of Zika virus strain H/PF/2013 diluted in 50 µl physiological saline, via footpad infection in the left hind leg. For mock vaccination, control mice (n = 5) were treated with inoculations of corresponding amounts of PBS. Mice were monitored daily for survival, weight loss and signs of illness for at least 3 weeks.

**Table 19: Clinical score for Zika virus infection**

| | | |
|---|---|---|
| **1. General condition** | shiny, smooth fur | 0 points |
| | normal posture | |
| | clear, clean eyes | |
| | good nutritional status | |
| | | |
| | slightly dull fur | 5 points each |
| | eyes moderately glued | |
| | squatting position | |
| | reduced nutritional status on palpation | 10 points each |
| | weight loss up to 20% starting weight | |
| | ruffled fur | |
| | sticky, closed eyes | |
| | emaciation visually visible | 15 points each |
| | prone position | |
| | weight loss> 20% starting weight | |
| **2. Behavior** | curious | 0 points |
| | attentive | |
| | Interested | |
| | reaction to external stimulus | |
| | normal social behavior | |
| | | |
| | unusual behavior | 5 points each |
| | hyperactive, nervous | |
| | afraid, hidden in little house | |
| | reduced, slowed response to external stimuli | |
| | | |
| | behavior caused by illness (coordination disorders, reflexes) | 10 points |
| | apathy / lethargy | 15 points |
| **3. ZIKV clinic** | reduced motor skills | 5 points each |
| | reduced reflexes | |
| | tiptoe | |
| | | |
| | hindquarters weakness / hindquarters lameness ; signs of paralysis on one of the two hind legs | 10 points each |
| | | 15 points each |
| | pronounced paralysis of the hind limbs | |

| | | |
|---|---|---|
| | tremor or staggering | |

| rating | With total points |
|---|---|
| Score 0 | 0 |
| Score 1 | 5-10 |
| Score 2 | 10-15 |
| Score 3 | 15+ |
| Score 4 | moribund or dead |

2.5.3. Depletion of CD8+ T cells

Experiments for depletion of CD8+ T cells were performed as described previously (Volz et al. 2014). Briefly, by intraperitoneal route of injection (i.p.) using 100 µg of a monoclonal anti-CD8 antibody (clone 2.43, Harlan Bioproducts, Indianapolis, IN, USA), mice were depleted of $CD8^+$ T cells on days −4; -2; −1 prior to immunization on day 0. Success of depletion was screened by flow-cytometric analysis of blood and spleen cells from depletion-antibody-treated animals.

2.5.4. Determination of ZIKV Loads in Mouse Organs

Preparation of organs from infected mice to determine the ZIKV load was performed as described earlier (Forster et al. 2020). In summary, the organs (brain, spinal cord and gonads) of sacrificed mice (n=5) were removed under aseptic conditions and stored in 2 ml tubes (Sarstedt, Nümbrecht, Germany) containing 300 µl of PBS + 20 % penicillin-streptomycin (SIGMA-ALDRICH, Taufkirchen, Germany). Samples were weighed and subsequently gently homogenized by a tissue lyser (Retsch Tissue Lyser MM300, Qiagen GmbH, Hilden, Germany) and hereinafter centrifuged for 1 min at 1500 rpm and 4 °C. The supernatants were taken and stored at –80 °C until further investigations. Viral titers in organs were determined by plaque assay as described before (Agbulos et al. 2016) and calculated in PFU per 1 g organ material. RNA from the sera of ZIKV-infected mice was extracted with the NucleoSpin® RNA Plus Kit (Macherey-Nagel, Düren, Germany). By using standard cycling conditions, ZikV RNA levels were determined by TaqMan

one-step quantitative reverse transcriptase PCR (qRT-PCR) on an AriaMx Real-Time PCR Instrument (Agilent, Santa Clara, USA). To determine the viral burden, we compared measured values in a log10 scale with a standard curve created by serial 10x dilutions of ZIKV RNA and determined readings as viral RNA equivalents per ml. The primer set used is based on sequences of ZIKV-nonstructural protein 5 of ZIKV isolate H/PF/2013, which was used for *in vivo* infection studies (SIGMA-ALDRICH, Taufkirchen, Germany).

### 2.5.5. Quantification of Total Antigen-Specific IgG Antibodies

To study antigen-specific IgG responses elicited by immunization of recombinant MVA alone or recombinant MVA plus ZIKV challenge, we examined sera of mice 18 days after immunization and 8 days after ZIKV challenge by ELISA using a peptide pool containing overlapping 15-mer peptides of ZIKV-NS2B. Flat bottom 96-well ELISA plates (Nunc™ MaxiSorp™ Plates, Thermo Scientific) were coated with 50 ng/well of peptide pools (100 µl volume) and incubated overnight at 4 °C. Plates were washed three times with 200 µl/well PBS + 0.05 % Tween (PBS/T) prior to blocking with buffer containing 1 % bovine serum albumin (SIGMA-ALDRICH, Taufkirchen, Germany) and 0.15 M sucrose (SIGMA-ALDRICH, Taufkirchen, Germany) in PBS at 37 °C. After 1 h plates were washed with PBS/T again. Sera were 3x serially diluted in PBS containing 1 % BSA (PBS/BSA) down the plate, starting at a dilution of 1:30 (100 µl volume/well) and incubated for 1 h at 37 °C. Hereinafter, plates were washed as described before and afterwards incubated with 100 µl/well goat anti-mouse IgG conjugated HRP (1:2000; Agilent Dako, Denmark) diluted in PBS/BSA for 1 h at 37 °C. Plates were then washed with PBS/T as described earlier. Next, 100 µl/well 3,3′,5,5′-Tetramethylbenzidine (TMB) Liquid Substrate System for ELISA (SIGMA-ALDRICH, Taufkirchen, Germany) was added, and plates were incubated until a color change was noticeable. To stop the reaction, 100 µl/well Stop Reagent for TMB Substrate (450 nm, SIGMA-ALDRICH, Taufkirchen, Germany) was added. Measurement of absorbance was performed on an ELISA plate reader (Tecan, Sunrise reader, Männedorf, Switzerland) at 450 nm with a 620 nm reference wavelength. Total IgG titers were calculated from the inflection point of the titration curve as logarithms of the reciprocal.

### 2.5.6. Analysis of antigen-specific $CD8^+$ T cells by enzyme-linked immunospot assay (ELISPOT)

To investigate specific CD4+ and CD8+ Tcell response induced by MVA-ZIKV-NS2B, mice were sacrificed 8 days after prime immunization and their spleens were removed. T cell responses were analyzed by ELISPOT as described before (Veit et al. 2018). After the preparation of single cell suspensions and the removal of red blood cells, splenocytes were resuspended in RPMI-10, containing RPMI-1640 (SIGMA-ALDRICH, Taufkirchen, Germany) with 10 % heat-inactivated FBS (SIGMA-ALDRICH, Taufkirchen, Germany) and 1 % penicillin–streptomycin (Sigma-Aldrich). Antigen-specific T cell responses were measured by IFN-γ ELISPOT assay using the mouse IFN-γ ELISpotPLUS kit (Mabtech, Nacka Strand, Sweden) according to the manufacturer's protocol.

Briefly, $2\times10^5$ splenocytes were seeded onto 96-well flat bottom plates (100 µl/well) (Sarstedt, Nümbrecht, Germany) and 100 µl/well of individual peptides were added (2 µg peptide/ml RPMI-10). Positive control cell cultures were treated with phorbol myristate acetate (PMA) and ionomycin (both from SIGMA-ALDRICH, Taufkirchen, Germany) or with the vaccinia virus (VACV)-specific $CD8^+$ T cell epitope $B8R_{20–27}$ (TSYKFESV) (Fiore-Gartland et al. 2016). Non-stimulated cells (mock) were used as controls. The splenocyte/peptide mixtures were added onto plates precoated with IFN-γ detection antibody and incubated at 37 °C. 48 h after incubation, the mixture was discarded and plates were processed following the kit manufacturer's protocol (Mabtech). The analysis and counting of spots were performed by using the automated ELISPOT plate reader and software as described in the manufacturer's protocol (A. EL. VIS Eli.Scan and A. EL. VIS ELISPOT Analysis Software, Hannover, Germany).

### 2.5.7. Intracellular Cytokine Staining (ICS) and Flow Cytometry (FACS)

Mice were sacrificed 8 days after prime immunization and spleens were harvested as described previously. Cells were stimulated, stained and analyzed by flow cytometry as described before (Kalodimou et al. 2019). Briefly, splenocytes were plated onto 96 well U-bottom plates at $10^6$ cells per well in a 100 µl volume. To each well, 100 µl of diluted peptides (16 µg/ml) were added

to give a final peptide concentration of 8 µg/ml. The VACV CD8 T cell epitope $B8R_{20–27}$ and PMA plus ionomycin were used as positive controls and unstimulated cells served as mock controls. After plating, cells were incubated for 2 hours at 37 ˚C before 20 µl/well of 10X Brefeldin A (Biolegend, San Diego, CA, USA) was added. Cells were then incubated for a further 4 hours at 37 °C. After the stimulation, plates were washed with FACS buffer (MACSQuant Running Buffer with 2 % FBS). Cells were then stained extracellularly for 30 min with 50 µl/well of antibody mixture containing anti-mouse CD3 phycoerithrin (PE)-Cy7 (clone 17A2, 1:100, Biolegend), anti-mouse CD4 Brilliant Violet 421 (clone GK1.5, 1:600, Biolegend), anti-mouse CD8α Alexa Fluor 488 (clone 53-6.8, 1:300, Biolegend) and purified CD16/CD32 (Fc block; clone 93, 1:500, Biolegend) diluted in FACS buffer on ice and protected from light. After staining, cells were washed with FACS buffer followed by PBS and then stained with 100 µl/well of the fixable dead cell viability dye Zombie Aqua (1:800, Biolegend) diluted in PBS for 30 minutes on ice in the dark. Cells were then washed with PBS and fixed with 100 µl/well Fixation Buffer (Biolegend) for 20 min at RT, protected from light. After fixation, cells were washed with PBS, resuspended in FACS buffer and stored overnight at 4 °C. The next day, cells were permeabilized using Intracellular Staining Permeabilization Wash Buffer (10X) (Biolegend) diluted to 1X with distilled water (1X Perm Wash buffer). Cells were stained intracellularly with 100 µl/well antibody mixture containing anti-mouse IFN-γ (clone XMG1.2, 1:200, Biolegend) and TNF-α (clone MP6-XT22, 1:200, Biolegend) diluted in 1X Perm Wash buffer for 30 min at RT, protected from light. Cells were then washed with 1X Perm Wash buffer and resuspended in FACS buffer. Prior to flow cytometry analysis, samples were filtered through a 50 µm nylon mesh (Sefar Pty Ltd, Huntingwood, NSW, Australia) into 5 ml round bottom FACS tubes (Sarstedt, Nümbrecht, Germany). Data was acquired using the MACSQuant VYB Flow Analyser (Miltenyi Biotec) and analyzed using FlowJo (FlowJo LLC, BD Life Sciences, Ashland, OR, USA).

### 2.5.8. Histopathology and Immunohistochemistry

Brain, spinal cord, gonads, uteri and epididymides of sacrificed mice were fixed in paraformaldehyde for 24 h and embedded in paraffin. Sections of 2 µm were stained with hematoxylin and eosin (HE) before being investigated by light microscopy. For immunohistochemistry (IHC), sections with 4 µm thickness

were used. After deparaffinization, sections were blocked with hydrogen peroxide followed by diluted normal goat serum (30 min). Tissue sections were stained with rabbit anti-Flavi-E antibody (1:1000; Oxford, UK) for 60 min at RT. Biotinylated goat-anti-rabbit antibody (1:200, Burlingame, CA, USA) was used as secondary antibody. Peroxidase-complexed avidin-biotin (ABC-HRP, Vector, PK-6100) and diaminobenzidine (DAB) were used for visualization and hemalaun as counterstain. Controls included chimeric rabbit IgG (abcam, AB172730, Cambridge, UK) and mixed cell cultures of ZIKV-infected and non-infected Vero cells stained with primary antibody. Images were taken with a Keyence microscope (Keyence BZ-X700, Keyence, Neu-Isenburg, Germany).

### 2.5.9. Statistical analysis

Data were analyzed using GraphPad Prism version 5.0 (GraphPad Software Inc., San Diego, CA, USA) and were expressed as mean ± standard error of the mean (SEM) unless stated otherwise. Statistical analysis was performed using one-way ANOVA and Kruskal-Wallis test to compare three or more groups. Comparison of different groups of mice was analyzed by one-way ANOVA test for the area under the curves (AUC). The threshold for statistical significance was $p < 0.05$.

# VI. RESULTS

## 1. Construction of recombinant MVAs expressing the Zika virus nonstructural proteins NS2B and NS3$^{pro}$

### 1.1. Construction of recombinant MVA-NS2B and MVA-NS3$^{pro}$

The recombinant viruses MVA-NS2B and MVA-NS3$^{pro}$ were created in chicken embryo fibroblasts (CEF), which were first infected with MVA and transfected with the shuttle plasmids pIIIH5red-NS2B and pIIIH5red-NS3$^{pro}$ (Figure 4). The specific sequences of these plasmids were chosen to allow the insertion of the ZIKV-NS2B or ZIKV-NS3$^{pro}$ gene encoding sequences into the site of deletion III within the MVA genome. To allow for a consistent quality control, the ZikV-NS3$^{pro}$ gene encoding sequence contains a tag sequence encoding nine amino acids from influenza virus hemagglutinin (HA tag) attached at the *C*-terminus of NS3$^{pro}$ since there was no NS3 protease-specific antibody available at the time of generation.

The co-expression of the red fluorescent reporter protein mCherry simplified the detection of MVA-NS2B and MVA-NS3$^{pro}$ during plaque purification. The incorporation of a short repetitive MVA-DNA sequence enabled the removal of mCherry from the genome of the final recombinant virus by intragenomic homologous recombination (see Figure 4).

## 2. Genetic characterization of constructed viruses

### 2.1. Verification of correct insertion of ZIKV genes

To verify the identity of the desired modification, standard quality control experiments were performed as described previously (Kremer et al. 2012). Polymerase chain reaction (PCR) analysis of genomic viral DNA was used to confirm the genetic identity and stability of the created MVA vector viruses. After we confirmed the integrity of MVA-NS2B and MVA-NS3$^{pro}$, we harvested plaques without mCherry fluorescence. To confirm the genetic integrity and correct insertion of the heterologous gene sequences within ZIKV-NS2B and NS3$^{pro}$ genome, we isolated viral DNA and analyzed the genome regions

adjacent to MVA Del IIII by PCR (Figure 6).

We performed additional PCRs to confirm the genetic identity and genomic stability of the MVA-NS2B and MVA-NS3$^{pro}$ by analyzing the C7L gene locus and the major deletion sites I, II, IV, V, and VI (see Figure 6, not alldata shown).

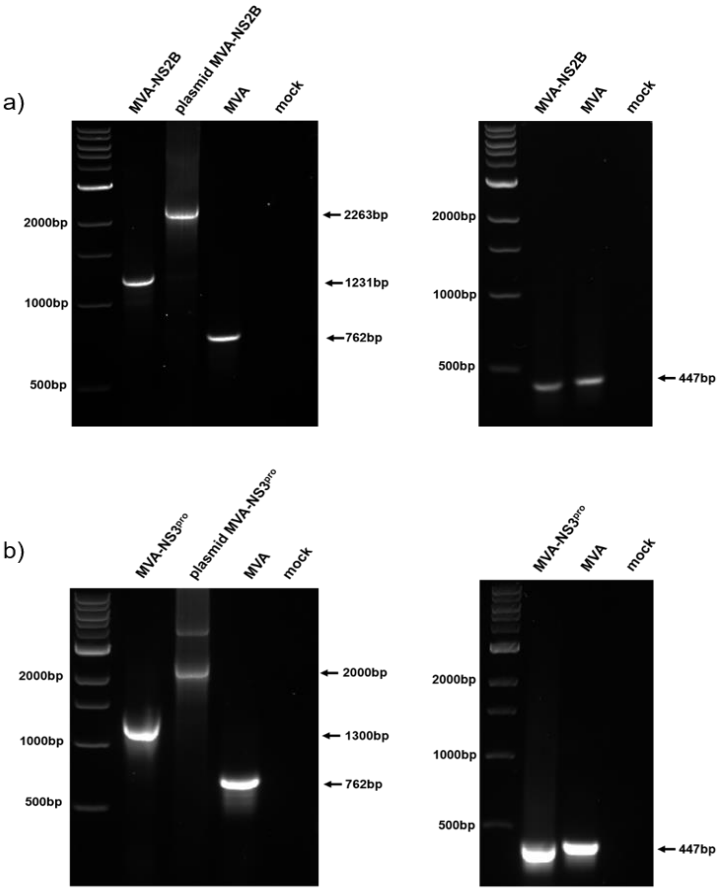


**Figure 6: Genetic stability of recombinant Modified Vaccinia virus Ankara.** (a+b) Specific PCRs for genome regions adjacent to MVA deletion site III and the C7L gene locus were performed to confirm the correct insertion of (a) recombinant ZIKV-NS2B and (b) ZIKV-NS3$^{pro}$ using isolated viral DNA of CEF infected for 24 h with viruses as indicated.

## 2.2. Multi-step growth kinetic of recombinant MVA viruses

The next step of our quality control procedure was to assess the growth of the recombinant viruses MVA-NS2B and MVA-NS3$^{pro}$ by multi-step growth analysis in different cell lines (Figure 7). We tested growth in CEF cells, which are routinely used for propagation of recombinant MVA vaccines and found that MVA-NS2B and MVA-NS3$^{pro}$ efficiently replicated to titer levels that were comparable to those of wild type MVA. As expected, the human cell line HaCat was non-permissive for productive virus growth, confirming that recombinant MVA-NS2B and MVA-NS3$^{pro}$ maintained the characteristic replication deficiency of MVA in cells of mammalian origin.

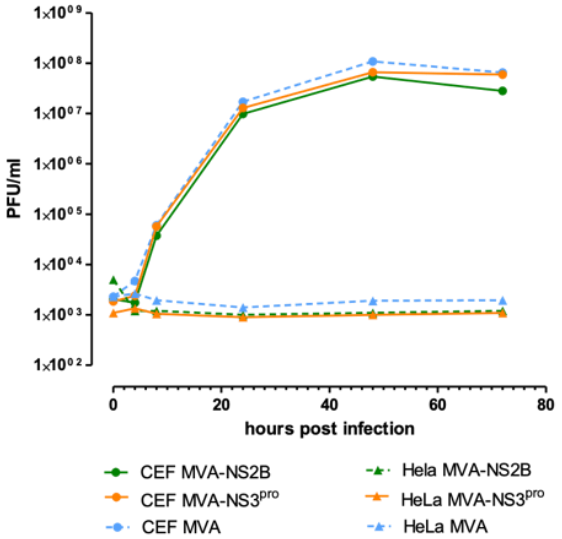


**Figure 7: Multiple-step growth analysis of recombinant MVA–NS2B and MVA–NS3$^{pro}$.** Recombinant MVA and wild-type MVA can be efficiently amplified in CEF (MOI 0.1) but fail to productively grow in human cell line HeLa (MOI 0.1).

## 2.3. Recombinant MVA viruses stably express ZIKV proteins

After determining the kinetics, we analyzed the production of recombinant NS2B and NS3$^{pro}$ protein by MVA-NS2B and MVA-NS3$^{pro}$ infected Vero cells by immunoblotting. Consistent with our expectations, we detected a ~14 kDa polypeptide using a ZIKV-NS2B-specific polyclonal antibody, as well as a 19kDa polypeptide using a HA-tag specific monoclonal antibody (Fig. 8).

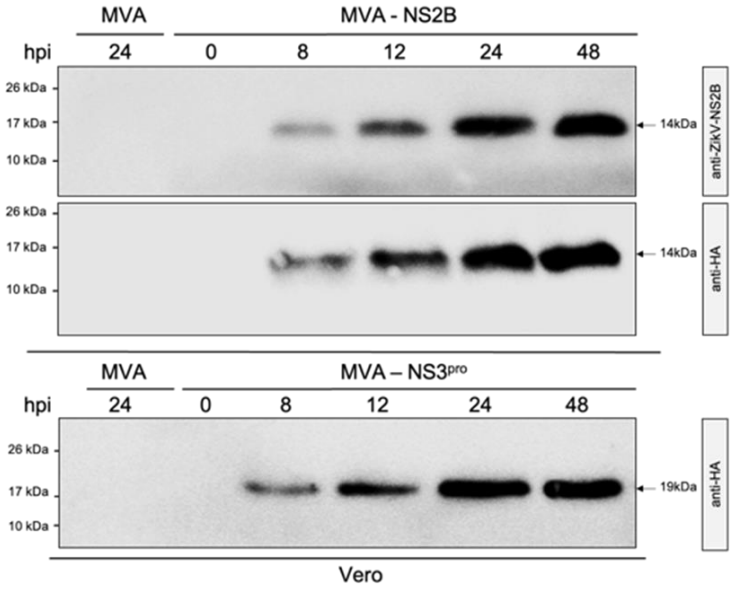


**Figure 8: Western blot analysis of recombinant Zika virus non-structural protein 2B and Zika virus non-structural protein 3 protease (ZIKV-NS2B / ZikV-NS3$^{pro}$) produced by Vero cells infected with MVA–NS2B and MVA–NS3$^{pro}$.** Cells were infected at a MOI of 5 with recombinant MVAs and harvested at indicated hours post-infection. Wild-type MVA served as control. Using a ZIKV-NS2B-specific polyclonal rabbit antibody or a monoclonal mouse HA-tag antibody for ZIKV-NS2B and ZIKV-NS3 pro, cell lysates were analyzed by immunoblotting. The recombinant proteins all show the expected molecular weights (ZIKV-NS2B: ~14 kDa and ZIKV-NS3$^{pro}$ protein: ~19 kDa).

To further investigate the synthesis of NS2B and NS3$^{pro}$ by infected cells, we analyzed the cellular localization of the recombinant proteins by immunofluorescence, which also allowed us to detect the juxtanuclear accumulation of both proteins when staining permeabilized cells. In non-permeabilized cells, however, no detection of the proteins was possible. From

both investigations, it can be concluded that NS2B and NS3$^{pro}$ are not expressed on the cell surface, which was expected (Figure 9).

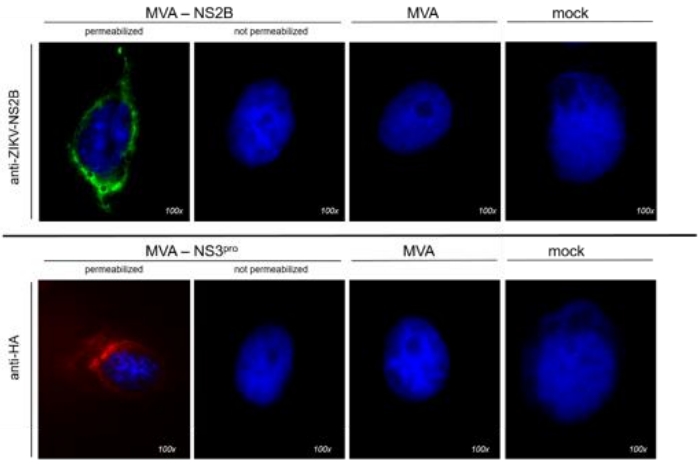


**Figure 9: Immunofluorescence staining of cells infected with MVA-NS2B and MVA-NS3 $^{pro}$.** Vero cells were infected at a MOI of 0.05 with the above viruses or wild-type MVA for 16 h. Non-infected cells (mock) served as controls. Cells were fixed, permeabilized and immunostained with rabbit polyclonal antibody for NS2B and anti-rabbit Alexa Fluor 488 (green) or with monoclonal mouse antibody for HA-tag and anti-mouse Alexa Fluor 647 (red). DAPI solution was used for staining of nuclei (blue). Panel shows representative pictures of permeabilized infected Vero cells at 100× magnification

## 3. Assessment of Immunogenicity and Protective Efficacy

### 3.1. Single dose of MVA-NS2B protects efficiently against ZIKV challenge infection

The protective capacity and immunogenicity of the candidate vaccines MVA-NS2B and MVA-NS3$^{pro}$ against ZIKV was evaluated in mice lacking the alpha/beta interferon receptor (IFNAR-/-) (Müller et al. 1994), a well-established mouse model for ZIKV disease (Lazear et al. 2016, Forster et al. 2020). Hence, we intramuscularly vaccinated six-week-old IFNAR-/- mice with our candidate vaccines or wild-type MVA as a control using a single dose of 10e8 PFU MVA vaccine. Four weeks later, the mice were subcutaneously infected with 10e3 FFU of ZIKV H/PF/13, or mock challenged with PBS. Mice were then monitored daily for signs of disease and survival. Blood was taken at day 18 and 21 before challenge to analyze neutralizing and binding antibodies in sera (Figure 10).

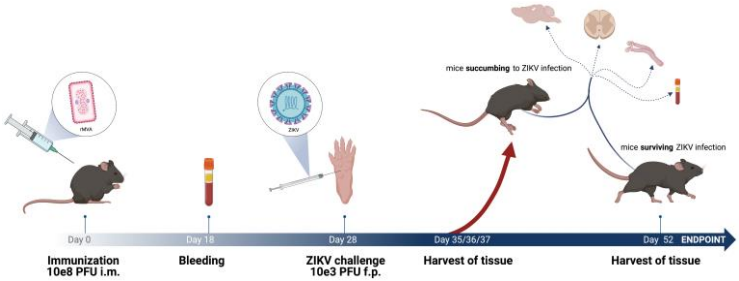


**Figure 10: Evaluation of protective capacity of MVA-based ZIKV vaccines.** Groups of IFNAR -/- mice (n=5) were i.m. vaccinated with 10e8 PFU wild-type MVA, MVA-NS2B, orMVA-NS3$^{pro}$ and sham-immunized with PBS. 28 days later mice were challenged with 10e3 PFU ZIKV via f.p. and observed for clinical symptoms and weight loss. Tissue and blood of mice which died from the ZIKV infection was subsequently harvested. Tissue and blood of mice that survived the infection was collected 28 days after ZIKV challenge. Created with BioRender.com

All animals receiving MVA-NS2B were fully protected against the ZIKV infection, showing no symptoms of disease, though a weight loss of approximately 10 % was observed during the observation period (Figure 11a; b).

However, all mice in this group fully regained their initial body weights by day 21 post-challenge according to the weights of the mock-challenged mice at this time point. This indicates that MVA-NS2B offered protection against ZIKV.

In contrast, mice treated with MVA-NS3$^{pro}$ did not show better protection than mice from the wild-type MVA control group or sham-immunized animals, demonstrating strong weight loss as well as significant signs of neurological disorders. All mice that had not received MVA-NS2B started to show conjunctivitis, reduced motility, partial limb weakness up to generalized paralysis before they died or had to be euthanized within 9 days after challenge infection (Figure 11).

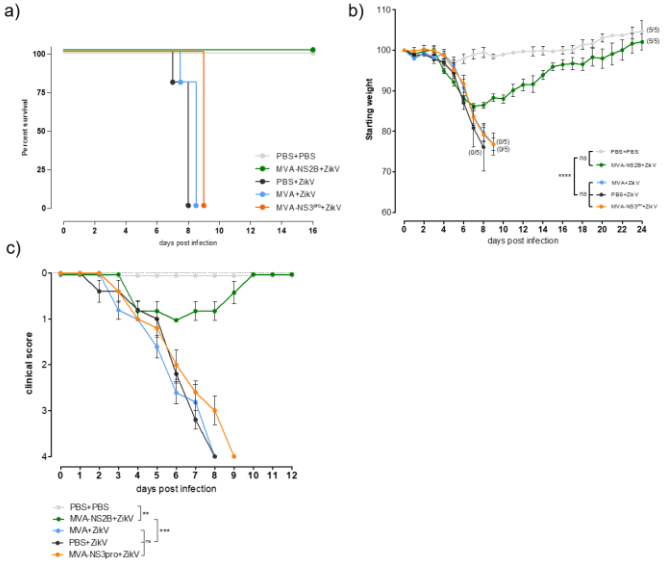


**Figure 11: MVA-NS2B mediates protection against ZIKV challenge infection.** (a) 5-6 week old IFNAR-/- mice were vaccinated with a total dose of $10^8$ PFU of recombinant MVA-NS2B, MVA-NS3$^{pro}$, wild-type MVA or saline (mock) by intramuscular application according to a prime only vaccination scheme. 28 days after immunization, mice were challenged by footpad infection with $10^3$ PFU of Zika virus H/PF/13. At the endpoint of the experiment (day 28 post challenge), the survival rate was analyzed by Mantel-Cox test, $p < 0.01$., and data are representative for two similar experiments. Data are censored at 16 days after infection. (b) Body weight was monitored daily and is expressed as a percentage of the starting weight. (c) Infected mice were monitored daily for clinical symptoms, which are shown as score, ranging from 0 (no symptoms) to 4 (moribund or dead). Error bars indicate SEMs, and the ratio of surviving/total animals are given in parentheses. Differences between individual groups were analyzed by determining area under curve (AUC) prior to analysis by one-way ANOVA test. Error bars indicate the interquartile range (IQR) from the median. Asterisks represent statistically significant differences between groups: ns = non-significant, **** $p < 0.0001$, *** $p < 0.001$, ** $p < 0.01$.

To figure out whether immunization with MVA-NS2B and MVA-NS3$^{pro}$ leads to a partial or complete elimination of ZIKV, we analyzed viral loads in the brain, spinal cord and gonads of vaccinated and mock-vaccinated mice at times of death or 21 days post challenge. Due to the neurotropism of ZIKV, these organs are particularly suitable for a reliable determination of viral load in this experiment (Miner and Diamond 2017).

The fact that we could not find any infectious ZIKV in the organs of MVA-NS2B vaccinated mice suggests that complete elimination of the challenge virus occurred. In contrast, we found high viral loads in all analyzed organs of groups immunized with MVA-NS3$^{pro}$, as well as MVA-WT and mock-vaccinated mice (Figure 12).

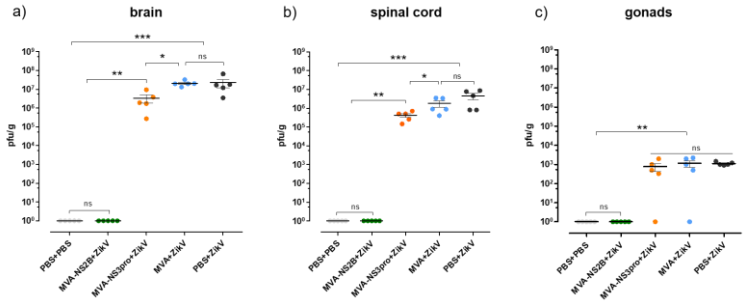


**Figure 12: MVA-NS2B vaccinated mice do not show any traces of infective ZIKV in their organs after challenge infection.** (a-c) According to the clinical score, mice were sacrificed at day 8 and 9 after challenge. (a) Brain, (b) spinal cord and (c) gonads were collected for analysis of virus loads. Organs of protected mice were analyzed 28 days after infection with ZIKV. Organs were homogenized, analyzed by plaque assay and infective viral loads were determined in plaque-forming-units (PFU). Differences between individual groups were analyzed by Kruskal-Wallis test. Error bars indicate the interquartile range (IQR) from the median. Asterisks represent statistically significant differences between groups: ns = non-significant, *** $p < 0.001$, ** $p < 0.01$, * $p < 0.05$.

Confirming the observation of a progressive disease, we have determined virus titers of 10e3 PFU ZIKV per gram in the gonads and up to 10e7 PFU ZIKV per gram in the brain of unprotected mice, comparable to the results of previous studies with ZIKV infected naive IFNAR (-/-) mice (Figure12) (Lazear et al. 2016, Elong Ngono et al. 2017, Marzi et al. 2018, Forster et al. 2020).

These results show that MVA-NS2B rapidly induces protective immunity with only a single vaccine dose, whereas MVA-NS3$^{pro}$ failed to provide protection in this mouse model.

### 3.2. Single MVA-NS2B immunization induces ZIKV specific antibody and CD8+ T cell responses

To ascertain possible correlates of protection induced by MVA-NS2B, we first analyzed neutralizing antibodies in blood, obtained 18 days after immunization and 8 days after ZIKV challenge using the PRNT90 assay.

We could not identify neutralizing antibodies in any of the tested groups on day 18 post immunization, whereas the titers of all animals noticeably increased after infection with ZIKV (virus neutralization titer of 1:512 to 1:1024), presumably induced by ZIKV, which is consistent with previous observations by others (Aid et al. 2017, Brault et al. 2017, Pérez et al. 2018) (Figure 14 a;b).

In contrast, MVA-NS2B immunization induced ZIKV-binding antibodies by day 18 after only a single application (IgG titers of 1:270 to 1:810). Eight days after the challenge infection, MVA-NS2B vaccinated mice produced higher levels of NS2B-specific antibodies, even increasing about 3- to 10-fold. Remarkably, we also could see NS2B-specific antibodies in mock vaccinated mice after infection with ZIKV (IgG titers of 1:90 to 1:270), though significantly lower than in MVA-NS2B immunized animals (Fig. 14c;d).

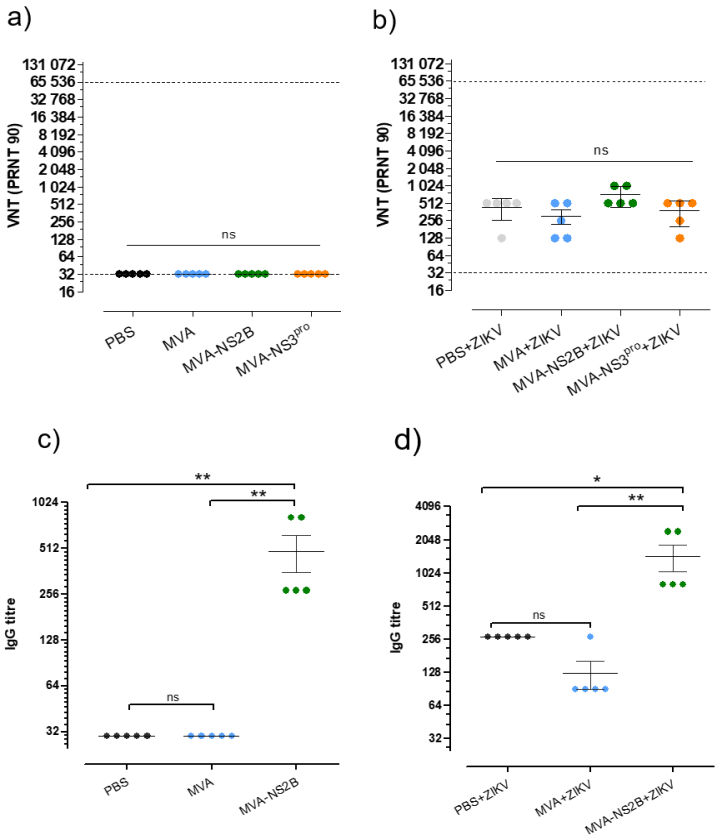


**Figure 13: Humoral immunity induced by recombinant MVA vaccines.** (a+b) Individual virus neutralization titers as determined from sera of IFNAR-/- mice vaccinated (prime only) with MVA-NS2B, MVA-NS3pro, wild-type MVA or saline (PBS) 18 days after immunization (a) and 8 days after ZIKV challenge (b). VNT is expressed as the ratio denominator only. Limit of detection is indicated by dashed lines. (c+d) ZIKV NS2B binding antibodies in IFNAR-/- mice. Sera of mice vaccinated (prime only) with MVA-NS2B, wild-type MVA or saline (PBS) were analyzed by ELISA (c) 18 days after immunization and (d) 8 days after ZIKV challenge. Differences between individual groups were analyzed by one-way ANOVA and Tukey post-hoc test. Asterisks represent statistically significant differences between two groups: ns = non-significant, * $p < 0.05$, ** $p < 0.01$

Previous studies had demonstrated that T cell immunity may play a key role in protection against flaviviruses (Shrestha and Diamond 2004, Hildner et al. 2008). Consequently, we monitored whether MVA-NS2B can induce a ZIKV-specific T cell response.

Hereby, we vaccinated mice using the same dose that we applied for the challenge experiment (10e8 PFU) and sacrificed them eight days later. We then collected their spleens, isolated splenocytes and analyzed them by IFN-γ-ELISPOT (Figure13). We detected substantial levels of NS2B-specific CD8+ T cells recognizing the previously described peptide epitope NS2B1478 (Hassert et al. 2019), with 50 to 170 NS2B specific IFN- γ-producing T cells in $10^6$ spleen cells.

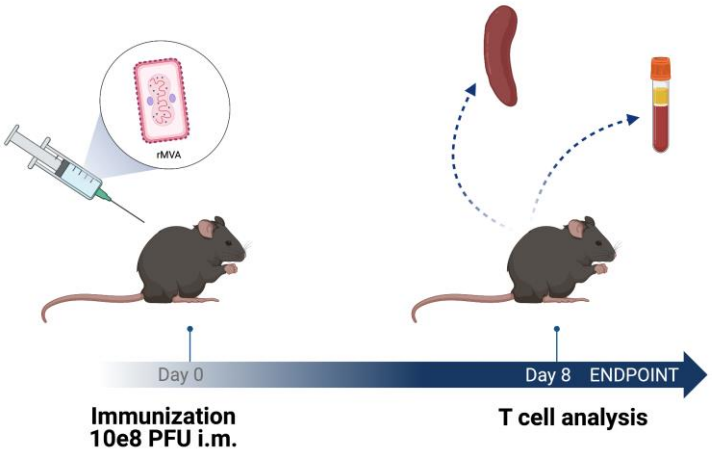


**Figure 14: Experimental scheme of prime only immunization.** Groups of IFNAR -/- mice (n=5) were vaccinated with 10e8 PFU of MVA-NS2B via the i.m. route. T cell responses were examined at day 8 post immunization. Created with BioRender.com

IFN-γ ICS analysis confirmed these findings, showing absolute numbers of IFN-γ-+CD8 T cells at a mean of 0.20 %, respectively 280 cells/10e6 splenocytes. Furthermore, we tested these splenocytes for the presence of induced ZIKV-specific CD4+ T cells stimulated with already described peptide $NS2B_{1486}$ (Hassert et al. 2018), but found no significant difference between the MVA-NS2B-vaccinated mice compared to control groups in the number of IFN producing splenocytes (Figure 15).

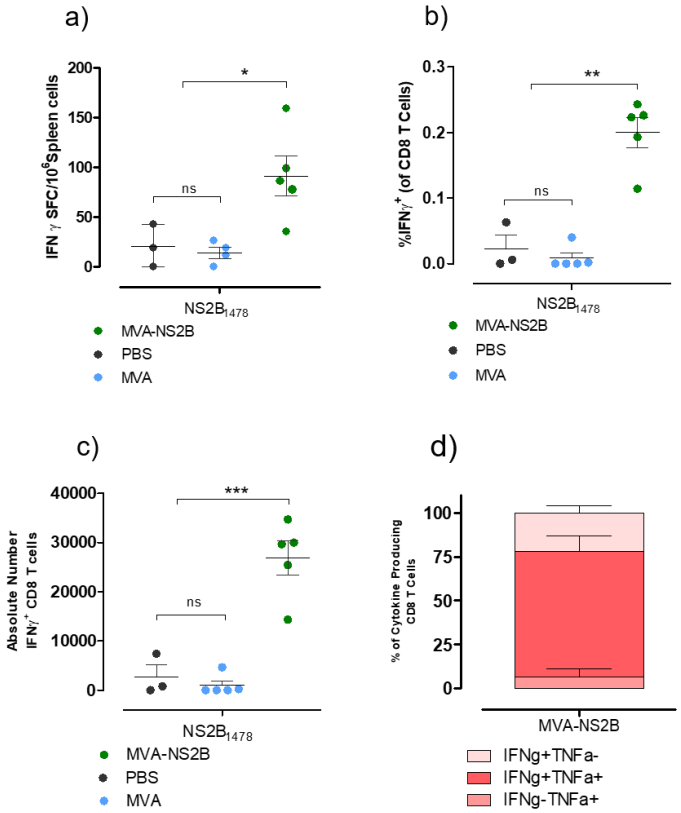


**Figure 15: Cellular immunity induced byMVA-NS2B.** (a-d) Following a prime only vaccination scheme, 5-6 week old IFNAR-/- mice were vaccinated by i.m. application with a total dose of 10e8 PFU of recombinant viruses, non-recombinant MVA and PBS. 8 days after immunization, all mice were sacrificed, splenocytes were removed and T cell analyses were carried out. (a) ZIKV NS2B-specific CD8+ T cell memory responses in IFNAR -/- mice. IFN-γ spot forming CD8+ T cells (IFN-γ SFC) were quantified by ELISPOT. (b) Frequency and (c) absolute number of antigen-specific CD8+ T cells measured by IFN-γ ICS plus FACS analysis. (d) Cytokine profile of NS2B-specific CD8+ T cells. Mean frequency of IFN-γ-TNF-α+, IFN-γ+TNF-α+ and IFN-γ+TNF-α- cells within the cytokine positive CD8+ T cell compartment are shown. Differences between individual groups were analyzed by one-way ANOVA and Tukey post-hoc test. Error bars indicate the interquartile range (IQR) from the median. Asteriks represent statistically significant differences between two groups. ns = non-significant, * $p < 0.05$, ** $p < 0.01$, *** $p < 0.001$.

These findings indicate that a prime immunization with MVA-NS2B is sufficient to elicit a significant number of ZIKV-specific antibodies and even to produce a substantial population of ZIKV-specific IFN-γ producing T cells, which both could mediate a protective capacity against ZIKV.

### 3.3. CD8+ T cells induced by recombinant MVA immunization are crucial for protection against ZIKV infection

Since we could not detect neutralizing antibodies in MVA-NS2B-vaccinated mice, we wanted to determine if CD8+ T cells elicited by MVA-NS2B are sufficient for protection as suggested in general for cytotoxic T cells in previous works on the immune response in ZIKV infections for cytotoxic T cells (Elong Ngono et al. 2017, Hickman and Pierson 2017, Hassert et al. 2018) and for ZIKV-NS2B corresponding CD8+ T cell specifities in particular (Hassert et al. 2019).

For this purpose, we chose the same vaccination and challenge infection scheme as before. On this occasion however, all mice received a monoclonal anti-CD8+ T cell depleting antibody daily for four days prior to challenge infection with ZIKV. Depletion of CD8+ T cells was confirmed by FACS analysis right before ZIKV infection (Figure 16).

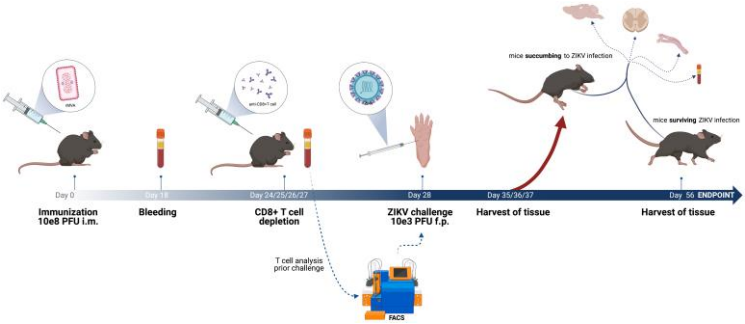


**Figure 16: Investigation of CD8+ T cell response for the protective effect of MVA-NS2B.** Groups of IFNAR-/- mice (n=5) were vaccinated with 10e8 PFU MVA-NS2B. One group of vaccinated animals received CD8+ T cell depletion treatment four days prior challenge with f.p. 10e3 PFU ZIKV. Mice were observed for clinical symptoms and weight loss. Tissue and blood of mice that succumbed to ZIKV infection were subsequently harvested. Tissue of mice that survived the infection was collected 28 days after ZIKV challenge. Created with BioRender.com

As expected, the non-depleted and MVA-NS2B vaccinated mice survived the challenge infection without any symptoms (Figure 17a). All vaccinated animals lacking CD8+ T cells however succumbed to the infection and showed neurological symptoms comparable to those observed in the depleted PBS sham-immunized group (Figure 17b,c). Remarkably, at the onset of the disease, the two groups of depleted mice showed rapidly increased disorders of the central nervous system, whereas non-depleted, mock-vaccinated mice initially exhibited predominantly disorders of the peripheral nervous system.

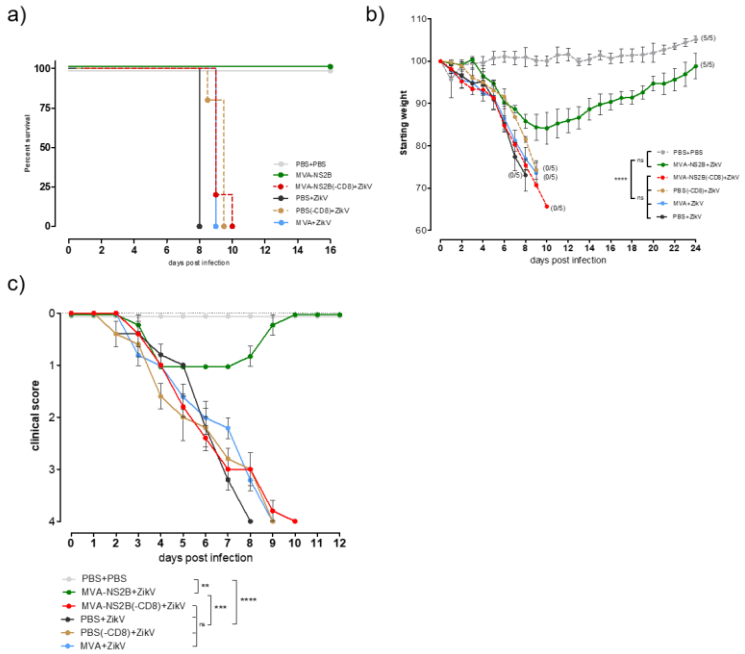


**Figure 17: Protection against Zika virus infection necessitates CD8+ T cell-mediated immunity after vaccination with MVA-NS2B.** (a) 5-6 week-old IFNAR-/- mice were depleted of CD8+ T cells before vaccinating with MVA-NS2B, wild-type MVA or PBS prior to inoculation with ZIKV strain H/PF/2013 by a subcutaneous route in the footpad. At the end of the experiment on day 28 post challenge the survival rate was analyzed by Mantel-Cox test, $p < 0.01$. Data are censored at 16 days after infection. (b) Weight progression of individual mice was monitored daily and is expressed as percentage of body weight. (c) Infected mice were monitored daily for clinical symptoms, expressed as a score from 0 (no symptoms) to 4 (moribund or dead). Data are representative for two similar experiments. Error bars indicate SEMs, and the ratio of surviving/total animals is given in parentheses. Differences between individual groups were analyzed by determining area under curve (AUC) prior to analysis with one-way ANOVA test. Error bars indicate the interquartile range (IQR) from the median. Asterisks represent statistically significant differences between groups: ns = non-significant, **** $p < 0.0001$, ** $p < 0.01$, *** $p < 0.001$

These observations also correlate with the viral loads we detected in the target organs at times of death. Impressively, mean virus titers in tissue of CD8+ T cell depleted animals ranged from 10e5 PFU in the gonads, up to 10e8 PFU in the brains and thus is 10 to 20 times higher compared to the unprotected groups that did not receive CD8+ T cell depletion treatment (Figure 18). While the

differences of viral loads in brain and spinal cord within the CD8+ T cell depleted and MVA-NS2B or PBS vaccinated groups did not differ significantly, clearly less challenge virus was detected in the gonads of the MVA-NS2B vaccinated group. Again, in the organs of MVA-NS2B-vaccinated and surviving mice, we failed to detect infectious virus 21 days after challenge.

In addition, we used qPCR to daily test the blood for viral loads after challenge infection, finding noticeable differences between the groups comparable to the data above. Three days after infection, the mean viral load in the blood was almost 10 times higher for all CD8+ T cell-depleted animals compared to all other groups (Figure 18).

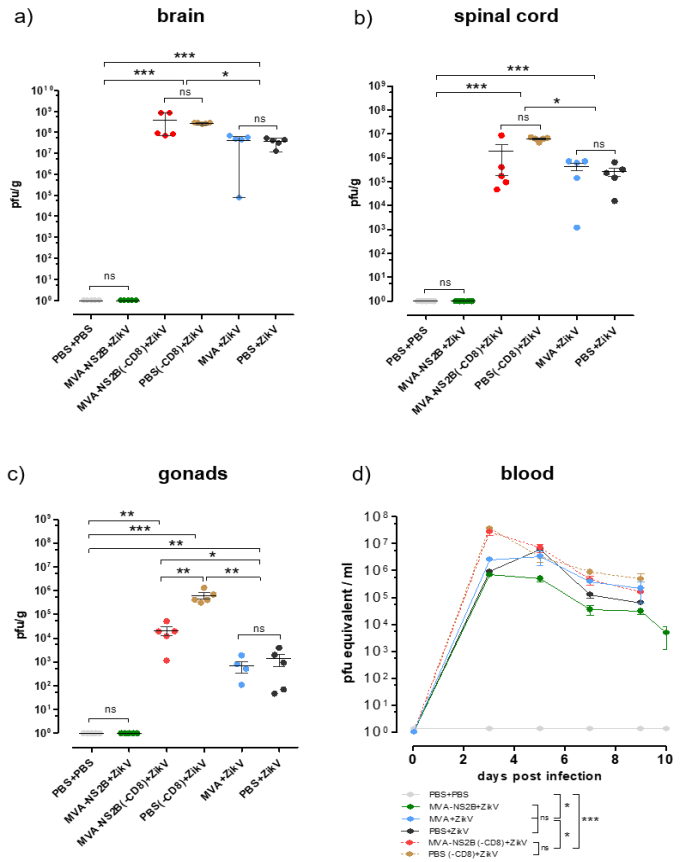


**Figure 18: Lack of cellular immune response leads to increased viral loads after ZIKV challenge.** (a) Brains, (b) spinal cord and (c) gonads of all mice were removed at the time of death, respectively the end of the experiments (day 28 p.i. for not depleted MVA-NS2B-vaccinated mice). Zika virus titers were analyzed by plaque assay and determined in PFU. Differences between individual groups were analyzed by Kruskal-Wallis test. Error bars indicate the interquartile range (IQR) from the median. Asterisks represent statistically significant differences between groups: ns = non-significant, *** $p < 0.001$. ** $p < 0.01$. * $p < 0.05$. (d) Blood was harvested on day 3, 5, 7, 9 and 10 after Zika virus infection from IFNAR −/− mice and viral RNA levels were determined by qRT-PCR to illustrate viremia. Differences between individual groups were analyzed by determining area under curve (AUC) prior to analysis with one-way ANOVA test. Error bars indicate the interquartile range (IQR) from the median. Asterisks represent statistically significant differences between groups: ns = non-significant, **** $p < 0.0001$.

Moreover, we performed histological analyses of brain, spinal cord and gonads. Organs from non-protected groups showed extensive ZIKV-specific staining, primarily in areas of the hypothalamus of inflamed brains. Both CD8+ T cell-depleted groups showed increased ZIKV-specific staining compared to the non-depleted groups in severely inflamed brain tissue. Immunohistochemical staining of organs from MVA-NS2B-vaccinated, non-depleted mice failed to detect ZIKV infected cells, indicating complete clearance of the virus 28 days after challenge (Figure 19).

Accordingly, a lack of CD8+ T cells increased susceptibility to ZIKV infection in MVA-NS2B vaccinated mice. Overall, the results of these studies confirmed the generation of ZIKV-specific CD8+ T cells as a correlate of protection for MVA-NS2B vaccination.

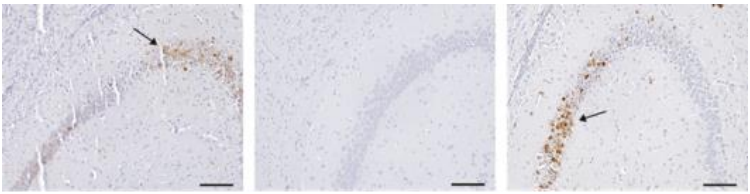


**Figure 19: Protection against Zika virus infection necessitates CD8+ T cell-mediated immunity after vaccination with MVA-NS2B.** Immunohistochemical analysis of brains from MVA-NS2B vaccinated IFNAR-/- mice with and without CD8+ T cell depletion and wild type MVA vaccinated IFNAR-/- mice after ZIKV challenge. At day of death, respectively the end of the experiments, sections of tissues were immunostained (IHC) with a monoclonal mouse antibody raised against the envelope protein of Zika virus to detect the presence of ZIKV antigen. Bars: 100 µm. The depicted sections show representative areas of brain all three groups.

# VII. DISCUSSION

Severe complications during pregnancy, devastating congenital abnormalities, together with neuropathies in adults caused by a Zika virus infection underline the indispensable development of a safe vaccine against this pathogen. Although the number of ZIKV infections clearly decreased in recent months (Organization 2019), the pandemic has highlighted the dangers of flaviviruses and the challenges they pose for vaccine development.

Here, we developed experimental ZIKV vaccines based on the highly attenuated vaccinia virus vector MVA expressing the ZIKV non-structural proteins 2B and $3^{pro}$. In this study, we investigated whether these ZIKV proteins can provide protective efficacy as antigenic components of a vaccine. We showed that MVA-NS2B induced robust humoral and cellular immune responses directed against the ZIKV non-structural protein 2B and was protective in a ZIKV challenge model using susceptible type I interferon-deficient mice. In contrast, MVA-$NS3^{pro}$ showed no protective properties in this model and was therefore not investigated in further detail. Notably this is the first study of a MVA-based vaccine expressing the nonstructural proteins NS2B and $NS3^{pro}$ of ZIKV.

**Challenges and requirements for vaccines against flaviviruses**

*In vitro* studies showed evidence of enhanced immunity between ZIKV and DENV (Dejnirattisai et al. 2016, Kawiecki and Christofferson 2016). Furthermore, the transfer of DENV and WNV convalescent plasma into ZIKV-susceptible mice led to increased morbidity and mortality after challenge infection (Bardina et al. 2017). Moreover, current prospective pediatric cohort studies show critical immunological interactions among ZIKV and different DENV serotypes. These findings suggest both protective and pathogenic interactions between DENV and ZIKV, that could affect efficacy and safety of existing vaccines and vaccines under development (Katzelnick et al., 2020). This is highly relevant since the majority of candidate vaccines against ZIKV, which have just now entered phase I and II clinical trials, predominantly incorporate structural proteins as key humoral targets, which in turn have the potential to cause ADE (Dejnirattisai et al. 2016, Kawiecki and Christofferson

2016, Bardina et al. 2017, Wilder-Smith et al. 2018). These insights must be taken into consideration, and large-scale Phase II and III clinical trials of these candidate vaccines must first demonstrate actual safety and prove that such adverse effects of vaccination cannot occur.

In contrast to humoral response, components of the cellular immune response have so far not been associated with ADE. CD8+ T cells have been confirmed as a primary cell type involved in the elimination of pathogens from tissue during flavivirus infections (Shrestha and Diamond 2004, Elong Ngono et al. 2017), thus providing effective virus clearance in neurons. However, the antiviral activity of cytotoxic T cells in the brain has also been shown to trigger ZIKV-associated paralysis and may therefore also pose a risk (Jurado et al. 2018). Therefore, it is essential to gain a more sophisticated understanding of the relevant components of the immune system that correlate with the best protective effects in ZIKV virus infection. This would enable us to find other potential virus antigens to improved vaccination strategies.

Nevertheless, the ideal vaccine against ZIKV should not only protect against ZIKV and prevent risks of ADE. Immunocompromised patients, the elderly and in particular pregnant women and children need special consideration. Furthermore, a vaccine should be inexpensive to produce, effective against the most common ZIKV strains and protective after a single application.

**MVA as a suitable platform for ZIKV vaccines**

MVA as a viral platform combines all the properties required for developing a vaccine that is safe, efficacious, cost-effective and prevents the risk of ADE. In terms of vaccine design which should strongly target the induction of a cellular immune response, the ability of MVA as a live vaccine to infect cells and induce intracellular expression of the corresponding antigen is a huge advantage (Draper and Heeney 2010). In particular, the fact that this virus efficiently infects antigen-presenting cells seems to play a crucial role in the activation of T cells (Altenburg et al. 2017). The *de novo* synthesis of antigenic proteins during the viral replication cycle within the host cell enables the processing and presentation of the antigens within MHC class I molecules. Thus, MVA efficiently induces antigen-specific CD8+ T cell responses (de Vries and

Rimmelzwaan 2016, Altenburg et al. 2017). In addition, MVA can efficiently induce antigen-specific antibodies thereby making it capable of stimulating a balanced immune response. Remarkably, these foreign antigens are expressed in their native conformation, or can be expressed exactly according to the corresponding antigen design (de Vries and Rimmelzwaan 2016). This guarantees a very specific and efficient immune response against the respective pathogen.

With regard to the characteristics necessary for the development of a safe ZIKV vaccine, MVA is especially suitable because it has successfully been used in immunocompromised and pregnant individuals. This concerns both studies for the approval of MVA as a vaccine against smallpox, as well as several phase I to III studies of recombinant MVA-based vaccines against infectious pathogens, which also included elderly people and HIV patients as subjects showing no adverse side effects associated with the vaccination (Harrer et al. 2005, Vollmar et al. 2006). Moreover, MVA showed no fetotoxic effect in studies of pregnant rats (Carroll and Moss 1997).

The fact that MVA is approved as a stand-alone vaccine against smallpox (Vollmar et al. 2006) or that a recombinant MVA-based vaccine has already been approved for immunization against Ebola (Ewer et al. 2016) proves that MVA also qualifies as a vaccine platform from an economic point of view. The corresponding industrial know-how and large-scale production capabilities are therefore sufficiently available. Moreover, since MVA shows little titer loss at room temperature, even without special cooling, this feature could facilitate its potential use in warmer regions without the ability to sufficiently maintain a cold chain compared to other, more heat-sensitive vaccines. This characteristic is crucial for the use of a vaccine against ZIKV in the predominantly warm regions where this virus is endemic.

**ZIKV-NS2B/NS3$^{pro}$ as target for vaccine developement**

Taken into account the issue of ADE, a possible approach for development of novel vaccines is considering certain non-structural proteins of ZIKV. Of note, using nonstructural protein 1 as antigen for vaccination in different studies showed strong humoral and cellular responses and it delivered protective capacity (Brault et al. 2017, Lai et al. 2017, Li et al. 2018). Although these applications are promising, further research on other nonstructural-based candidate vaccines is needed.

As described earlier, the NS2B-NS3 protease-complex plays a crucial role in the post-translational cleavage of the viral polyprotein that is required to produce viral progeny (Hill et al. 2018). The *N*-terminal part of the NS3 protein (NS3$^{pro}$), harboring the catalytic triad, forms the chymotrypsin-like viral protease (Phoo et al. 2016, Hilgenfeld et al. 2018). To ensure correct folding, enzymatic activity and sufficient substrate binding, the protease requires the nonstructural protein 2B as cofactor (Chambers et al. 1990, Falgout et al. 1991, Stocks and Lobigs 1998, Li et al. 2018). Thus, the essential role of the NS2B/NS3 protease complex in replication of flaviviruses makes it one of the most promising targets in antiviral drug research and should also be considered for vaccine design (Kang et al. 2017).

In terms of its ability to be used as part of a broad-spectrum flavivirus antiviral agent, the NS2B/NS3 complex may offer previously unappreciated opportunities, at least as a component of novel vaccine design (Barrows et al. 2016, Xu et al. 2016). This assumption is not only based on the fact that the protease-complex plays a very decisive role in virus replication, it also exhibits several vulnerabilities that potential vaccines or drugs can target. Moreover, this protease has a high sequence similarity between different flaviviruses (80 %), which could be advantageous in terms of a cross-reactive effect of a broad-range anti-flaviviral agent (Kang et al. 2017).

A few vaccine designs have also taken the ZIKV protease into account. For example, virus-like particle (VLP)-based vaccines have been described, in which the expression of NS2B/NS3$^{pro}$ aimed to facilitate the processing of co-expressed CprME, thereby leading to self-assembly and release of VLPs.

However, none of these studies have considered our approach to investigate any direct influence of single protease components on immunogenicity or protection (Stocks and Lobigs 1998, Boigard et al. 2017, Garg et al. 2019).

**ZIKV-NS2B and ZIKV-NS3$^{pro}$ are expressed in a native state by MVA**

MVA is a suitable platform for investigating new and different approaches to ZIKV vaccines, as it allows for the analysis of target antigens in an experimental vaccine model. MVA is able to express high levels of ZIKV NS2B and NS3$^{pro}$, as shown in western blot and immunofluorescence analyses.

This important property is due to the use of the modified VACV early/late promoter H5 (mH5) (Wang et al. 2010), which is thought to induce potent gene expression that persists throughout the replication cycle and contains a particularly strong early component. The high early gene expression is known to be beneficial for the initiation of a cellular immune response (Wyatt et al. 1996) and thus purposeful for the vaccine-design we aimed at. Immunofluorescence assays show that ZIKV-NS2B and ZIKV-NS3$^{pro}$ expressed by MVA are not present on the surface of infected cells. This indicates that the proteins are not packaged into ZIKV virions, just as in native processing.

**Single dose of MVA-NS2B protects against ZIKV challenge infection**

We found that ZIKV-NS2B induces protection against lethal ZIKV infection in our model system. Using IFNAR-/- mice, a single dose of the candidate vaccine MVA-NS2B provided substantial protection even in the absence of detectable neutralizing antibodies. Moreover, no detectable ZIKV was observed in the organs of MVA-NS2B vaccinated animals after challenge infection, indicating that a single vaccination is sufficient to eliminate the virus. By contrast, ZIKV-NS3$^{pro}$, offered no protective capacity. Challenged mice immunized with MVA-NS3$^{pro}$ developed Zika disease and showed high viral loads in organs. The observations may be due to the fact that ZIKV-NS2B is required for both correct folding and catalytic activity of the protease (Phoo et al. 2016, Kang et al. 2017, Li et al. 2018) and therefore is a crucial target for inhibiting the complete enzyme, which in turn inhibits viral replication. ZIKV-NS3$^{pro}$ is consequently inactive without its co-factor and has no significance as a single antigen for immune response. The protective effect of ZIKV-NS2B can be explained not

only by its role in viral replication but also in pathogenesis. Aguirre et al. described, that DENV NS2B/NS3 protease counteracts the type-I interferon response via digesting the stimulator of interferon genes (STING) in dendritic cells (Aguirre et al. 2012). Since ZIKV also permissively infects this cell type, the catalytic activity of ZIKV-NS2B/NS3$^{pro}$ could also cause cleavage of STING, leading to an enhanced suppression of the host innate immune response. Thus, immune responses directed against ZIKV-NS2B could also inhibit the function of the protease, thereby delivering a protective effect.

**MVA-NS2B induces strong humoral and cellular immune response**

As ZIKV-virions do not contain any non-structural proteins, it can be assumed that antibodies against NS2B will not neutralize ZIKV. This property makes the protein a valuable alternative antigen for vaccine development, as it could potentially avoid the risk of ADE. Indeed, we were only able to detect neutralizing antibodies after, but not prior ZIKV challenge infection. From these observations, it can be concluded that the induction of neutralizing antibodies in this study setup is conveyed by the infection with the challenge virus itself and is probably directed against the structural proteins of the virus and not an effect of the vaccination with MVA-NS2B. In contrast, MVA-NS2B elicited high levels of ZIKV-NS2B specific antibodies, which may contribute to protection at low level, perhaps through antibody-dependent cell-mediated cytotoxicity (Ochoa et al. 2017).

Numerous studies show that CD8+ T cells play a crucial role in protectivity against ZIKV (Pardy et al. 2017, Ricciardi et al. 2017, Wen et al. 2017). Moreover, Hassert et al. identified a novel ZIKV CD8+ T cell epitope of NS2B that could be a target for cytotoxic T cells and postulated the possibility of an associated protective capacity (Hassert et al. 2019).

This suggests that the CD8+ T cell response induced by MVA-NS2B could be a major correlate of protection associated with this vaccine. This is substantiated by the fact that MVA-NS2B vaccinated IFNAR-/- mice depleted of CD8+ T cells remained completely unprotected and their organs contained even higher virus loads than those of unprotected, sham-vaccinated control mice. Perhaps, these observations indicate the efficacy of a developing CD8+ T cell

response to control ZIKV infection in naive IFNAR-/- mice, reflecting the observations of Jurado et al. in CD8+ T cell depleted IFNAR -/- mice (Jurado et al. 2018). The lower viral loads in the gonads compared to the depleted sham-immunized group is the only indication that ZIKV-NS2B-specific antibodies may have contributed to a reduction of the challenge virus beyond the effect of the cellular immune response.

**Future perspective**

The poor induction of DENV-specific T cells by a recently licensed DENV vaccine is suggested to be the reason for its low efficacy (Scherwitzl et al. 2017). This problem demonstrates the importance of developing a ZIKV vaccine that aims to induces both arms of the adaptive immune system. Although humoral immune responses play an important role in reducing viremia (Hurtado-Monzón et al. 2020), it is essential to study the protective capacity of T cells in ZIKV infection in more detail. Thus, a vaccine that can stimulate both humoral and cellular responses may not just be more efficient, but could also potentially avoid ADE, as several studies have suggested (Elong Ngono et al. 2017, Rivino and Lim 2017, Ngono and Shresta 2018).

The potent ZIKV-specific CD8+ T cell mediated immunogenicity induced by MVA-NS2B warrants further investigation to determine if ZIKV-NS2B is a suitable vaccine antigen. Nevertheless, it should be noted that our study showed that NS2B cannot serve as the sole antigenic component of a future vaccine. This is particularly demonstrated by the fact that MVA-NS2B does not elicit neutralizing antibodies and mice show moderate weight loss after challenge with ZIKV. However, MVA-NS2B could be a promising component of a vaccine that targets two or more ZIKV antigens. In addition, the strong T cell response of MVA-NS2B should be further analyzed in the mouse pregnancy model of ZIKV, as pregnant mice show a decreased CD8+ T cell response in general (Winkler et al. 2017).

# VIII. SUMMARY

More than sixty years after its discovery in Africa, Zika virus (ZIKV) has been associated with congenital malformations in infants and Guillain-Barré syndrome in adults during outbreaks in the South Pacific and Latin America. Even five years after the WHO declared a "Public Health Emergency of International Concern" due to these outbreaks, there is still no approved medication, nor licensed vaccination against this pathogen. Since the risk of further outbreaks is also very high in the Western Hemisphere, the development of a safe and effective vaccine is essential. Previous approaches to ZIKV vaccine development have focused on structural proteins to elicit neutralizing antibodies, although numerous studies have shown that stimulation of a suboptimal humoral immune response can lead to severe flavivirus-related disease through the phenomenon of antibody-dependent enhancement. However, little is known about the role of nonstructural proteins in ZIKV-specific immune response and protection.

This work investigates an alternative strategy of immunization involving the two components of the ZIKV protease NS2B and $NS3^{pro}$ by using the live attenuated Modified Vaccinia virus Ankara (MVA) as vector. Growth characterizations of newly generated candidate vaccines showed replication deficiency in mammalian cells, as well as high level genetic stability upon large scale amplification. Further, immunoblot analyses demonstrated robust expression of both antigens. Remarkably, the recombinant MVA expressing the entire ZIKV-protease $NS3^{pro}$ showed no protective potential, whereas a single vaccination with the cofactor NS2B as antigen induced a protective T cell response in an established mouse model for ZIKV challenge infection. The MVA-NS2B vaccine did not induce neutralizing antibodies but elicited CD8+ T cells that prevented death in lethally infected mice.

These results contribute to a better understanding of the involvement of CD8+ T cells in protection against ZIKV and thus to improve future flavivirus vaccine design.

# IX. ZUSAMMENFASSUNG

Mehr als sechzig Jahre nachdem das Zika Virus (ZIKV) seiner Entdeckung in Afrika, wurde das Virus bei Ausbrüchen im Südpazifik und in Lateinamerika mit kongenitalen Fehlbildungen bei Säuglingen und dem Guillain-Barré-Syndrom bei Erwachsenen in Verbindung gebracht. Auch fünf Jahre nachdem die WHO aufgrund dieser Ausbrüche einen „Öffentlichen Gesundheitsnotstand internationalen Ausmaßes“ ausgerufen hatte, gibt es noch immer weder ein zugelassenes Medikament, noch eine zugelassene Impfung gegen diesen Erreger. Da das Risiko weiterer Ausbrüche zwischenzeitlich auch in der westlichen Hemisphäre sehr hoch ist, stellt die Entwicklung eines sicheren und wirksamen Impfstoffs weiterhin eine unerlässliche Aufgabe für die weltweite Wissenschaftsgemeinde dar. Um Impfstoffe zu entwickeln, die hohe Titer neutralisierender Antikörper induzieren, fokusieren sich bisherige Ansätze zur Entwicklung von ZIKV-Impfstoffen auf Strukturproteine als Antigene. Jedoch haben zahlreiche Studien gezeigt, dass die Anregung einer suboptimalen humoralen Immunantwort bei der Infektion mit Flaviviren durch das Phänomen infektionsverstärkender Antikörpern (antibody-dependent enhancement, ADE) zu einem schweren Krankheitsverlauf führen kann. Zugleich ist jedoch wenig über die Rolle von Nicht-Strukturproteinen bei der ZIKV-spezifischen Immunantwort und deren möglichen Interaktion bei einer Schutzwirkung bekannt.

Diese Arbeit untersucht eine alternative Strategie der Immunisierung, bei der das Modifizierte Vaccinia virus Ankara (MVA) als Vektorimpfstoff für die der beiden Antigen-Komponenten der ZIKV-Protease NS2B und NS3$^{pro}$ dient. Virologische Untersuchungen der neu generierten Impfstoffkandidaten belegten deren Unfähigkeit sich in Säugetierzellen zu vermehren, sowie deren hohe genetische Stabilität bei der Vermehrung in für die Impfstoffproduktion geeigneten Zellkulturen. Weiterhin konnten Immunoblot-Analysen eine robuste Expression der beiden Antigene nachweisen. In einem etablierten Mausmodel zur Untersuchung der Pathogenesemechanismen nach ZIKV-Infektion wies bemerkenswerterweise jener Impfstoffkandidat, der die gesamte ZIKV-Protease NS3$^{pro}$ exprimiert, keine Schutzwirkung auf. Dagegen vermittelte eine einzige Impfung mit NS2B, dem Kofaktor der Protease, einen vollständigen

Schutz gegen eine letale Belastungsinfektion mit ZIKV. Der MVA-NS2B-Impfstoff induzierte zwar keine neutralisierenden Antikörper, rief aber CD8+ T-Zellen hervor, die essentiell waren, um eine schwere Erkrankung der mit ZIKV infizierten Mäuse zu verhindern.

Diese Ergebnisse tragen zu einem besseren Verständnis der Beteiligung von CD8+ T-Zellen an der Schutzwirkung gegen ZIKV und damit zur Verbesserung eines zukünftigen Designs von Flavivirus-Impfstoffen bei.

# X. REFERENCES

Abrams, R. P. M., J. Solis and A. Nath (2017). "Therapeutic Approaches for Zika Virus Infection of the Nervous System." Neurotherapeutics **14**(4): 1027-1048.

Adebanjo, T., S. Godfred-Cato, L. Viens, M. Fischer, J. E. Staples, W. Kuhnert-Tallman, H. Walke, T. Oduyebo, K. Polen, G. Peacock, D. Meaney-Delman, M. A. Honein, S. A. Rasmussen and C. A. Moore (2017). "Update: Interim Guidance for the Diagnosis, Evaluation, and Management of Infants with Possible Congenital Zika Virus Infection - United States, October 2017." MMWR Morb Mortal Wkly Rep **66**(41): 1089-1099.

Agbulos, D. S., L. Barelli, B. V. Giordano and F. F. Hunter (2016). "Zika Virus: Quantification, Propagation, Detection, and Storage." Curr Protoc Microbiol **43**: 15d.14.11-15d.14.16.

Aguirre, S., A. M. Maestre, S. Pagni, J. R. Patel, T. Savage, D. Gutman, K. Maringer, D. Bernal-Rubio, R. S. Shabman, V. Simon, J. R. Rodriguez-Madoz, L. C. Mulder, G. N. Barber and A. Fernandez-Sesma (2012). "DENV inhibits type I IFN production in infected cells by cleaving human STING." PLoS Pathog **8**(10): e1002934.

Aid, M., P. Abbink, R. A. Larocca, M. Boyd, R. Nityanandam, O. Nanayakkara, A. J. Martinot, E. T. Moseley, E. Blass, E. N. Borducchi, A. Chandrashekar, A. L. Brinkman, K. Molloy, D. Jetton, L. J. Tartaglia, J. Liu, K. Best, A. S. Perelson, R. A. De La Barrera, M. G. Lewis and D. H. Barouch (2017). "Zika Virus Persistence in the Central Nervous System and Lymph Nodes of Rhesus Monkeys." Cell **169**(4): 610-620.e614.

Allison, S. L., J. Schalich, K. Stiasny, C. W. Mandl, C. Kunz and F. X. Heinz (1995). "Oligomeric rearrangement of tick-borne encephalitis virus envelope proteins induced by an acidic pH." J Virol **69**(2): 695-700.

Altenburg, A. F., C. E. van de Sandt, B. W. S. Li, R. J. MacLoughlin, R. A. M. Fouchier, G. van Amerongen, A. Volz, R. W. Hendriks, R. L. de Swart, G. Sutter, G. F. Rimmelzwaan and R. D. de Vries (2017). "Modified Vaccinia Virus Ankara Preferentially Targets Antigen Presenting Cells In Vitro, Ex Vivo and In Vivo." Sci Rep **7**(1): 8580.

Antoine, G., F. Scheiflinger, F. Dorner and F. G. Falkner (1998). "The complete genomic sequence of the modified vaccinia Ankara strain: comparison with other orthopoxviruses." Virology **244**(2): 365-396.

Aubry, M., A. Teissier, M. Huart, S. Merceron, J. Vanhomwegen, C. Roche, A. L. Vial, S. Teururai, S. Sicard, S. Paulous, P. Desprès, J. C. Manuguerra, H. P. Mallet, D. Musso, X. Deparis and V. M. Cao-Lormeau (2017). "Zika Virus Seroprevalence, French Polynesia, 2014-2015." Emerg Infect Dis **23**(4): 669-672.

Badolo, A., F. Burt, S. Daniel, R. Fearns, E. S. Gudo, M. Kielian, J. Lescar, Y. Shi, A. von Brunn, S. R. Weiss and R. Hilgenfeld (2019). "Third Tofo Advanced Study Week on Emerging and Re-emerging Viruses, 2018." Antiviral Res **162**: 142-150.

Bardina, S. V., P. Bunduc, S. Tripathi, J. Duehr, J. J. Frere, J. A. Brown, R. Nachbagauer, G. A. Foster, D. Krysztof, D. Tortorella, S. L. Stramer, A. García-Sastre, F. Krammer and J. K. Lim (2017). "Enhancement of Zika virus pathogenesis by preexisting antiflavivirus immunity." Science **356**(6334): 175-180.

Baronti, C., G. Piorkowski, R. N. Charrel, L. Boubis, I. Leparc-Goffart and X. de Lamballerie (2014). "Complete coding sequence of zika virus from a French polynesia outbreak in 2013." Genome Announc **2**(3).

Barrows, Nicholas J., Rafael K. Campos, S. T. Powell, K. R. Prasanth, G. Schott-Lerner, R. Soto-Acosta, G. Galarza-Muñoz, Erica L. McGrath, R. Urrabaz-Garza, J. Gao, P. Wu, R. Menon, G. Saade, I. Fernandez-Salas, Shannan L. Rossi, N. Vasilakis, A. Routh, Shelton S. Bradrick and Mariano A. Garcia-Blanco (2016). "A Screen of FDA-Approved Drugs for Inhibitors of Zika Virus Infection." Cell Host & Microbe **20**(2): 259-270.

Bayer, A., N. J. Lennemann, Y. Ouyang, J. C. Bramley, S. Morosky, E. T. Marques, Jr., S. Cherry, Y. Sadovsky and C. B. Coyne (2016). "Type III Interferons Produced by Human Placental Trophoblasts Confer Protection against Zika Virus Infection." Cell Host Microbe **19**(5): 705-712.

Baz, M. and G. Boivin (2019). "Antiviral Agents in Development for Zika Virus Infections." Pharmaceuticals (Basel) **12**(3).

Bernatchez, J. A., L. T. Tran, J. Li, Y. Luan, J. L. Siqueira-Neto and R. Li (2020). "Drugs for the Treatment of Zika Virus Infection." J Med Chem **63**(2): 470-489.

Bhattacharya, S. (2008). "The World Health Organization and global smallpox eradication." J Epidemiol Community Health **62**(10): 909-912.

Blanchard, T. J., A. Alcami, P. Andrea and G. L. Smith (1998). "Modified vaccinia virus Ankara undergoes limited replication in human cells and lacks several immunomodulatory proteins: implications for use as a human vaccine." J Gen Virol **79 ( Pt 5)**: 1159-1167.

Bloch, E. M., P. M. Ness, A. A. R. Tobian and J. Sugarman (2018). "Revisiting Blood Safety Practices Given Emerging Data about Zika Virus." N Engl J Med **378**(19): 1837-1841.

Boehme, K. W., J. Singh, S. T. Perry and T. Compton (2004). "Human cytomegalovirus elicits a coordinated cellular antiviral response via envelope glycoprotein B." J Virol **78**(3): 1202-1211.

Boigard, H., A. Alimova, G. R. Martin, A. Katz, P. Gottlieb and J. M. Galarza (2017). "Zika virus-like particle (VLP) based vaccine." PLoS Negl Trop Dis **11**(5): e0005608.

Boukamp, P., R. T. Petrussevska, D. Breitkreutz, J. Hornung, A. Markham and N. E. Fusenig (1988). "Normal keratinization in a spontaneously immortalized aneuploid human keratinocyte cell line." J Cell Biol **106**(3): 761-771.

Bowen, J. R., K. M. Quicke, M. S. Maddur, J. T. O'Neal, C. E. McDonald, N. B. Fedorova, V. Puri, R. S. Shabman, B. Pulendran and M. S. Suthar (2017). "Zika Virus Antagonizes Type I Interferon Responses during Infection of Human Dendritic Cells." PLoS Pathog **13**(2): e1006164.

Brasil, P., J. P. Pereira, Jr., M. E. Moreira, R. M. Ribeiro Nogueira, L. Damasceno, M. Wakimoto, R. S. Rabello, S. G. Valderramos, U. A. Halai, T. S. Salles, A. A. Zin, D. Horovitz, P. Daltro, M. Boechat, C. Raja Gabaglia, P. Carvalho de Sequeira, J. H. Pilotto, R. Medialdea-Carrera, D. Cotrim da Cunha, L. M. Abreu de Carvalho, M. Pone, A. Machado Siqueira, G. A. Calvet, A. E. Rodrigues Baiao, E. S. Neves, P. R. Nassar de Carvalho, R. H. Hasue, P. B. Marschik, C. Einspieler, C. Janzen, J. D. Cherry, A. M. Bispo de Filippis and K. Nielsen-Saines (2016). "Zika Virus Infection in Pregnant Women in Rio de Janeiro." N Engl J Med **375**(24): 2321-2334.

Brault, A. C., A. Domi, E. M. McDonald, D. Talmi-Frank, N. McCurley, R. Basu, H. L. Robinson, M. Hellerstein, N. K. Duggal, R. A. Bowen and F. Guirakhoo (2017). "A Zika Vaccine Targeting NS1 Protein Protects Immunocompetent Adult Mice in a Lethal Challenge Model." Sci Rep **7**(1): 14769.

Brien, J. D., J. L. Uhrlaub and J. Nikolich-Zugich (2007). "Protective capacity and epitope specificity of CD8(+) T cells responding to lethal West Nile virus infection." Eur J Immunol **37**(7): 1855-1863.

Brinton, M. A. (2002). "The molecular biology of West Nile Virus: a new invader of the western hemisphere." Annu Rev Microbiol **56**: 371-402.

Broyles, S. S. (2003). "Vaccinia virus transcription." J Gen Virol **84**(Pt 9): 2293-2303.

Büttner, M., C. P. Czerny, K. H. Lehner and K. Wertz (1995). "Interferon induction in peripheral blood mononuclear leukocytes of man and farm animals by poxvirus vector candidates and some poxvirus constructs." Vet Immunol Immunopathol **46**(3-4): 237-250.

Cao-Lormeau, V. M., A. Blake, S. Mons, S. Lastère, C. Roche, J. Vanhomwegen, T. Dub, L. Baudouin, A. Teissier, P. Larre, A. L. Vial, C. Decam, V. Choumet, S. K. Halstead, H. J. Willison, L. Musset, J. C. Manuguerra, P. Despres, E. Fournier, H. P. Mallet, D. Musso, A. Fontanet, J. Neil and F. Ghawché (2016). "Guillain-Barré Syndrome outbreak associated with Zika virus infection in French Polynesia: a case-control study." Lancet **387**(10027): 1531-1539.

Carroll, M. W. and B. Moss (1997). "Host range and cytopathogenicity of the highly attenuated MVA strain of vaccinia virus: propagation and generation of recombinant viruses in a nonhuman mammalian cell line." Virology **238**(2): 198-211.

Chambers, T. J., C. S. Hahn, R. Galler and C. M. Rice (1990). "Flavivirus genome organization, expression, and replication." Annu Rev Microbiol **44**: 649-688.

Chouin-Carneiro, T., M. R. David, F. de Bruycker Nogueira, F. B. Dos Santos and R. Lourenço-de-Oliveira (2020). "Zika virus transmission by Brazilian Aedes aegypti and Aedes albopictus is virus dose and temperature-dependent." PLoS Negl Trop Dis **14**(9): e0008527.

Chung, K. M., B. S. Thompson, D. H. Fremont and M. S. Diamond (2007). "Antibody recognition of cell surface-associated NS1 triggers Fc-gamma receptor-mediated phagocytosis and clearance of West Nile Virus-infected cells." J Virol **81**(17): 9551-9555.

Colombage, G., R. Hall, M. Pavy and M. Lobigs (1998). "DNA-based and alphavirus-vectored immunisation with prM and E proteins elicits long-lived and protective immunity against the flavivirus, Murray Valley encephalitis virus." Virology **250**(1): 151-163.

Cosma, A., R. Nagaraj, S. Bühler, J. Hinkula, D. H. Busch, G. Sutter, F. D. Goebel and V. Erfle (2003). "Therapeutic vaccination with MVA-HIV-1 nef elicits Nef-specific T-helper cell responses in chronically HIV-1 infected individuals." Vaccine **22**(1): 21-29.

Costa, F., M. Sarno, R. Khouri, B. de Paula Freitas, I. Siqueira, G. S. Ribeiro, H. C. Ribeiro, G. S. Campos, L. C. Alcântara, M. G. Reis, S. C. Weaver, N.

Vasilakis, A. I. Ko and A. R. Almeida (2016). "Emergence of Congenital Zika Syndrome: Viewpoint From the Front Lines." Ann Intern Med **164**(10): 689-691.

Davis, C. W., L. M. Mattei, H. Y. Nguyen, C. Ansarah-Sobrinho, R. W. Doms and T. C. Pierson (2006). "The location of asparagine-linked glycans on West Nile virions controls their interactions with CD209 (dendritic cell-specific ICAM-3 grabbing nonintegrin)." J Biol Chem **281**(48): 37183-37194.

de Jong, M. D. and T. T. Hien (2006). "Avian influenza A (H5N1)." J Clin Virol **35**(1): 2-13.

de Vries, R. D. and G. F. Rimmelzwaan (2016). "Viral vector-based influenza vaccines." Hum Vaccin Immunother **12**(11): 2881-2901.

Dejnirattisai, W., A. Jumnainsong, N. Onsirisakul, P. Fitton, S. Vasanawathana, W. Limpitikul, C. Puttikhunt, C. Edwards, T. Duangchinda, S. Supasa, K. Chawansuntati, P. Malasit, J. Mongkolsapaya and G. Screaton (2010). "Cross-reacting antibodies enhance dengue virus infection in humans." Science **328**(5979): 745-748.

Dejnirattisai, W., P. Supasa, W. Wongwiwat, A. Rouvinski, G. Barba-Spaeth, T. Duangchinda, A. Sakuntabhai, V. M. Cao-Lormeau, P. Malasit, F. A. Rey, J. Mongkolsapaya and G. R. Screaton (2016). "Dengue virus sero-cross-reactivity drives antibody-dependent enhancement of infection with zika virus." Nat Immunol **17**(9): 1102-1108.

Delaloye, J., T. Roger, Q. G. Steiner-Tardivel, D. Le Roy, M. Knaup Reymond, S. Akira, V. Petrilli, C. E. Gomez, B. Perdiguero, J. Tschopp, G. Pantaleo, M. Esteban and T. Calandra (2009). "Innate immune sensing of modified vaccinia virus Ankara (MVA) is mediated by TLR2-TLR6, MDA-5 and the NALP3 inflammasome." PLoS Pathog **5**(6): e1000480.

Dhanda, S. K., S. Mahajan, S. Paul, Z. Yan, H. Kim, M. C. Jespersen, V. Jurtz, M. Andreatta, J. A. Greenbaum, P. Marcatili, A. Sette, M. Nielsen and B. Peters (2019). "IEDB-AR: immune epitope database-analysis resource in 2019." Nucleic Acids Res **47**(W1): W502-w506.

Diamond, M. S., B. Shrestha, A. Marri, D. Mahan and M. Engle (2003). "B cells and antibody play critical roles in the immediate defense of disseminated infection by West Nile encephalitis virus." J Virol **77**(4): 2578-2586.

Diamond, M. S., E. M. Sitati, L. D. Friend, S. Higgs, B. Shrestha and M. Engle (2003). "A critical role for induced IgM in the protection against West Nile virus infection." J Exp Med **198**(12): 1853-1862.

Dick, G. W., S. F. Kitchen and A. J. Haddow (1952). "Zika virus. I. Isolations and serological specificity." Trans R Soc Trop Med Hyg **46**(5): 509-520.

Dirlikov, E., C. G. Major, N. A. Medina, R. Lugo-Robles, D. Matos, J. L. Muñoz-Jordan, C. Colon-Sanchez, M. Garcia, M. Olivero-Segarra, G. Malave, G. M. Rodríguez-Vega, D. L. Thomas, S. H. Waterman, J. J. Sejvar, C. A. Luciano, T. M. Sharp and B. Rivera-García (2018). "Clinical Features of Guillain-Barré Syndrome With vs Without Zika Virus Infection, Puerto Rico, 2016." JAMA Neurol **75**(9): 1089-1097.

do Rosario, M. S., P. A. de Jesus, N. Vasilakis, D. S. Farias, M. A. Novaes, S. G. Rodrigues, L. C. Martins, P. F. Vasconcelos, A. I. Ko, L. C. Alcantara and I. C. de Siqueira (2016). "Guillain-Barre Syndrome After Zika Virus Infection in Brazil." Am J Trop Med Hyg **95**(5): 1157-1160.

Dos Santos, T., A. Rodriguez, M. Almiron, A. Sanhueza, P. Ramon, W. K. de Oliveira, G. E. Coelho, R. Badaró, J. Cortez, M. Ospina, R. Pimentel, R. Masis, F. Hernandez, B. Lara, R. Montoya, B. Jubithana, A. Melchor, A. Alvarez, S.

Aldighieri, C. Dye and M. A. Espinal (2016). "Zika Virus and the Guillain-Barré Syndrome - Case Series from Seven Countries." N Engl J Med **375**(16): 1598-1601.

Draper, S. J. and J. L. Heeney (2010). "Viruses as vaccine vectors for infectious diseases and cancer." Nat Rev Microbiol **8**(1): 62-73.

Drexler, I., K. Heller, B. Wahren, V. Erfle and G. Sutter (1998). "Highly attenuated modified vaccinia virus Ankara replicates in baby hamster kidney cells, a potential host for virus propagation, but not in various human transformed and primary cells." J Gen Virol **79 ( Pt 2)**: 347-352.

Drexler, I., C. Staib, W. Kastenmuller, S. Stevanović, B. Schmidt, F. A. Lemonnier, H. G. Rammensee, D. H. Busch, H. Bernhard, V. Erfle and G. Sutter (2003). "Identification of vaccinia virus epitope-specific HLA-A*0201-restricted T cells and comparative analysis of smallpox vaccines." Proc Natl Acad Sci U S A **100**(1): 217-222.

Duffy, M. R., T. H. Chen, W. T. Hancock, A. M. Powers, J. L. Kool, R. S. Lanciotti, M. Pretrick, M. Marfel, S. Holzbauer, C. Dubray, L. Guillaumot, A. Griggs, M. Bel, A. J. Lambert, J. Laven, O. Kosoy, A. Panella, B. J. Biggerstaff, M. Fischer and E. B. Hayes (2009). "Zika virus outbreak on Yap Island, Federated States of Micronesia." N Engl J Med **360**(24): 2536-2543.

Duggal, N. K., J. M. Ritter, E. M. McDonald, H. Romo, F. Guirakhoo, B. S. Davis, G. J. Chang and A. C. Brault (2017). "Differential Neurovirulence of African and Asian Genotype Zika Virus Isolates in Outbred Immunocompetent Mice." Am J Trop Med Hyg **97**(5): 1410-1417.

Elong Ngono, A., E. A. Vizcarra, W. W. Tang, N. Sheets, Y. Joo, K. Kim, M. J. Gorman, M. S. Diamond and S. Shresta (2017). "Mapping and Role of the CD8(+) T Cell Response During Primary Zika Virus Infection in Mice." Cell Host Microbe **21**(1): 35-46.

Ewer, K., T. Rampling, N. Venkatraman, G. Bowyer, D. Wright, T. Lambe, E. B. Imoukhuede, R. Payne, S. K. Fehling, T. Strecker, N. Biedenkopf, V. Krähling, C. M. Tully, N. J. Edwards, E. M. Bentley, D. Samuel, G. Labbé, J. Jin, M. Gibani, A. Minhinnick, M. Wilkie, I. Poulton, N. Lella, R. Roberts, F. Hartnell, C. Bliss, K. Sierra-Davidson, J. Powlson, E. Berrie, R. Tedder, F. Roman, I. De Ryck, A. Nicosia, N. J. Sullivan, D. A. Stanley, O. T. Mbaya, J. E. Ledgerwood, R. M. Schwartz, L. Siani, S. Colloca, A. Folgori, S. Di Marco, R. Cortese, E. Wright, S. Becker, B. S. Graham, R. A. Koup, M. M. Levine, A. Volkmann, P. Chaplin, A. J. Pollard, S. J. Draper, W. R. Ballou, A. Lawrie, S. C. Gilbert and A. V. Hill (2016). "A Monovalent Chimpanzee Adenovirus Ebola Vaccine Boosted with MVA." N Engl J Med **374**(17): 1635-1646.

Falgout, B., M. Pethel, Y. M. Zhang and C. J. Lai (1991). "Both nonstructural proteins NS2B and NS3 are required for the proteolytic processing of dengue virus nonstructural proteins." J Virol **65**(5): 2467-2475.

Faria, N. R., R. Azevedo, M. U. G. Kraemer, R. Souza, M. S. Cunha, S. C. Hill, J. Thézé, M. B. Bonsall, T. A. Bowden, I. Rissanen, I. M. Rocco, J. S. Nogueira, A. Y. Maeda, F. Vasami, F. L. L. Macedo, A. Suzuki, S. G. Rodrigues, A. C. R. Cruz, B. T. Nunes, D. B. A. Medeiros, D. S. G. Rodrigues, A. L. N. Queiroz, E. V. P. da Silva, D. F. Henriques, E. S. T. da Rosa, C. S. de Oliveira, L. C. Martins, H. B. Vasconcelos, L. M. N. Casseb, D. B. Simith, J. P. Messina, L. Abade, J. Lourenço, L. C. J. Alcantara, M. M. de Lima, M. Giovanetti, S. I. Hay, R. S. de Oliveira, P. D. S. Lemos, L. F. de Oliveira, C. P. S. de Lima, S. P. da Silva, J. M. de Vasconcelos, L. Franco, J. F. Cardoso, J. Vianez-Júnior, D. Mir, G. Bello, E. Delatorre, K. Khan, M. Creatore, G. E. Coelho, W. K. de Oliveira, R. Tesh, O. G. Pybus, M. R. T. Nunes and P. F. C. Vasconcelos (2016). "Zika virus in the Americas: Early epidemiological and genetic findings." Science **352**(6283): 345-349.

Feldmann, H., A. Sprecher and T. W. Geisbert (2020). "Ebola." N Engl J Med **382**(19): 1832-1842.

Fiore-Gartland, A., B. A. Manso, D. P. Friedrich, E. E. Gabriel, G. Finak, Z. Moodie, T. Hertz, S. C. De Rosa, N. Frahm, P. B. Gilbert and M. J. McElrath (2016). "Pooled-Peptide Epitope Mapping Strategies Are Efficient and Highly Sensitive: An Evaluation of Methods for Identifying Human T Cell Epitope Specificities in Large-Scale HIV Vaccine Efficacy Trials." PLoS One **11**(2): e0147812.

Forster, D., J. H. Schwarz, K. Brosinski, U. Kalinke, G. Sutter and A. Volz (2020). "Obstetric Ultrasonography to Detect Fetal Abnormalities in a Mouse Model for Zika Virus Infection." Viruses **12**(1).

Förster, R., G. Wolf and A. Mayr (1994). "Highly attenuated poxviruses induce functional priming of neutrophils in vitro." Arch Virol **136**(1-2): 219-226.

Garg, H., T. Mehmetoglu-Gurbuz, G. M. Ruddy and A. Joshi (2019). "Capsid containing virus like particle vaccine against Zika virus made from a stable cell line." Vaccine **37**(48): 7123-7131.

George, J., W. G. Valiant, M. J. Mattapallil, M. Walker, Y. S. Huang, D. L. Vanlandingham, J. Misamore, J. Greenhouse, D. E. Weiss, D. Verthelyi, S. Higgs, H. Andersen, M. G. Lewis and J. J. Mattapallil (2017). "Prior Exposure to Zika Virus Significantly Enhances Peak Dengue-2 Viremia in Rhesus Macaques." Sci Rep **7**(1): 10498.

Giron, S., F. Franke, A. Decoppet, B. Cadiou, T. Travaglini, L. Thirion, G. Durand, C. Jeannin, G. L'Ambert, G. Grard, H. Noël, N. Fournet, M. Auzet-Caillaud, C. Zandotti, S. Aboukaïs, P. Chaud, S. Guedj, L. Hamouda, X. Naudot, A. Ovize, C. Lazarus, H. de Valk, M. C. Paty and I. Leparc-Goffart (2019). "Vector-borne transmission of Zika virus in Europe, southern France, August 2019." Euro Surveill **24**(45).

Gollins, S. W. and J. S. Porterfield (1985). "Flavivirus infection enhancement in macrophages: an electron microscopic study of viral cellular entry." J Gen Virol **66 ( Pt 9)**: 1969-1982.

Grant, A., S. S. Ponia, S. Tripathi, V. Balasubramaniam, L. Miorin, M. Sourisseau, M. C. Schwarz, M. P. Sánchez-Seco, M. J. Evans, S. M. Best and A. García-Sastre (2016). "Zika Virus Targets Human STAT2 to Inhibit Type I Interferon Signaling." Cell Host Microbe **19**(6): 882-890.

Greiner, S., J. Y. Humrich, P. Thuman, B. Sauter, G. Schuler and L. Jenne (2006). "The highly attenuated vaccinia virus strain modified virus Ankara induces apoptosis in melanoma cells and allows bystander dendritic cells to generate a potent anti-tumoral immunity." Clin Exp Immunol **146**(2): 344-353.

Guirakhoo, F., R. A. Bolin and J. T. Roehrig (1992). "The Murray Valley encephalitis virus prM protein confers acid resistance to virus particles and alters the expression of epitopes within the R2 domain of E glycoprotein." Virology **191**(2): 921-931.

Guirakhoo, F., F. X. Heinz, C. W. Mandl, H. Holzmann and C. Kunz (1991). "Fusion activity of flaviviruses: comparison of mature and immature (prM-containing) tick-borne encephalitis virions." J Gen Virol **72 ( Pt 6)**: 1323-1329.

Gutiérrez-Bugallo, G., L. A. Piedra, M. Rodriguez, J. A. Bisset, R. Lourenço-de-Oliveira, S. C. Weaver, N. Vasilakis and A. Vega-Rúa (2019). "Vector-borne transmission and evolution of Zika virus." Nat Ecol Evol **3**(4): 561-569.

Haagmans, B. L., J. M. van den Brand, V. S. Raj, A. Volz, P. Wohlsein, S. L. Smits, D. Schipper, T. M. Bestebroer, N. Okba, R. Fux, A. Bensaid, D. Solanes Foz, T. Kuiken, W. Baumgärtner, J. Segalés, G. Sutter and A. D. Osterhaus (2016). "An orthopoxvirus-based vaccine reduces virus excretion after MERS-CoV infection in dromedary camels." Science **351**(6268): 77-81.

Haddow, A. D., A. J. Schuh, C. Y. Yasuda, M. R. Kasper, V. Heang, R. Huy, H. Guzman, R. B. Tesh and S. C. Weaver (2012). "Genetic characterization of Zika virus strains: geographic expansion of the Asian lineage." PLoS Negl Trop Dis **6**(2): e1477.

Halle, S., H. C. Dujardin, N. Bakocevic, H. Fleige, H. Danzer, S. Willenzon, Y. Suezer, G. Hämmerling, N. Garbi, G. Sutter, T. Worbs and R. Förster (2009). "Induced bronchus-associated lymphoid tissue serves as a general priming site for T cells and is maintained by dendritic cells." J Exp Med **206**(12): 2593-2601.

Halstead, S. B. (2014). "Dengue Antibody-Dependent Enhancement: Knowns and Unknowns." Microbiol Spectr **2**(6).

Hamel, R., O. Dejarnac, S. Wichit, P. Ekchariyawat, A. Neyret, N. Luplertlop, M. Perera-Lecoin, P. Surasombatpattana, L. Talignani, F. Thomas, V. M. Cao-Lormeau, V. Choumet, L. Briant, P. Desprès, A. Amara, H. Yssel and D. Missé (2015). "Biology of Zika Virus Infection in Human Skin Cells." J Virol **89**(17): 8880-8896.

Harrer, E., M. Bäuerle, B. Ferstl, P. Chaplin, B. Petzold, L. Mateo, A. Handley, M. Tzatzaris, J. Vollmar, S. Bergmann, M. Rittmaier, K. Eismann, S. Müller, J. R. Kalden, B. Spriewald, D. Willbold and T. Harrer (2005). "Therapeutic vaccination of HIV-1-infected patients on HAART with a recombinant HIV-1 nef-expressing MVA: safety, immunogenicity and influence on viral load during treatment interruption." Antivir Ther **10**(2): 285-300.

Hassert, M., M. G. Harris, J. D. Brien and A. K. Pinto (2019). "Identification of Protective CD8 T Cell Responses in a Mouse Model of Zika Virus Infection." Front Immunol **10**: 1678.

Hassert, M., K. J. Wolf, K. E. Schwetye, R. J. DiPaolo, J. D. Brien and A. K. Pinto (2018). "CD4+T cells mediate protection against Zika associated severe disease in a mouse model of infection." PLoS Pathog **14**(9): e1007237.

Hay, J. A., P. Nouvellet, C. A. Donnelly and S. Riley (2018). "Potential inconsistencies in Zika surveillance data and our understanding of risk during pregnancy." PLoS Negl Trop Dis **12**(12): e0006991.

Hayes, E. B. (2009). "Zika virus outside Africa." Emerg Infect Dis **15**(9): 1347-1350.

Heinz, F. X. and K. Stiasny (2012). "Flaviviruses and their antigenic structure." J Clin Virol **55**(4): 289-295.

Heller, K. N., C. Gurer and C. Münz (2006). "Virus-specific CD4+ T cells: ready for direct attack." J Exp Med **203**(4): 805-808.

Herrlich, A. and A. Mayr (1957). "[Smallpox vaccine from tissue culture from a bull's tongue; at the same time a contribution to the question of culture vaccines]." Arch Gesamte Virusforsch **7**(3): 284-296.

Hickman, H. D. and T. C. Pierson (2017). "T Cells Take on Zika Virus." Immunity **46**(1): 13-14.

Hildner, K., B. T. Edelson, W. E. Purtha, M. Diamond, H. Matsushita, M. Kohyama, B. Calderon, B. U. Schraml, E. R. Unanue, M. S. Diamond, R. D. Schreiber, T. L. Murphy and K. M. Murphy (2008). "Batf3 deficiency reveals a critical role for CD8alpha+ dendritic cells in cytotoxic T cell immunity." Science **322**(5904): 1097-1100.

Hilgenfeld, R., J. Lei and L. Zhang (2018). "The Structure of the Zika Virus Protease, NS2B/NS3(pro)." Adv Exp Med Biol **1062**: 131-145.

Hill, M. E., A. Kumar, J. A. Wells, T. C. Hobman, O. Julien and J. A. Hardy (2018). "The Unique Cofactor Region of Zika Virus NS2B–NS3 Protease Facilitates Cleavage of Key Host Proteins." ACS Chemical Biology **13**(9): 2398-2405.

Hill, S. C., J. Vasconcelos, Z. Neto, D. Jandondo, L. Zé-Zé, R. S. Aguiar, J. Xavier, J. Thézé, M. Mirandela, A. L. Micolo Cândido, F. Vaz, C. D. S. Sebastião, C. H. Wu, M. U. G. Kraemer, A. Melo, B. L. F. Schamber-Reis, G. S. de Azevedo, A. Tanuri, L. M. Higa, C. Clemente, S. P. da Silva, D. da Silva Candido, I. M. Claro, D. Quibuco, C. Domingos, B. Pocongo, A. G. Watts, K. Khan, L. C. J. Alcantara, E. C. Sabino, E. Lackritz, O. G. Pybus, M. J. Alves, J. Afonso and N. R. Faria (2019). "Emergence of the Asian lineage of Zika virus in Angola: an outbreak investigation." Lancet Infect Dis **19**(10): 1138-1147.

Hugo, L. E., L. Stassen, J. La, E. Gosden, O. Ekwudu, C. Winterford, E. Viennet, H. M. Faddy, G. J. Devine and F. D. Frentiu (2019). "Vector competence of Australian Aedes aegypti and Aedes albopictus for an epidemic strain of Zika virus." PLoS Negl Trop Dis **13**(4): e0007281.

Hurtado-Monzón, A. M., C. D. Cordero-Rivera, C. N. Farfan-Morales, J. F. Osuna-Ramos, L. A. De Jesús-González, J. M. Reyes-Ruiz and R. M. Del Ángel (2020). "The role of anti-flavivirus humoral immune response in protection and pathogenesis." Rev Med Virol **30**(4): e2100.

Jameson, B., F. Baribaud, S. Pöhlmann, D. Ghavimi, F. Mortari, R. W. Doms and A. Iwasaki (2002). "Expression of DC-SIGN by dendritic cells of intestinal and genital mucosae in humans and rhesus macaques." J Virol **76**(4): 1866-1875.

Jurado, K. A., L. J. Yockey, P. W. Wong, S. Lee, A. J. Huttner and A. Iwasaki (2018). "Antiviral CD8 T cells induce Zika-virus-associated paralysis in mice." Nat Microbiol **3**(2): 141-147.

Kalodimou, G., S. Veit, S. Jany, U. Kalinke, C. C. Broder, G. Sutter and A. Volz (2019). "A Soluble Version of Nipah Virus Glycoprotein G Delivered by Vaccinia Virus MVA Activates Specific CD8 and CD4 T Cells in Mice." Viruses **12**(1).

Kang, C., T. H. Keller and D. Luo (2017). "Zika Virus Protease: An Antiviral Drug Target." Trends Microbiol **25**(10): 797-808.

Karaghiosoff, M., H. Neubauer, C. Lassnig, P. Kovarik, H. Schindler, H. Pircher, B. McCoy, C. Bogdan, T. Decker, G. Brem, K. Pfeffer and M. Müller (2000). "Partial impairment of cytokine responses in Tyk2-deficient mice." Immunity **13**(4): 549-560.

Katzelnick, L. C., L. Gresh, M. E. Halloran, J. C. Mercado, G. Kuan, A. Gordon, A. Balmaseda and E. Harris (2017). "Antibody-dependent enhancement of severe dengue disease in humans." Science **358**(6365): 929-932.

Katzelnick, L. C., C. Narvaez, S. Arguello, B. Lopez Mercado, D. Collado, O. Ampie, D. Elizondo, T. Miranda, F. Bustos Carillo, J. C. Mercado, K. Latta, A. Schiller, B. Segovia-Chumbez, S. Ojeda, N. Sanchez, M. Plazaola, J. Coloma, M. E. Halloran, L. Premkumar, A. Gordon, F. Narvaez, A. M. de Silva, G. Kuan, A. Balmaseda and E. Harris (2020). "Zika virus infection enhances future risk of severe dengue disease." Science **369**(6507): 1123-1128.

Kawiecki, A. B. and R. C. Christofferson (2016). "Zika Virus-Induced Antibody Response Enhances Dengue Virus Serotype 2 Replication In Vitro." J Infect Dis **214**(9): 1357-1360.

Kim, S. Y., J. Zhao, X. Liu, K. Fraser, L. Lin, X. Zhang, F. Zhang, J. S. Dordick and R. J. Linhardt (2017). "Interaction of Zika Virus Envelope Protein with Glycosaminoglycans." Biochemistry **56**(8): 1151-1162.

Koch, T., C. Dahlke, A. Fathi, A. Kupke, V. Krähling, N. M. A. Okba, S. Halwe, C. Rohde, M. Eickmann, A. Volz, T. Hesterkamp, A. Jambrecina, S. Borregaard, M. L. Ly, M. E. Zinser, E. Bartels, J. S. H. Poetsch, R. Neumann, R. Fux, S. Schmiedel, A. W. Lohse, B. L. Haagmans, G. Sutter, S. Becker and M. M. Addo (2020). "Safety and immunogenicity of a modified vaccinia virus Ankara vector vaccine candidate for Middle East respiratory syndrome: an open-label, phase 1 trial." Lancet Infect Dis **20**(7): 827-838.

Kraemer, M. U. G., R. C. Reiner, Jr., O. J. Brady, J. P. Messina, M. Gilbert, D. M. Pigott, D. Yi, K. Johnson, L. Earl, L. B. Marczak, S. Shirude, N. Davis Weaver, D. Bisanzio, T. A. Perkins, S. Lai, X. Lu, P. Jones, G. E. Coelho, R. G. Carvalho, W. Van Bortel, C. Marsboom, G. Hendrickx, F. Schaffner, C. G. Moore, H. H. Nax, L. Bengtsson, E. Wetter, A. J. Tatem, J. S. Brownstein, D. L. Smith, L. Lambrechts, S. Cauchemez, C. Linard, N. R. Faria, O. G. Pybus, T. W. Scott, Q. Liu, H. Yu, G. R. W. Wint, S. I. Hay and N. Golding (2019). "Past and future spread of the arbovirus vectors Aedes aegypti and Aedes albopictus." Nat Microbiol **4**(5): 854-863.

Kreijtz, J. H., Y. Suezer, G. de Mutsert, G. van Amerongen, A. Schwantes, J. M. van den Brand, R. A. Fouchier, J. Löwer, A. D. Osterhaus, G. Sutter and G. F. Rimmelzwaan (2009). "MVA-based H5N1 vaccine affords cross-clade protection in mice against influenza A/H5N1 viruses at low doses and after single immunization." PLoS One **4**(11): e7790.

Kremer, M., A. Volz, J. H. Kreijtz, R. Fux, M. H. Lehmann and G. Sutter (2012). "Easy and efficient protocols for working with recombinant vaccinia virus MVA." Methods Mol Biol **890**: 59-92.

Krow-Lucal, E. R., M. R. de Andrade, J. N. A. Cananéa, C. A. Moore, P. L. Leite, B. J. Biggerstaff, C. M. Cabral, M. Itoh, J. Percio, M. Y. Wada, A. M. Powers, A. Barbosa, R. B. Abath, J. E. Staples and G. E. Coelho (2018). "Association and birth prevalence of microcephaly attributable to Zika virus infection among infants in Paraíba, Brazil, in 2015-16: a case-control study." Lancet Child Adolesc Health **2**(3): 205-213.

Lai, Y. C., Y. C. Chuang, C. C. Liu, T. S. Ho, Y. S. Lin, R. Anderson and T. M. Yeh (2017). "Antibodies Against Modified NS1 Wing Domain Peptide Protect Against Dengue Virus Infection." Sci Rep **7**(1): 6975.

Lazear, H. M., J. Govero, A. M. Smith, D. J. Platt, E. Fernandez, J. J. Miner and M. S. Diamond (2016). "A Mouse Model of Zika Virus Pathogenesis." Cell Host Microbe **19**(5): 720-730.

Lehmann, M. H., W. Kastenmuller, J. D. Kandemir, F. Brandt, Y. Suezer and G. Sutter (2009). "Modified vaccinia virus ankara triggers chemotaxis of monocytes and early respiratory immigration of leukocytes by induction of CCL2 expression." J Virol **83**(6): 2540-2552.

Li, A., J. Yu, M. Lu, Y. Ma, Z. Attia, C. Shan, M. Xue, X. Liang, K. Craig, N. Makadiya, J. J. He, R. Jennings, P. Y. Shi, M. E. Peeples, S. L. Liu, P. N. Boyaka and J. Li (2018). "A Zika virus vaccine expressing premembrane-envelope-NS1 polyprotein." Nat Commun **9**(1): 3067.

Li, Y., Z. Zhang, W. W. Phoo, Y. R. Loh, R. Li, H. Y. Yang, A. E. Jansson, J. Hill, T. H. Keller, K. Nacro, D. Luo and C. Kang (2018). "Structural Insights into the Inhibition of Zika Virus NS2B-NS3 Protease by a Small-Molecule Inhibitor." Structure **26**(4): 555-564.e553.

Lindenbach, B. D. and C. M. Rice (2003). "Molecular biology of flaviviruses." Adv Virus Res **59**: 23-61.

Liu, R., X. Wang, Y. Ma, J. Wu, C. Mao, L. Yuan and J. Lu (2019). "Prevalence of Zika virus in blood donations: a systematic review and meta-analysis." BMC Infect Dis **19**(1): 590.

Liu, Z. Y., W. F. Shi and C. F. Qin (2019). "The evolution of Zika virus from Asia to the Americas." Nat Rev Microbiol **17**(3): 131-139.

López-Medina, E., C. A. Rojas, J. P. Calle-Giraldo, N. Alexander, I. C. Hurtado, D. M. Dávalos, P. López, C. Barco, D. Libreros, A. Arias, M. C. Lesmes, E. Pinzón and V. A. Ortiz (2020). "Risks of Adverse Childhood Outcomes According to Prenatal Time of Exposure to Zika Virus: Assessment in a Cohort Exposed to Zika During an Outbreak in Colombia." J Pediatric Infect Dis Soc.

Lucas, C. G. O., J. Z. Kitoko, F. M. Ferreira, V. G. Suzart, M. P. Papa, S. V. A. Coelho, C. B. Cavazzoni, H. A. Paula-Neto, P. C. Olsen, A. Iwasaki, R. M. Pereira, P. M. Pimentel-Coelho, A. M. Vale, L. B. de Arruda and M. T. Bozza (2018). "Critical role of CD4(+) T cells and IFNγ signaling in antibody-mediated resistance to Zika virus infection." Nat Commun **9**(1): 3136.

Luo, D., T. Xu, R. P. Watson, D. Scherer-Becker, A. Sampath, W. Jahnke, S. S. Yeong, C. H. Wang, S. P. Lim, A. Strongin, S. G. Vasudevan and J. Lescar (2008). "Insights into RNA unwinding and ATP hydrolysis by the flavivirus NS3 protein." Embo j **27**(23): 3209-3219.

Ma, L., C. T. Jones, T. D. Groesch, R. J. Kuhn and C. B. Post (2004). "Solution structure of dengue virus capsid protein reveals another fold." Proc Natl Acad Sci U S A **101**(10): 3414-3419.

Martinez-Vega, R. A., G. Carrasquila, E. Luna and J. Ramos-Castaneda (2017). "ADE and dengue vaccination." Vaccine **35**(32): 3910-3912.

Marzi, A., J. Emanuel, J. Callison, K. L. McNally, N. Arndt, S. Chadinha, C. Martellaro, R. Rosenke, D. P. Scott, D. Safronetz, S. S. Whitehead, S. M. Best and H. Feldmann (2018). "Lethal Zika Virus Disease Models in Young and Older Interferon α/β Receptor Knock Out Mice." Front Cell Infect Microbiol **8**: 117.

Masmejan, S., D. Baud, D. Musso and A. Panchaud (2018). "Zika virus, vaccines, and antiviral strategies." Expert Rev Anti Infect Ther **16**(6): 471-483.

Mayr, A. and K. Danner (1978). "Vaccination against pox diseases under immunosuppressive conditions." Dev Biol Stand **41**: 225-234.

Mayr, A., Hochstein-Mintzel, V. & Stickl, H. (1975). "Passage history, properties, and use of the attenuated vaccinia virus strain Ankara." Infection **3**.

Mead, P. S., N. K. Duggal, S. A. Hook, M. Delorey, M. Fischer, D. Olzenak McGuire, H. Becksted, R. J. Max, M. Anishchenko, A. M. Schwartz, W. P. Tzeng, C. A. Nelson, E. M. McDonald, J. T. Brooks, A. C. Brault and A. F. Hinckley (2018). "Zika Virus Shedding in Semen of Symptomatic Infected Men." N Engl J Med **378**(15): 1377-1385.

Mehrjardi, M. Z. (2017). "Is Zika Virus an Emerging TORCH Agent? An Invited Commentary." Virology (Auckl) **8**: 1178122x17708993.

Meisinger-Henschel, C., M. Schmidt, S. Lukassen, B. Linke, L. Krause, S. Konietzny, A. Goesmann, P. Howley, P. Chaplin, M. Suter and J. Hausmann (2007). "Genomic sequence of chorioallantois vaccinia virus Ankara, the ancestor of modified vaccinia virus Ankara." J Gen Virol **88**(Pt 12): 3249-3259.

Metsky, H. C., C. B. Matranga, S. Wohl, S. F. Schaffner, C. A. Freije, S. M. Winnicki, K. West, J. Qu, M. L. Baniecki, A. Gladden-Young, A. E. Lin, C. H. Tomkins-Tinch, S. H. Ye, D. J. Park, C. Y. Luo, K. G. Barnes, R. R. Shah, B. Chak, G. Barbosa-Lima, E. Delatorre, Y. R. Vieira, L. M. Paul, A. L. Tan, C. M. Barcellona, M. C. Porcelli, C. Vasquez, A. C. Cannons, M. R. Cone, K. N. Hogan, E. W. Kopp, J. J. Anzinger, K. F. Garcia, L. A. Parham, R. M. G. Ramírez, M. C. M. Montoya, D. P. Rojas, C. M. Brown, S. Hennigan, B. Sabina, S. Scotland, K. Gangavarapu, N. D. Grubaugh, G. Oliveira, R. Robles-Sikisaka, A. Rambaut, L. Gehrke, S. Smole, M. E. Halloran, L. Villar, S. Mattar, I. Lorenzana, J. Cerbino-Neto, C. Valim, W. Degrave, P. T. Bozza, A. Gnirke, K. G. Andersen, S. Isern, S. F. Michael, F. A. Bozza, T. M. L. Souza, I. Bosch, N. L. Yozwiak, B. L. MacInnis and P. C. Sabeti (2017). "Zika virus evolution and spread in the Americas." Nature **546**(7658): 411-415.

Meyer, H., G. Sutter and A. Mayr (1991). "Mapping of deletions in the genome of the highly attenuated vaccinia virus MVA and their influence on virulence." J Gen Virol **72 ( Pt 5)**: 1031-1038.

Mier, Y. T.-R. L., M. J. Delorey, J. J. Sejvar and M. A. Johansson (2018). "Guillain-Barré syndrome risk among individuals infected with Zika virus: a multi-country assessment." BMC Med **16**(1): 67.

Miner, J. J. and M. S. Diamond (2017). "Zika Virus Pathogenesis and Tissue Tropism." Cell Host Microbe **21**(2): 134-142.

Miranda-Filho Dde, B., C. M. Martelli, R. A. Ximenes, T. V. Araújo, M. A. Rocha, R. C. Ramos, R. Dhalia, R. F. França, E. T. Marques Júnior and L. C. Rodrigues (2016). "Initial Description of the Presumed Congenital Zika Syndrome." Am J Public Health **106**(4): 598-600.

Mondotte, J. A., P. Y. Lozach, A. Amara and A. V. Gamarnik (2007). "Essential role of dengue virus envelope protein N glycosylation at asparagine-67 during viral propagation." J Virol **81**(13): 7136-7148.

Moore, C. A., J. E. Staples, W. B. Dobyns, A. Pessoa, C. V. Ventura, E. B. Fonseca, E. M. Ribeiro, L. O. Ventura, N. N. Neto, J. F. Arena and S. A. Rasmussen (2017). "Characterizing the Pattern of Anomalies in Congenital Zika Syndrome for Pediatric Clinicians." JAMA Pediatr **171**(3): 288-295.

Mukhopadhyay, S., R. J. Kuhn and M. G. Rossmann (2005). "A structural perspective of the flavivirus life cycle." Nat Rev Microbiol **3**(1): 13-22.

Mulkey, S. B., M. Arroyave-Wessel, C. Peyton, D. I. Bulas, Y. Fourzali, J. Jiang, S. Russo, R. McCarter, M. E. Msall, A. J. du Plessis, R. L. DeBiasi and C. Cure (2020). "Neurodevelopmental Abnormalities in Children With In Utero Zika Virus Exposure Without Congenital Zika Syndrome." JAMA Pediatr **174**(3): 269-276.

Muller, U., U. Steinhoff, L. F. Reis, S. Hemmi, J. Pavlovic, R. M. Zinkernagel and M. Aguet (1994). "Functional role of type I and type II interferons in antiviral defense." Science **264**(5167): 1918-1921.

Müller, U., U. Steinhoff, L. F. Reis, S. Hemmi, J. Pavlovic, R. M. Zinkernagel and M. Aguet (1994). "Functional role of type I and type II interferons in antiviral defense." Science **264**(5167): 1918-1921.

Musso, D., H. Bossin, H. P. Mallet, M. Besnard, J. Broult, L. Baudouin, J. E. Levi, E. C. Sabino, F. Ghawche, M. C. Lanteri and D. Baud (2018). "Zika virus in French Polynesia 2013-14: anatomy of a completed outbreak." Lancet Infect Dis **18**(5): e172-e182.

Musso, D. and D. J. Gubler (2016). "Zika Virus." Clin Microbiol Rev **29**(3): 487-524.

Musso, D., A. I. Ko and D. Baud (2019). "Zika Virus Infection — After the Pandemic." New England Journal of Medicine **381**(15): 1444-1457.

Musso, D., E. J. Nilles and V. M. Cao-Lormeau (2014). "Rapid spread of emerging Zika virus in the Pacific area." Clin Microbiol Infect **20**(10): O595-596.

Musso, D., S. L. Stramer and M. P. Busch (2016). "Zika virus: a new challenge for blood transfusion." Lancet **387**(10032): 1993-1994.

Ngono, A. E. and S. Shresta (2018). "Immune Response to Dengue and Zika." Annu Rev Immunol **36**: 279-308.

Ochoa, M. C., L. Minute, I. Rodriguez, S. Garasa, E. Perez-Ruiz, S. Inogés, I. Melero and P. Berraondo (2017). "Antibody-dependent cell cytotoxicity: immunotherapy strategies enhancing effector NK cells." Immunol Cell Biol **95**(4): 347-355.

Organization, W. H. (2019). "ZIKA EPIDEMIOLOGY UPDATE." https://www.who.int/emergencies/zika-virus/situation-report/1-july-2019/en/.

Pardy, R. D., M. M. Rajah, S. A. Condotta, N. G. Taylor, S. M. Sagan and M. J. Richer (2017). "Analysis of the T Cell Response to Zika Virus and Identification of a Novel CD8+ T Cell Epitope in Immunocompetent Mice." PLoS Pathog **13**(2): e1006184.

Parola, P. and D. Musso (2020). "Zika, dengue, chikungunya and yellow fever infections in Europe? - Winter is over, warm days are coming - So hedge your bets." Travel Med Infect Dis **35**: 101614.

Pascutti, M. F., A. M. Rodríguez, J. Falivene, L. Giavedoni, I. Drexler and M. M. Gherardi (2011). "Interplay between modified vaccinia virus Ankara and dendritic cells: phenotypic and functional maturation of bystander dendritic cells." J Virol **85**(11): 5532-5545.

Pattnaik, A., B. R. Sahoo and A. K. Pattnaik (2020). "Current Status of Zika Virus Vaccines: Successes and Challenges." Vaccines (Basel) **8**(2).

Perera-Lecoin, M., L. Meertens, X. Carnec and A. Amara (2013). "Flavivirus entry receptors: an update." Viruses **6**(1): 69-88.

Pérez, P., Q. M. M, A. Lázaro-Frías, N. Jiménez de Oya, A. B. Blázquez, E. Escribano-Romero, S. S. CÓ, J. Ortego, J. C. Saiz, M. Esteban, M. A. Martín-Acebes and J. García-Arriaza (2018). "A Vaccine Based on a Modified Vaccinia Virus Ankara Vector Expressing Zika Virus Structural Proteins Controls Zika Virus Replication in Mice." Sci Rep **8**(1): 17385.

Petersen, L. R., D. J. Jamieson, A. M. Powers and M. A. Honein (2016). "Zika Virus." N Engl J Med **374**(16): 1552-1563.

Petzold, S., N. Agbaria, A. Deckert, P. Dambach, V. Winkler, J. F. Drexler, O. Horstick and T. Jaenisch (2021). "Congenital abnormalities associated with Zika virus infection-Dengue as potential co-factor? A systematic review." PLoS Negl Trop Dis **15**(1): e0008984.

Phoo, W. W., Y. Li, Z. Zhang, M. Y. Lee, Y. R. Loh, Y. B. Tan, E. Y. Ng, J. Lescar, C. Kang and D. Luo (2016). "Structure of the NS2B-NS3 protease from Zika virus after self-cleavage." Nature Communications **7**(1): 13410.

Polen, K. D., S. M. Gilboa, S. Hills, T. Oduyebo, K. S. Kohl, J. T. Brooks, A. Adamski, R. M. Simeone, A. T. Walker, D. M. Kissin, L. R. Petersen, M. A. Honein and D. Meaney-Delman (2018). "Update: Interim Guidance for Preconception Counseling and Prevention of Sexual Transmission of Zika Virus for Men with Possible Zika Virus Exposure - United States, August 2018." MMWR Morb Mortal Wkly Rep **67**(31): 868-871.

Pomar, L., M. Vouga, V. Lambert, C. Pomar, N. Hcini, A. Jolivet, G. Benoist, D. Rousset, S. Matheus, G. Malinger, A. Panchaud, G. Carles and D. Baud (2018). "Maternal-fetal transmission and adverse perinatal outcomes in pregnant women infected with Zika virus: prospective cohort study in French Guiana." Bmj **363**: k4431.

Price, P. J., L. E. Torres-Domínguez, C. Brandmüller, G. Sutter and M. H. Lehmann (2013). "Modified Vaccinia virus Ankara: innate immune activation and induction of cellular signalling." Vaccine **31**(39): 4231-4234.

Purtha, W. E., N. Myers, V. Mitaksov, E. Sitati, J. Connolly, D. H. Fremont, T. H. Hansen and M. S. Diamond (2007). "Antigen-specific cytotoxic T lymphocytes protect against lethal West Nile virus encephalitis." Eur J Immunol **37**(7): 1845-1854.

Quicke, K. M., J. R. Bowen, E. L. Johnson, C. E. McDonald, H. Ma, J. T. O'Neal, A. Rajakumar, J. Wrammert, B. H. Rimawi, B. Pulendran, R. F. Schinazi, R. Chakraborty and M. S. Suthar (2016). "Zika Virus Infects Human Placental Macrophages." Cell Host Microbe **20**(1): 83-90.

Ramos, H. J., M. C. Lanteri, G. Blahnik, A. Negash, M. S. Suthar, M. M. Brassil, K. Sodhi, P. M. Treuting, M. P. Busch, P. J. Norris and M. Gale, Jr. (2012). "IL-1β signaling promotes CNS-intrinsic immune control of West Nile virus infection." PLoS Pathog **8**(11): e1003039.

Reynolds, M. R., A. M. Jones, E. E. Petersen, E. H. Lee, M. E. Rice, A. Bingham, S. R. Ellington, N. Evert, S. Reagan-Steiner, T. Oduyebo, C. M. Brown, S. Martin, N. Ahmad, J. Bhatnagar, J. Macdonald, C. Gould, A. D. Fine, K. D. Polen, H. Lake-Burger, C. L. Hillard, N. Hall, M. M. Yazdy, K. Slaughter, J. N. Sommer, A. Adamski, M. Raycraft, S. Fleck-Derderian, J. Gupta, K. Newsome, M. Baez-Santiago, S. Slavinski, J. L. White, C. A. Moore, C. K. Shapiro-Mendoza, L. Petersen, C. Boyle, D. J. Jamieson, D. Meaney-Delman and M. A. Honein (2017). "Vital Signs: Update on Zika Virus-Associated Birth Defects and Evaluation of All U.S. Infants with Congenital Zika Virus Exposure - U.S. Zika Pregnancy Registry, 2016." MMWR Morb Mortal Wkly Rep **66**(13): 366-373.

Ricciardi, M. J., D. M. Magnani, A. Grifoni, Y. C. Kwon, M. J. Gutman, N. D. Grubaugh, K. Gangavarapu, M. Sharkey, C. G. T. Silveira, V. K. Bailey, N. Pedreño-Lopez, L. Gonzalez-Nieto, H. S. Maxwell, A. Domingues, M. A. Martins, J. Pham, D. Weiskopf, J. Altman, E. G. Kallas, K. G. Andersen, M. Stevenson, P. Lichtenberger, H. Choe, S. S. Whitehead, A. Sette and D. I. Watkins (2017). "Ontogeny of the B- and T-cell response in a primary Zika virus infection of a dengue-naïve individual during the 2016 outbreak in Miami, FL." PLoS Negl Trop Dis **11**(12): e0006000.

Rivino, L. and M. Q. Lim (2017). "CD4(+) and CD8(+) T-cell immunity to Dengue - lessons for the study of Zika virus." Immunology **150**(2): 146-154.

Rochlitz, C., R. Figlin, P. Squiban, M. Salzberg, M. Pless, R. Herrmann, E. Tartour, Y. Zhao, N. Bizouarne, M. Baudin and B. Acres (2003). "Phase I immunotherapy with a modified vaccinia virus (MVA) expressing human MUC1 as antigen-specific immunotherapy in patients with MUC1-positive advanced cancer." J Gene Med **5**(8): 690-699.

Rodriguez-Barraquer, I., F. Costa, E. J. M. Nascimento, N. J. Nery, P. M. S. Castanha, G. A. Sacramento, J. Cruz, M. Carvalho, D. De Olivera, J. E. Hagan, H. Adhikarla, E. A. Wunder, Jr., D. F. Coêlho, S. R. Azar, S. L. Rossi, N. Vasilakis, S. C. Weaver, G. S. Ribeiro, A. Balmaseda, E. Harris, M. L. Nogueira, M. G. Reis, E. T. A. Marques, D. A. T. Cummings and A. I. Ko (2019). "Impact of preexisting dengue immunity on Zika virus emergence in a dengue endemic region." Science **363**(6427): 607-610.

Rossi, S. L., G. D. Ebel, C. Shan, P. Y. Shi and N. Vasilakis (2018). "Did Zika Virus Mutate to Cause Severe Outbreaks?" Trends Microbiol **26**(10): 877-885.

Saiz, J. C., Á. Vázquez-Calvo, A. B. Blázquez, T. Merino-Ramos, E. Escribano-Romero and M. A. Martín-Acebes (2016). "Zika Virus: the Latest Newcomer." Front Microbiol **7**: 496.

Scherwitzl, I., J. Mongkolsapaja and G. Screaton (2017). "Recent advances in human flavivirus vaccines." Curr Opin Virol **23**: 95-101.

Sen, J., P. Bossu, S. J. Burakoff and A. K. Abbas (1992). "T cell surface molecules regulating noncognate B lymphocyte activation. Role of CD2 and LFA-1." J Immunol **148**(4): 1037-1042.

Shapiro-Mendoza, C. K., M. E. Rice, R. R. Galang, A. C. Fulton, K. VanMaldeghem, M. V. Prado, E. Ellis, M. S. Anesi, R. M. Simeone, E. E. Petersen, S. R. Ellington, A. M. Jones, T. Williams, S. Reagan-Steiner, J. Perez-Padilla, C. C. Deseda, A. Beron, A. J. Tufa, A. Rosinger, N. M. Roth, C. Green, S. Martin, C. D. Lopez, L. deWilde, M. Goodwin, H. P. Pagano, C. T. Mai, C. Gould, S. Zaki, L. N. Ferrer, M. S. Davis, E. Lathrop, K. Polen, J. D. Cragan, M. Reynolds, K. B. Newsome, M. M. Huertas, J. Bhatangar, A. M. Quiñones, J. F. Nahabedian, L. Adams, T. M. Sharp, W. T. Hancock, S. A. Rasmussen, C. A. Moore, D. J. Jamieson, J. L. Munoz-Jordan, H. Garstang, A. Kambui, C. Masao, M. A. Honein and D. Meaney-Delman (2017). "Pregnancy Outcomes After Maternal Zika Virus Infection During Pregnancy - U.S. Territories, January 1, 2016-April 25, 2017." MMWR Morb Mortal Wkly Rep **66**(23): 615-621.

Sheridan, M. A., V. Balaraman, D. J. Schust, T. Ezashi, R. M. Roberts and A. W. E. Franz (2018). "African and Asian strains of Zika virus differ in their ability to infect and lyse primitive human placental trophoblast." PLoS One **13**(7): e0200086.

Shimoda, K., K. Kato, K. Aoki, T. Matsuda, A. Miyamoto, M. Shibamori, M. Yamashita, A. Numata, K. Takase, S. Kobayashi, S. Shibata, Y. Asano, H. Gondo, K. Sekiguchi, K. Nakayama, T. Nakayama, T. Okamura, S. Okamura, Y. Niho and K. Nakayama (2000). "Tyk2 plays a restricted role in IFN alpha signaling, although it is required for IL-12-mediated T cell function." Immunity **13**(4): 561-571.

Shrestha, B. and M. S. Diamond (2004). "Role of CD8+ T cells in control of West Nile virus infection." J Virol **78**(15): 8312-8321.

Shrestha, B., M. A. Samuel and M. S. Diamond (2006). "CD8+ T cells require perforin to clear West Nile virus from infected neurons." J Virol **80**(1): 119-129.

Shrestha, B., T. Wang, M. A. Samuel, K. Whitby, J. Craft, E. Fikrig and M. S. Diamond (2006). "Gamma interferon plays a crucial early antiviral role in protection against West Nile virus infection." J Virol **80**(11): 5338-5348.

Simonin, Y., D. van Riel, P. Van de Perre, B. Rockx and S. Salinas (2017). "Differential virulence between Asian and African lineages of Zika virus." PLoS Negl Trop Dis **11**(9): e0005821.

Sitati, E. M. and M. S. Diamond (2006). "CD4+ T-cell responses are required for clearance of West Nile virus from the central nervous system." J Virol **80**(24): 12060-12069.

Song, F., R. Fux, L. B. Provacia, A. Volz, M. Eickmann, S. Becker, A. D. Osterhaus, B. L. Haagmans and G. Sutter (2013). "Middle East respiratory syndrome coronavirus spike protein delivered by modified vaccinia virus Ankara efficiently induces virus-neutralizing antibodies." J Virol **87**(21): 11950-11954.

Staib, C. and G. Sutter (2003). "Live viral vectors: vaccinia virus." Methods Mol Med **87**: 51-68.

Stocks, C. E. and M. Lobigs (1998). "Signal peptidase cleavage at the flavivirus C-prM junction: dependence on the viral NS2B-3 protease for efficient processing requires determinants in C, the signal peptide, and prM." J Virol **72**(3): 2141-2149.

Sutter, G. and B. Moss (1992). "Nonreplicating vaccinia vector efficiently expresses recombinant genes." Proc Natl Acad Sci U S A **89**(22): 10847-10851.

Sutter, G., L. S. Wyatt, P. L. Foley, J. R. Bennink and B. Moss (1994). "A recombinant vector derived from the host range-restricted and highly attenuated

MVA strain of vaccinia virus stimulates protective immunity in mice to influenza virus." Vaccine **12**(11): 1032-1040.

Thomas, S. J. and I. K. Yoon (2019). "A review of Dengvaxia®: development to deployment." Hum Vaccin Immunother **15**(10): 2295-2314.

Throsby, M., C. Geuijen, J. Goudsmit, A. Q. Bakker, J. Korimbocus, R. A. Kramer, M. Clijsters-van der Horst, M. de Jong, M. Jongeneelen, S. Thijsse, R. Smit, T. J. Visser, N. Bijl, W. E. Marissen, M. Loeb, D. J. Kelvin, W. Preiser, J. ter Meulen and J. de Kruif (2006). "Isolation and characterization of human monoclonal antibodies from individuals infected with West Nile Virus." J Virol **80**(14): 6982-6992.

Tolonen, N., L. Doglio, S. Schleich and J. Krijnse Locker (2001). "Vaccinia virus DNA replication occurs in endoplasmic reticulum-enclosed cytoplasmic mini-nuclei." Mol Biol Cell **12**(7): 2031-2046.

Vannice, K. S., M. C. Cassetti, R. W. Eisinger, J. Hombach, I. Knezevic, H. D. Marston, A. Wilder-Smith, M. Cavaleri and P. R. Krause (2019). "Demonstrating vaccine effectiveness during a waning epidemic: A WHO/NIH meeting report on approaches to development and licensure of Zika vaccine candidates." Vaccine **37**(6): 863-868.

Vázquez, S., M. G. Guzmán, G. Guillen, G. Chinea, A. B. Pérez, M. Pupo, R. Rodriguez, O. Reyes, H. E. Garay, I. Delgado, G. García and M. Alvarez (2002). "Immune response to synthetic peptides of dengue prM protein." Vaccine **20**(13-14): 1823-1830.

Veit, S., S. Jany, R. Fux, G. Sutter and A. Volz (2018). "CD8+ T Cells Responding to the Middle East Respiratory Syndrome Coronavirus Nucleocapsid Protein Delivered by Vaccinia Virus MVA in Mice." Viruses

**10**(12).

Victora, C. G., L. Schuler-Faccini, A. Matijasevich, E. Ribeiro, A. Pessoa and F. C. Barros (2016). "Microcephaly in Brazil: how to interpret reported numbers?" Lancet **387**(10019): 621-624.

Vollmar, J., N. Arndtz, K. M. Eckl, T. Thomsen, B. Petzold, L. Mateo, B. Schlereth, A. Handley, L. King, V. Hülsemann, M. Tzatzaris, K. Merkl, N. Wulff and P. Chaplin (2006). "Safety and immunogenicity of IMVAMUNE, a promising candidate as a third generation smallpox vaccine." Vaccine **24**(12): 2065-2070.

Volz, A., M. Langenmayer, S. Jany, U. Kalinke and G. Sutter (2014). "Rapid expansion of CD8+ T cells in wild-type and type I interferon receptor-deficient mice correlates with protection after low-dose emergency immunization with modified vaccinia virus Ankara." J Virol **88**(18): 10946-10957.

Volz, A. and G. Sutter (2017). "Modified Vaccinia Virus Ankara: History, Value in Basic Research, and Current Perspectives for Vaccine Development." Adv Virus Res **97**: 187-243.

Wang, Z., J. Martinez, W. Zhou, C. La Rosa, T. Srivastava, A. Dasgupta, R. Rawal, Z. Li, W. J. Britt and D. Diamond (2010). "Modified H5 promoter improves stability of insert genes while maintaining immunogenicity during extended passage of genetically engineered MVA vaccines." Vaccine **28**(6): 1547-1557.

Watts, A. G., C. Huber, Bogoch, II, O. J. Brady, M. U. G. Kraemer and K. Khan (2018). "Potential Zika virus spread within and beyond India." J Travel Med

**25**(1).

Webster, D. P., S. Dunachie, S. McConkey, I. Poulton, A. C. Moore, M. Walther, S. M. Laidlaw, T. Peto, M. A. Skinner, S. C. Gilbert and A. V. Hill (2006). "Safety of recombinant fowlpox strain FP9 and modified vaccinia virus Ankara vaccines against liver-stage P. falciparum malaria in non-immune volunteers." Vaccine **24**(15): 3026-3034.

Wen, J., W. W. Tang, N. Sheets, J. Ellison, A. Sette, K. Kim and S. Shresta (2017). "Identification of Zika virus epitopes reveals immunodominant and protective roles for dengue virus cross-reactive CD8(+) T cells." Nat Microbiol **2**: 17036.

Wilder-Smith, A., C. R. Chang and W. Y. Leong (2018). "Zika in travellers 1947-2017: a systematic review." J Travel Med **25**(1).

Wilder-Smith, A., K. Vannice, A. Durbin, J. Hombach, S. J. Thomas, I. Thevarjan and C. P. Simmons (2018). "Zika vaccines and therapeutics: landscape analysis and challenges ahead." BMC Med **16**(1): 84.

Winkler, C. W., L. M. Myers, T. A. Woods, R. J. Messer, A. B. Carmody, K. L. McNally, D. P. Scott, K. J. Hasenkrug, S. M. Best and K. E. Peterson (2017). "Adaptive Immune Responses to Zika Virus Are Important for Controlling Virus Infection and Preventing Infection in Brain and Testes." J Immunol **198**(9): 3526-3535.

Wolford, R. W. and T. J. Schaefer (2020). Zika Virus. StatPearls. Treasure Island (FL), StatPearls Publishing Copyright © 2020, StatPearls Publishing LLC.

Wongsurawat, T., N. Athipanyasilp, P. Jenjaroenpun, S. R. Jun, B. Kaewnapan, T. M. Wassenaar, N. Leelahakorn, N. Angkasekwinai, W. Kantakamalakul, D.

W. Ussery, R. Sutthent, I. Nookaew and N. Horthongkham (2018). "Case of Microcephaly after Congenital Infection with Asian Lineage Zika Virus, Thailand." Emerg Infect Dis **24**(9): 1758-1761.

WorldHealthOrganization. (2016). "Mosquito (vector) control emergency response and preparedness for Zika virus." from https://www.who.int/neglected_diseases/news/mosquito_vector_control_response/en/.

WorldHealthOrganization (2019). WHO Zika Epidemiology Update.

Wu, J., G. Lu, B. Zhang and P. Gong (2015). "Perturbation in the conserved methyltransferase-polymerase interface of flavivirus NS5 differentially affects polymerase initiation and elongation." J Virol **89**(1): 249-261.

Wyatt, L. S., P. L. Earl, W. Xiao, J. L. Americo, C. A. Cotter, J. Vogt and B. Moss (2009). "Elucidating and minimizing the loss by recombinant vaccinia virus of human immunodeficiency virus gene expression resulting from spontaneous mutations and positive selection." J Virol **83**(14): 7176-7184.

Wyatt, L. S., S. T. Shors, B. R. Murphy and B. Moss (1996). "Development of a replication-deficient recombinant vaccinia virus vaccine effective against parainfluenza virus 3 infection in an animal model." Vaccine **14**(15): 1451-1458.

Xu, M., E. M. Lee, Z. Wen, Y. Cheng, W.-K. Huang, X. Qian, J. Tcw, J. Kouznetsova, S. C. Ogden, C. Hammack, F. Jacob, H. N. Nguyen, M. Itkin, C. Hanna, P. Shinn, C. Allen, S. G. Michael, A. Simeonov, W. Huang, K. M. Christian, A. Goate, K. J. Brennand, R. Huang, M. Xia, G.-l. Ming, W. Zheng, H. Song and H. Tang (2016). "Identification of small-molecule inhibitors of Zika virus infection and induced neural cell death via a drug repurposing screen." Nature Medicine **22**(10): 1101-1107.

# XI. APPENDIX

## 1.1. Chemicals

| Chemical | Supplier |
|---|---|
| 2-Propanol ≥ 99.8 % | Carl Roth, Karlsruhe, Germany |
| Acetone ≥ 99.5 % | Carl Roth, Karlsruhe, Germany |
| Albumine, IgG-free | Carl Roth, Karlsruhe, Germany |
| Biozym LE Agarose | Biozym Scientific, Hessisch Oldendorf, Germany |
| Brefeldin A | Biolegend, London, United Kingdom |
| cOMPLETE, EDTA free | Roche Diagnostics, Mannheim, Germany |
| DAPI | Thermo Fisher Scientific, Planegg, Germany |
| DMSO | Sigma-Aldrich, Taufkirchen, Germany |
| Ethanol 96 %, | Carl Roth, Karlsruhe, Germany |
| GelRed Nucleic Acid Gel Stain, 10 000x | Biozol GmbH, Eching, Germany |
| Glycin | PanReac AppliChem, Darmstadt, Germany |
| KPL TrueBlue™ Peroxidase Substrate | HiSS Diagnostics GmbH, Freiburg im Breigau, Germany |
| Methanol ≥ 99 % | Carl Roth, Karlsruhe, Germany |
| MACSQuant Running Buffer | Milenyi Biotec, Bergisch Gladbach, Germany |
| Nonfat dried milk powder | PanReac AppliChem, Darmstadt, Germany |
| Red Blood Cell Lysing Buffer Hybri-Mix | Sigma-Aldrich, Taufkirchen, Germany |
| Roti-Load 1, reducing, 4 x | Carl Roth, Karlsruhe, Germany |
| Stop Reagent for ELISA | Sigma-Aldrich, Taufkirchen, |

| | |
|---|---|
| | Germany |
| Sucrose | Sigma-Aldrich, Taufkirchen, Germany |
| TMB for ELISA | Sigma-Aldrich, Taufkirchen, Germany |
| Tris-Ultrapure | PanReac AppliChem, Darmstadt, Germany |
| Triton-X100 | Sigma-Aldrich, Taufkirchen, Germany |
| Trypan blue | Sigma-Aldrich, Taufkirchen, Germany |
| Tween20 | Sigma-Aldrich, Taufkirchen, Germany |
| Zombie dye | Biolegend, London, United Kingdom |

### 1.2. Consumables

| Material | Supplier |
|---|---|
| 6- well tissue culture plates | Sarstedt, Nümbrecht, Germany |
| 24-well tissue culture plates | Sarstedt, Nümbrecht, Germany |
| 96-well tissue culture plates | Sarstedt, Nümbrecht, Germany |
| CryoPure tube | Sarstedt, Nümbrecht, Germany |
| Disposal bag | Sarstedt, Nümbrecht, Germany |
| Ep T.I.P.S Standard 20-300 µl | Eppendorf AG, Hamburg, Germany |
| Filter tips (20 µl) | Sarstedt, Nümbrecht, Germany |
| Filter tips (100 µl) | Sarstedt, Nümbrecht, Germany |
| Filter tips (200 µl) | Sarstedt, Nümbrecht, Germany |
| Filtopur S0.45 | Sarstedt, Nümbrecht, Germany |
| Microtest plate 96-well | Sarstedt, Nümbrecht, Germany |
| MiniCollect vials | Greiner Bio-One, Frickenhausen, Germany |
| Nitrocelluose Blotting Membrane | GE Healthcare Europe, Freiburg, Germany |

| | |
|---|---|
| Nunc-Immuno Plate | Thermo Fisher Scientific, Planegg, Germany |
| SafeSeal reaction tube 1.5 ml | Sarstedt, Nümbrecht, Germany |
| SafeSeal reaction tube 2 ml | Sarstedt, Nümbrecht, Germany |
| Serological pipette 5 ml | Sarstedt, Nümbrecht, Germany |
| Serological pipette 10 ml | Sarstedt, Nümbrecht, Germany |
| Serological pipette 25 ml | Sarstedt, Nümbrecht, Germany |
| TC flask 25 | Sarstedt, Nümbrecht, Germany |
| TC flask 75 | Sarstedt, Nümbrecht, Germany |
| TC flask 175 | Sarstedt, Nümbrecht, Germany |
| Tube 15 ml | Sarstedt, Nümbrecht, Germany |
| Tube 50 ml | Sarstedt, Nümbrecht, Germany |

### 1.3. Laboratory equipment

| **Laboratory equipment** | **Supplier** |
|---|---|
| A.EL.VIS Universal plate reader V3.0 | A.EL.VIS GmbH, Hannover, Germany |
| Avanti® J-26 XP Centrifuge | Beckmann Coulter, Krefeld, Germany |
| Biofuge fresco | Heraeus, Hanau, Germany |
| Centrifuge 5424 | Eppendorf AG, Hamburg, Germany |
| ChemiDocTMMP, Imaging System | Bio-Rad, Munich, Germany |
| FACS Calibur cytofluorometer | Becton Dickinson, Heidelberg, Germany |

| | |
|---|---|
| Galaxy 170S Incubator | New Brunswick (Eppendorf), Hamburg, Germany |
| KEYENCE BZ-X710 All-in one Fluorescence Microscope | KEYENCE Deutschland GmbH, NeuIsenburg, Germany |
| Microplate reader Sunrice | Tecan, |
| MJ Research PTC-200 Peltier Thermal Cycler | GMI, Ramsey, USA |
| Olympus CKX41 | Olympus Life Sciences, Hamburg, Germany |
| OptimaTMLE-80K Ultracentrifuge | Beckman Coulter, Krefeld, Germany |
| Sonoplus | Bandelin electronic, Berlin, Germany |

### 1.4. DNA and protein marker

| Material | Supplier |
|---|---|
| 1 kb DNA ladder | New England Biolabs, Frankfurt, Germany |
| Color Protein Standard Broad range | New England Biolabs, Frankfurt, Germany |

### 1.5. Commercial Kits

| Material | Supplier |
|---|---|
| 2.5 mM dNTP Mix | Invitrogen, Darmstadt, Germany |
| MINI-Protean TGX | Bio-Rad, Feldkirchen, Germany |
| Mouse IFN-y ELISpot$^{Plus}$ kit (ALP) | Mabtech, Nacka Strand, Germany |
| NucleoBond Xtra Midi | Macherey-Nagel, Düren, Germany |
| NucleoSpin Blood QuickPure | Macherey-Nagel, Düren, Germany |
| NucleoSpin Gel and PCR Clean-up | Macherey-Nagel, Düren, Germany |
| NucleoSpin Plasmid | Macherey-Nagel, Düren, Germany |
| OneStep RT-PCR Kit | Qiagen, Hilden, Germany |
| RNeasy Mini kit | Qiagen, Hilden, Germany |
| SuperSignal West Dura Extended Duration Substrate | Thermo Fisher Scientific, Planegg, Germany |
| Taq DNA Polymerase | Invitrogen, Darmstadt, Germany |

### 1.6. Media and supplements for cell culture

| Material | Supplier |
|---|---|
| DMEM | Sigma-Aldrich, Taufkirchen, Germany |
| DMEM (high glucose) | Sigma-Aldrich, Taufkirchen, Germany |
| DPBS | Thermo Fisher Scientific, Planegg, Germany |
| FBS | Thermo Fisher Scientific, Planegg, Germany Fisher Scientific |
| HEPES solution | Sigma-Aldrich, Taufkirchen, Germany |
| L-Glutamine | Thermo Fisher Scientific, Planegg, Germany |
| MEM | Sigma-Aldrich, Taufkirchen, Germany |
| MEM non-essential amino acid solution | Sigma-Aldrich, Taufkirchen, Germany |
| Penicillin-Streptomycin | Sigma-Aldrich, Taufkirchen, Germany |
| RPMI-1640 medium | Sigma-Aldrich, Taufkirchen, Germany |
| SFP eggs | VALO BioMedia GmbH, Cuxhaven, Germany |
| TrypLE™ Select Enzym | Thermo Fisher Scientific, Planegg, Germany |
| VP-SFM | Thermo Fisher Scientific, Planegg, Germany |

### 1.7. Buffer

| **Lysis buffer** | **Transfer buffer (conc.)** |
|---|---|
| 1 % Triton X-100 | 24 g Tris |
| 25 mM Tris | 114,6 g Glycin |
| 1 M NaCl | |
| **5x Running buffer** | **Transfer (working solution)** |
| 72.5 g Glycin | 80 ml Towbin buffer (conc.) |
| 15,2 g Tris | 200 ml Methanol |
| 25 ml 20 % SDS | Ad 1 l ddH2O |

| **Vaccine buffer (pH=7.4)** | **50x TAE buffer (pH= 7.4)** |
|---|---|
| 10 mM Tris | 242 g Tris |
| 140 mM NaCl | 57.1 ml acetic acid glacial |
| | 18.6 g EDTA |
| **LB-Medium (pH= 7.5)** | **LB-agar** |
| 5 g/l NaCl | 1,5 % Agar-Agar in LB-Medium |
| 5 g/l Yeast extract | |
| 10 g/l Trypton | |
| **10x PBS** | |
| 2 g/l KCl | |
| 2 g/l $KH_2PO_4$ | |
| 80 g/l NaCl | |
| 11.5 g/l $Na_2HPO_4$ | |

### 1.8. Software

| | |
|---|---|
| Adobe Reader | Adobe Systems, San Jose, USA |
| A.EL.VIS V6.1 | A.EL.VIS GmbH, Hannover, Germany |
| BioRender | BioRender, Toronto, USA |
| DNASTAR Lasergene | DNASTAR, Inc., Madison, Wisconsin, USA |
| FlowJo LLC | BD Life Sciences, Ashland, USA |
| GraphPad prism | GraphPad Software, San Diego, USA |
| Image Lab 5.0 Software | Bio-Rad, Feldkirchen, Germany |
| Microsoft Office 2016 | Microsoft Corp., Redmond, USA |
| NetNGlyc 1.0 Server | http://www.cbs.dtu.dk/services/NetNGlyc/ |

# XII. DANKSAGUNG

Meinem Doktorvater Herrn **Prof. Dr. Gerd Sutter** möchte ich für die Möglichkeit, diese Arbeit am Institut für Infektionsmedizin und Zoonosen anfertigen zu können, sowie für seine unzähligen Ratschlägen und seiner Unterstützung ganz herzlich danken. Vielmehr aber gilt mein größter Dank seiner Art und Weise, wie er mich an das wissenschaftliche Arbeiten herangeführt hat, welches stets von der notwendigen Freiheit und Leidenschaft für die Sache geprägt war und ist. Von allen Erkenntnissen und Erfahrungen die ich während dieser Zeit hier sammeln durfte, hat sich besonders jene eingeprägt, als ich erstmals den beeindruckenden Schutzeffekt einer Impfung beobachten konnte. Die daraus resultierende Faszination hat mich auch entgegen vieler Widrigkeiten in meiner Arbeit immerzu angetrieben und unermüdlich neugierig gemacht.

Bei Frau **Prof. Dr. Asisa Volz** möchte ich mich für die Möglichkeit an diesem wirklich tollen Projekt mitarbeiten und dieses mitgestalten zu dürfen bedanken. Besonders danke ich ihr für die Verantwortung, die sie mir in diesem Projekt anvertraut hat, sowie für die Möglichkeit, die Ergebnisse auf mehreren Tagungen in Hamburg und Berlin vorstellen zu dürfen.

**Astrid Freudenstein** und **Sylvia Jany** danke ich für ihre Geduld, die sie sowohl bei meiner Einführung in die Laborarbeit, als auch bei den unzähligen Momenten beweisen mussten, in denen Domi, Leo und ich sie
mit einfachem Quatsch unaufhaltsam überrumpelt haben. Ohne euer Wissen, eure Hilfe und Ideen wären die Hürden dieser Arbeit wohl viel höher gelegen.

Auch ohne die engagierte Hilfe von **Ursula Klostermeier**, **Patrizia Bonert**, **Axel Groß** und **Johannes Döring**, wäre die Umsetzung der Tierversuche ganz sicher nicht möglich gewesen. Euer Wissen, Engagement und der kollegiale Umgang haben mir stets die notwendige Sicherheit für die verantwortungsvolle Arbeit mit unseren Versuchstieren gegeben.

Bei **Dr. Robert Fux** möchte ich mich für seine unentwegt offene Art und seiner von größter Begeisterung geprägten Wissensvermittlung danken. Das gemeinsame Musizieren zu den Weihnachtsfeiern war immer ein großer und unvergesslicher Spaß, an den ich mich gerne zurückerinnern werde!

**Dr. Georg Wolf** möchte ich dafür danken, dass auch er immerwährend ein offenes Ohr für Fragen wirklich aller Art hat, auf die er immer kluge Antworten findet. Jedes noch so kurze Aufeinandertreffen mit ihm ist bereichernd, da es stets damit verbunden ist, Neues aus seinem offensichtlich unendlichen Wissensschatz zu lernen.

Seinen unzähligen Erklärungen und Hilfen aller Art gilt **Dr. Martin Langenmayr** mein Dank in gleichem Maße wie für seine Aufmerksamkeit bei persönlichen Belangen!

**Corinna Macheel**, **Wanda Schroppa** und **Nina Hechtberger** danke ich ihrer Hilfe bei der Bewältigung akademischer Bürokratie und sonstigem universitärem Wahnsinn.

Ein besonderer Dank gilt auch meiner Bürokollegin **Alina Tscherne**, ohne deren Akribie und Fleiß das Abenteuer MVA-S so nicht möglich gewesen wäre!

**Dr. Georgia Kalodimou** danke ich ganz herzlich für die schnelle Korrektur dieser Arbeit und die tolle Zusammenarbeit.

Wenngleich ich Titel jeglicher Form gewissermaßen nur als Produkt von menschlichem Rigorismus betrachte, so bedeutet mir diese Arbeit doch eine ganze Menge. Dies begründet sich vor allem in der Unterstützung, die ich auf diesem Weg von so vielen besonderen Menschen erhalten habe.

An erster Stelle sind hier meine lieben Eltern **Susann** und **Andreas** zu nennen, deren Umgang mit den Schwierigkeiten des Lebens mir immerzu ein Vorbild ist. Durch sie weiß ich, dass Aufgeben niemals eine Option ist, dass sich „Mutigsein“ und tiefe Aufrichtigkeit auch nach quälend langer Zeit letztlich immer lohnt - sofern man nur so unfassbar stark wie sie zusammenhält.

Meinem großen Bruder **Frederik** danke ich unter anderem dafür, dass ich immer auf ihn zählen kann. Nur dank seines Rückhalts kann ich mich meiner Arbeit fernab der Heimat auch immer mit einem guten Gewissen widmen.

In erster Linie verdanke ich **Arne Auste** im Reich der Viren gelandet zu sein. Sein unvergleichlicher Enthusiasmus hat die notwendige Neugierde und den Mut in mir geweckt, diese Arbeit überhaupt zu beginnen. Die unzähligen Stunden, in denen wir über den neuesten „Virologen-Klatsch“ diskutiert und in alten Erinnerungen an unsere Abenteuer in Kanada geschwelgt haben, bleiben mir unvergessen.

Meine Zeit als Doktorand möchte ich vor allem wegen zwei weiterer wunderbarer Freunde nicht missen – **Dominik Forster** und seinem würdigen Nachfolger **Leonard Limpinsel** verdanke ich unfassbar schöne, lustige, quatschige, aber auch philosophische, häufig mit großer Sorge erfüllte Momente inner- wie außerhalb des Instituts, die uns zusammengeschweißt haben. Danke für das gemeinsame Durchstehen und das aufrichtige Zusammenhalten!

Arne, Domi, Leo – es ist schön und unendlich bereichernd wahre Freunde wie euch zu haben!

Das Schicksal hätte es nicht besser mit mir meinen können, um diesen wie auch die vorherigen Wege schon so lange gemeinsam mit meiner großen Liebe **Bianca Faletti** beschreiten zu dürfen. Danke für deine unendliche Geduld mit mir, deinen unaufhaltsamen Optimismus, deine ansteckende Fröhlichkeit, dein gesunder Pragmatismus und deine Kreativität – du bist meine Konstante; du gibst alledem erst einen Sinn!